FACULTY OF MARITIME STUDIES

Marko Zubčić

DETECTION OF A BROKEN ROTOR BAR IN A SQUIRREL CAGE INDUCTION MOTOR AT STEADY STATE USING MAGNETIC STRAY FLUX PORTABLE TRIAXIAL AIR COIL SENSOR

DOCTORAL THESIS

Split, 2024

FACULTY OF MARITIME STUDIES

Marko Zubčić

DETECTION OF A BROKEN ROTOR BAR IN A SQUIRREL CAGE INDUCTION MOTOR AT STEADY STATE USING MAGNETIC STRAY FLUX PORTABLE TRIAXIAL AIR COIL SENSOR

DOCTORAL THESIS

Supervisor: Petar Matić, Ph.D.
Co-supervisor: Ivan Pavić, Ph.D.

Split, 2024

DATA ON EVALUATION AND DEFENCE OF THE DISSERTATION

Doctoral thesis evaluation committee:

1 prof. Danko Kezić, Ph. D., president, Full Professor with tenure, University of Split, Faculty of Maritime Studies
2 Adamczyk Arkadiusz, Ph. D., member, Assistant professor, Polish Naval Academy of the Heroes of Westerplatte, Faculty of Mechanical and Electrical Engineering
3 Joško Šoda, Ph. D., member, Associate professor, University of Split, Faculty of Maritime Studies

Doctoral thesis defense committee:

1 prof. Danko Kezić, Ph. D., president, Full Professor with tenure, University of Split, Faculty of Maritime Studies
2 Adamczyk Arkadiusz, Ph. D., member, Assistant Professor, Polish Naval Academy of the Heroes of Westerplatte, Faculty of Mechanical and Electrical Engineering
3 Joško Šoda, Ph. D., member, Associate professor, University of Split, Faculty of Maritime Studies
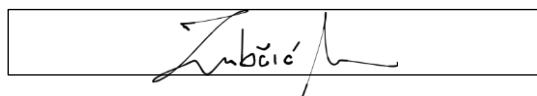
Doctoral thesis defended on:

The Doctoral thesis defence committee for *Marko Zubčić* certifies that this is the approved version of the

DETECTION OF A BROKEN ROTOR BAR IN A SQUIRREL CAGE INDUCTION MOTOR AT STEADY STATE USING MAGNETIC STRAY FLUX PORTABLE TRIAXIAL AIR COIL SENSOR

President:	prof. Danko Kezić, Ph. D., Full Professor with tenure	University of Split, Faulty of Maritime Studies
Member:	Adamczyk Arkadiusz, Ph. D., Assistant Professor	Polish Naval Academy of the Heroes of Westerplatte, Faculty of Mechanical and Electrical Engineering
Member:	Joško Šoda, Ph. D., Associate Professor	University of Split, Faulty of Maritime Studies

ABSTRACT

Squirrel cage induction motors (SCIMs) account for approximately 87% of all AC motors in the industry. However, during their operational lifetime, SCIMs are subjected to various stresses, including thermal, mechanical, electrical, and environmental factors, which can lead to faults despite robust design and manufacturing standards. Faults in SCIMs are classified into electrical (stator and rotor faults) and mechanical (bearing and rotor faults). This study investigates the detection of broken rotor bar (BRB) faults in SCIMs using stray magnetic flux measurements with randomly positioned sensor. The research aims to validate the measurement method and assess its efficacy in detecting BRB faults in a steady state using random sensor positioning. The experimental setup involved two groups of SCIMs (Siemens and Končar), each comprising two identical motors—one maintained in a healthy state and the other with an induced BRB. Three analytical approaches were employed: statistical analysis of raw data, time-domain feature analysis, and Fast Fourier Transformation (FFT) analysis. The statistical analysis aimed to validate the consistency of the measurement method. Results showed that the measurements were time-independent for each motor condition, indicating the method's reliability. However, statistical analysis alone was inconclusive for BRB detection due to significant differences between healthy motors. The feature analysis focused on 19 time-domain features, revealing that peak-to-rms, impulse factor, and clearance factor were reliable indicators for detecting BRB in Siemens motors, especially when a large number of measurements were used. For Končar motors, however, no features consistently indicated BRB faults at high reliability levels. The FFT analysis proved to be the most effective approach for BRB detection. By averaging the frequency spectra over the interval of 0-100 Hz and analysing specific frequency indicators, the FFT method reliably detected BRB faults. The reliability of detection increased with the number of measurements, achieving high accuracy with as few as 10 random measurements. This research demonstrates that BRB faults in SCIMs can be reliably detected using stray magnetic flux measurements with random sensor positioning, particularly when employing FFT analysis. Future research should explore shorter measurement durations, a wider variety of motor types, and the detection of multiple broken rotor bars. The limitations of this study include the controlled laboratory environment, the specific motor types tested, and the constant measurement duration and sampling frequency.

Key words: Broken rotor bar; Squirrel cage induction motor; Stray flux; Triaxial air coil; Sensor random positioning;

Table of Contents

1. INTRODUCTION

The induction motor (IM) is an alternating current (AC) electrical machine used to drive various industrial utility components such as compressors, pumps, fans, elevators, cranes, etc. There are two types of IMs: wound rotor induction motors (WRIMs) and squirrel cage induction motors (SCIMs). As stated in [1], SCIMs account for aproximately 87 % of the total AC motor population in the industry.

SCIMs are designed and tested in accordance with standards (e.g., International Electrotechnical Commission - IEC, National Electrical Manufacturers Association - NEMA) that specify working conditions for motors. During their lifetime, motors may be subjected to different types of stresses (thermal, mechanical, electrical, environmental conditions - chemical pollution) with varying intensity [2]. Since standards cannot cover all scenarios in the industry and manufacturing process has a certain level of imperfection (quality of materials used and quality of the assembly process), it is to be expected that even robust machines such as SCIMs have defects [3].

Faults in SCIMs are divided into two categories: electrical and mechanical faults [4], [5]. Electrical faults are further divided into:

- stator (turn-to-turn, coil-to-coil, phase-to-phase, phase-to-ground, and open circuit)
- rotor (broken rotor bar and broken end ring)
- power supply faults (phase imbalance and single phasing)

Mechanical faults are divided into:
- stator (frame vibrations)
- rotor (unbalanced, bent rotor, static, dynamic, and mixed eccentricity)
- bearing faults (outer ring, inner ring, rolling elements, and loss of lubricant)

Division of the SCIM faults is shown in Figure 1.
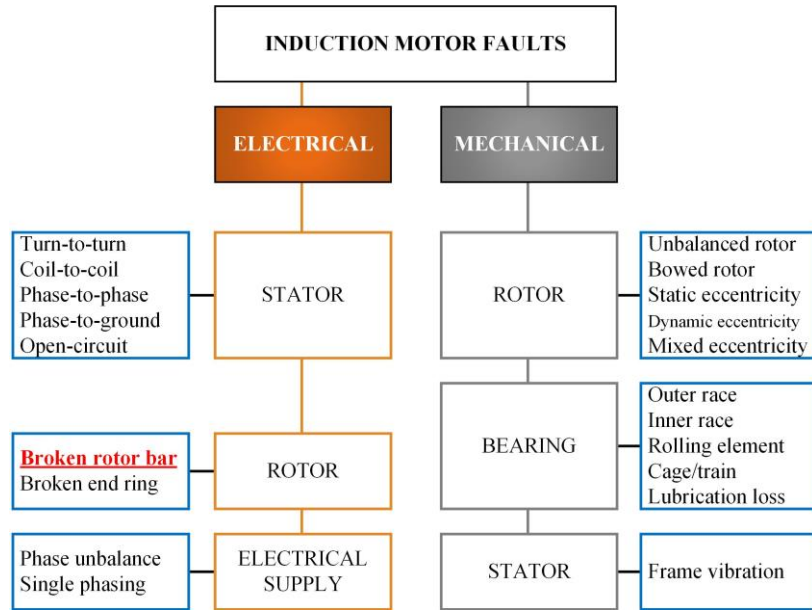
Figure 1. Division of the squirrel cage induction motor faults.

The rotor of the SCIM is a solid body produced by casting or fabrication. In all casting processes, molten aluminium or an aluminium alloy is injected into a preheated, stacked rotor core. During fabrication, the rotor bars are inserted individually and then shorted with rings at each end [6]. As stated in [7] and [8], during motor service the rotor can be subjected to various stresses that can lead to rotor bar fracture: thermal, magnetic, dynamic, mechanical and environmental stresses. Calculations and measurements from [9], [10] and [11] have shown that a broken rotor bar increases the total harmonic distortion, motor current, and power dissipation, thus reducing motor efficiency. Calculations have also shown that a broken rotor bar leads to an increase in the currents in the neighbouring bars and thus to their potential breakage. Examples in [12] show that at rated load, one broken bar can lead to a relative increase of 30% in the current in the neighbouring bars, and in the case of three neighbouring broken bars, the relative increase can reach about 60%. As shown in [13] this type of fault can be random in nature, rotor of a 6.6 kV, 500 kW motor has 8 nonadjacent broken bars that are unevenly distributed. Early detection of the rotor bar is important because bearing failures may occur over time due to the induced shaft vibrations [14].

Broken rotor bar fault and broken end ring fault are illustrated in Figure 2.

The distribution of the fault types analysed in various studies is shown in Figure 3. The studies shown in Figure 3 are the Electric Power Research Institute (EPRI) study, the Motor Reliability Working Group (MRWG) study of the Institute of Electrical and Electronics Engineers (IEEE), the 1995 study, and the Allianz study [15]. The EPRI study deals with

SCIMs, WRIMs, and synchronous motors (100 hp and above at low voltage levels 460 V and 575 V, and medium voltage motors 2.3 kV, 4 kV, 6.6 kV, and 13.2 kV) [16].

(a)　　　　　　　　　　　　　　　　　　**(b)**
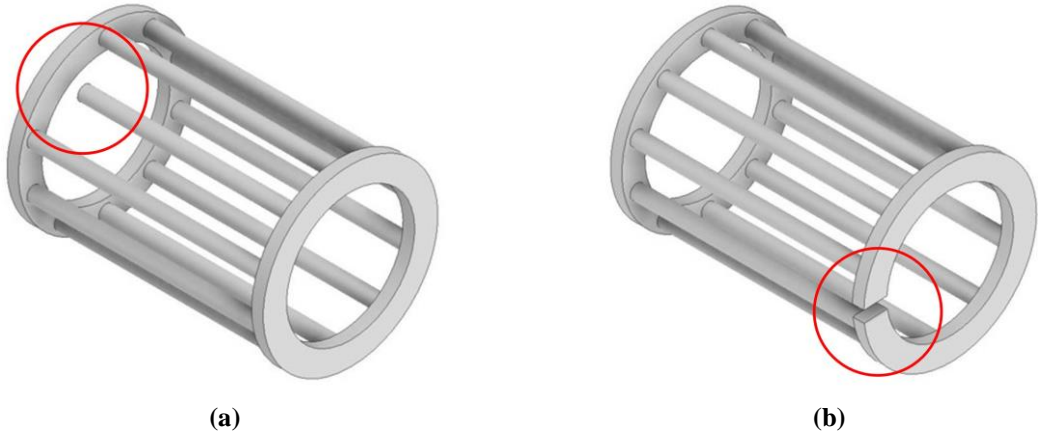
Figure 2. Illustration of broken rotor: **(a)** bar; **(b)** end ring.
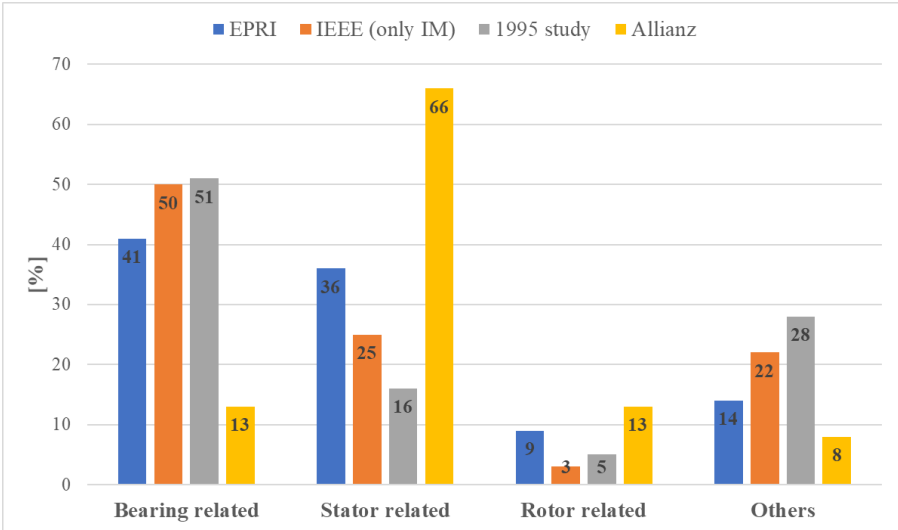
Figure 3. Squirrel cage induction motor fault distribution.

The 1995 study [17] covers SCIMs of 10 kW and above. The IEEE MRWG study covers asynchronous, synchronous, wound-rotor, and DC motors over 200 hp that are not older than 15 years [18], [19]. The Alliance study covers medium-voltage motors with high power [14].

The methods for detecting broken rotor bars are divided into model-based and signal-processing methods [7], [8].

The model-based methods are further divided into:

- methods based on resistance estimation (they use the deviation of the estimated rotor resistance from the known value as a fault indicator)
- methods based on estimation of other parameters (estimation of stator current, rotor flux, rotor speed, etc.)

3

- methods based on a digital twin (they automatically measure and estimate motor parameters and variables based on online data)

The methods based on signal processing are divided into:
- the time domain (decomposition products of currents and voltages, differential measurement of the air-gap magnetic field [20], etc.)
- the frequency domain (fast Fourier transform)
- time–frequency domain (short-time Fourier transform, Chriplet transform, Wigner–Ville distribution, Hilbert–Huang transform, continuous wavelet transform, discrete wavelet transform, etc.)

Magnetic flux fault detection is based on the direct or indirect measurement of the magnetic flux or magnetic flux density. Depending on the location of the measurement, there is an external or internal detection method. Internal magnetic flux or air gap flux detection is based on the measurement of the magnetic flux or magnetic flux density in the air gap of the electrical machine. Although air-gap flux detection was developed in the 1970s to detect faults in the stator winding of synchronous generators, it is still an active field of research [21]. This type of fault detection is considered invasive as it requires access to the air gap or stator slots. This means that the work process must be stopped, the electrical machine dismantled, and the sensor carefully positioned. Proper installation of air gap sensors can be carried out during an overhaul or manufacturing process.

The external magnetic flux or stray flux is the magnetic flux that radiates into the environment of the electrical machine. Although the magnitude of the stray flux is much weaker than the air-gap flux, this physical quantity reflects the anomalies (asymmetries) of the total magnetic field in the electrical machine [22]. The oldest paper on monitoring stray flux available on the Web of Science dates back to 1971 [23]. In the paper, the authors investigated an unbalanced supply. The aim was to detect certain frequency components in the spectrum of the coil voltage and use this information to activate the protective device that disconnects the motor from the mains in the event of an unbalanced supply. The air-core coil was placed on the non-drive side of the motor.

The modern ship is a complex industrial environment built and maintained according to the classification rules of various classification societies (Det Norske Veritas, Lloyd's Register, Bureau Veritas, etc.). The topic of the dissertation relates to ship industry through the category of ship maintenance. Maintenance includes all technical, administrative, and managerial

activities during the life cycle of an object to maintain or restore it to a condition in which it can perform its required function. Maintenance has an impact on safety, the environment, product quality, and overall profit [24]. Maintenance can be divided into four categories: corrective, preventive, predictive, and proactive. The philosophy of corrective maintenance is to take corrective actions after equipment failure. This strategy may be acceptable if the failure does not cause serious problems. Preventive maintenance is time-based maintenance, meaning that maintenance actions are scheduled at specific time intervals. The philosophy is to repair or replace damaged equipment before failure occurs [25]. Predictive maintenance is divided into two categories: condition-based maintenance (CBM) and reliability centred maintenance (RCM). There are many similar definitions for CBM [26]. This document paraphrases a description from Bureau Veritas that uses the term condition monitoring system: Condition Monitoring Systems (CMS) are computer-based systems that use complex algorithms, machine learning, and knowledge of asset defect data to make diagnoses and predictions. A CMS generally consists of the following main functions: data acquisition, data processing, diagnostic assessment, prognostic assessment, and health management [27]. RCM is a strategy that integrates a mix of corrective, preventive, predictive, and proactive maintenance strategies to ensure adequate reliability levels in a cost-effective manner [28]. Proactive maintenance includes CMB, RCM with the addition of risk-based maintenance (RBM) [29]. RBM is designed to investigate all failure modes, determine the risk associated with these failure modes, and develop a maintenance strategy that minimises the occurrence of the high-risk failure modes [30].

According to [31], the maintenance requirements for SCIMs are as follows: high insulation resistance and low contact resistance, proper lubrication of bearings, ensuring that both the inside and the outside are always clean and dry. Maintenance mainly concerns the stator winding and bearings, as shown in Figure 3. Rotor maintenance requires only visual inspection, i.e., signs of damage and overheating in the cage winding and laminations. The manual is mainly focused on the maintenance of the stator winding (insulation resistance) and bearings (lubrication).

The motivation for extracting information about the motor state, i.e., broken rotor bar (BRB), with random positioning of the sensor is based on the review articles [8], [32], [33] and [34], the literature review presented in the next section of this paper, and the assumption that the human factor plays a role in the monitoring process. From the review articles and the literature review, it can be observed that the research papers study BRB faults with a stationary

position of the sensor, i.e., the sensor is placed at a fixed position. There can be more sensors but all of them have fixed positions. The question that can be asked, can reliably information of BRB fault be obtained if the measurement is performed with random positioning of the sensor over the motor surface? The context of this question can fall into a category of routine maintenance, where operator would be free to choose the position of the sensor on every motor health inspection.

Two objectives of this research are to validate the measurement method and to investigate BRB detection in a steady state using the magnetic stray flux method with random positioning of the sensor over the surface of the motor. The validation of the measurement method requires that the information about the state of the motor (healthy or BRB) is time-independent, i.e., if the measurement is performed with random positioning at different times for a given motor, then all measurements must not show a difference if the motor has not changed its state. If the motor changes its state from healthy to BRB at a certain point in time, the measurements before and after must show a difference. Difference in measurement implies difference in data which must numerically show the difference between healthy and BRB state or must not numerically show difference in the case of measurement validation.

In this dissertation three approaches are taken for BRB detection. First approach to measurement validation and BRB detection is statistical analysis conducted on raw data. Appropriate statistical tests based on the distribution of measurement data are used for the validation and detection of BRB. Second approach is based on time-domain feature analysis and third approach is the application of Fast Fourier Transformation (FFT). A simplified diagram of BRB detection is shown in Figure 4.

The investigations carried out in this dissertation took place under laboratory conditions.
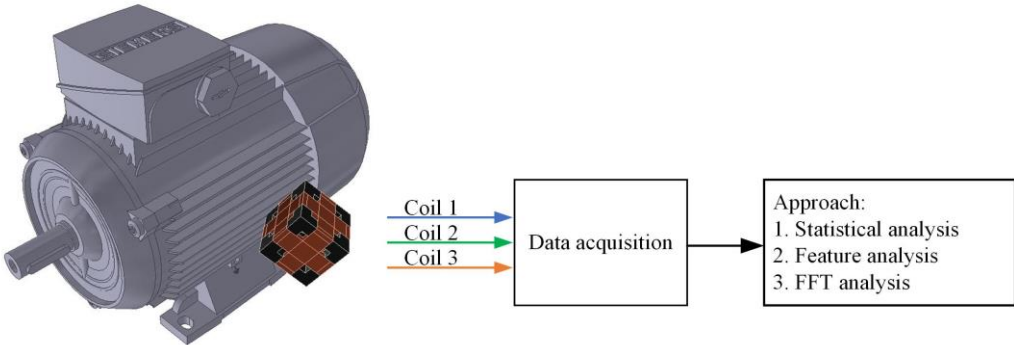
Figure 4. Simplified diagram of BRB detection;
IM 3D model source: *https://mall.industry.siemens.com/mall/en/mx/Catalog/Product/1LE10030DB222AA4*

The dissertation is divided into six chapters. After the introduction, Chapter 2 presents the literature that is relevant to the research of this dissertation. Chapter 3 describes the

dissertation's primary goal and research plan, which addresses the idea of developing portable triaxial air core sensor along with data logging system that can detect broken roto bar with random position approach. Chapter 4 describes the components used to develop a triaxial air coil sensor. Furthermore, test objects, experimental setup and methodology is also described in Chapter 4. Obtained results are presented in Chapter 5 and finally conclusion is given in Chapter 6.

2. THEORETICAL BACKGROUND

In this section theoretical background of stray magnetic flux and its link to broken rotor bar detection is given. The theoretical background is based on the theory presented in following references: [35], [36], [32], [37], [38] and [39].

IM is a rotating electrical machine. Its basic parts are stator and rotor. Cross section of the IM is shown in Figure 5.
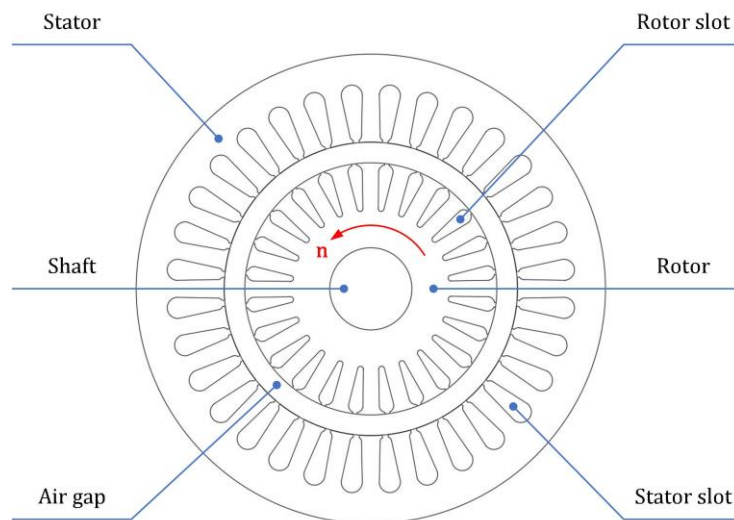
Figure 5. Cross section of the induction motor - basic parts.

Stator windings are connected to three phase power supply with frequency f_s (when there is no need for speed regulations the supply frequencies are grid frequencies, 50 or 60 Hz). Stator windings generate rotating magnetic field that induces electromotive force in rotor conductors. Induced electromotive force drives the current through rotor conductors. Due to presence of rotor currents in rotor conductors and the fact that these conductors are located in the rotating stator magnetic field, the electrodynamical force ($F = BIl$) is generated on conductors which results with the rotation of the rotor. For IM to work there must always be difference in stator rotating magnetic field and the speed of the rotor. The normalized difference in speed is called slip:

$$s = \frac{n_s - n}{n_s} \qquad (1)$$

where n_s is synchronous speed, i.e., rotating speed of stator magnetic field and n is rotational speed of the rotor (mechanical speed).

Theoretical background is based on a simplified magnetic circuit of the induction motor [35]. Figure 6 shows illustrative diagram of one quarter of the induction motor cross section.
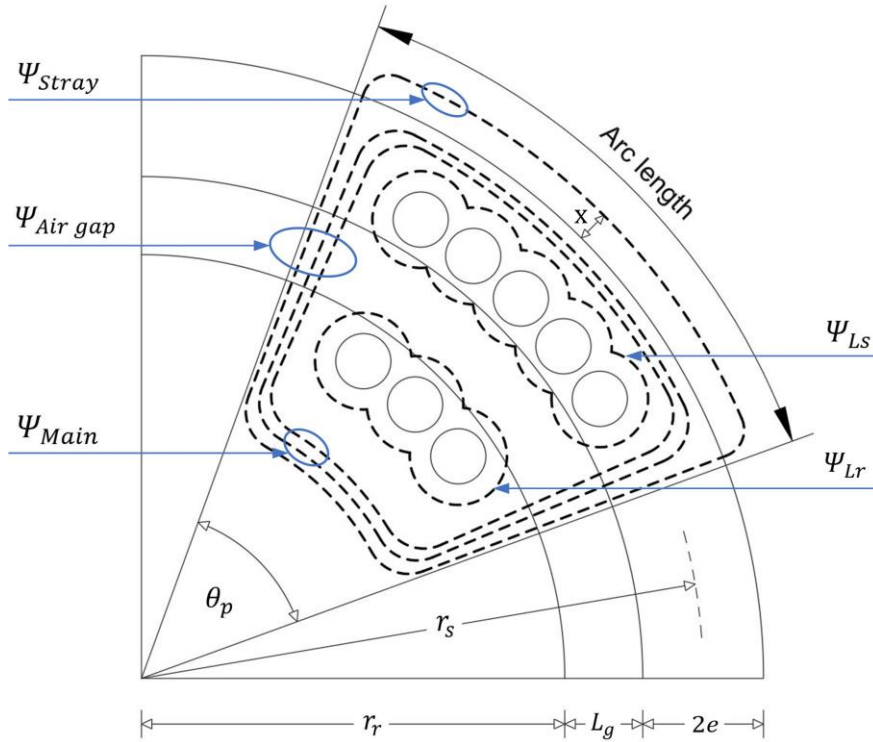
Figure 6. Illustration of one quarter of IM cross section with geometrical quantities and magnetic flux lines; Source: Koroglu, S., Adam, A.A., Umurkan, N. et al. Leakage magnetic flux density in the vicinity of induction motor during operation. Electr Eng 91, 15–21 (2009). https://doi.org/10.1007/s00202-009-0111-4.

Figure 6 shows geometrical parameters of the induction motor construction: r_r – radius of the rotor, r_s – radius of the stator slots, L_g – air gap length, $2e$ – thickens of the stator yoke, θ_p – pole angle in $[rad]$ and x – distance from rotor surface. It also shows magnetic flux lines (highlighted dashed lines) and corresponding magnetic flux components: Ψ_{Stray} – stray flux, $\Psi_{Air\ gap}$ – air gap flux, Ψ_{Main} – main flux, Ψ_{Ls} – leakage stator flux and Ψ_{Lr} – leakage rotor flux.

Equivalent magnetic circuit of the geometry presented on Figure 6 is shown in Figure 7.
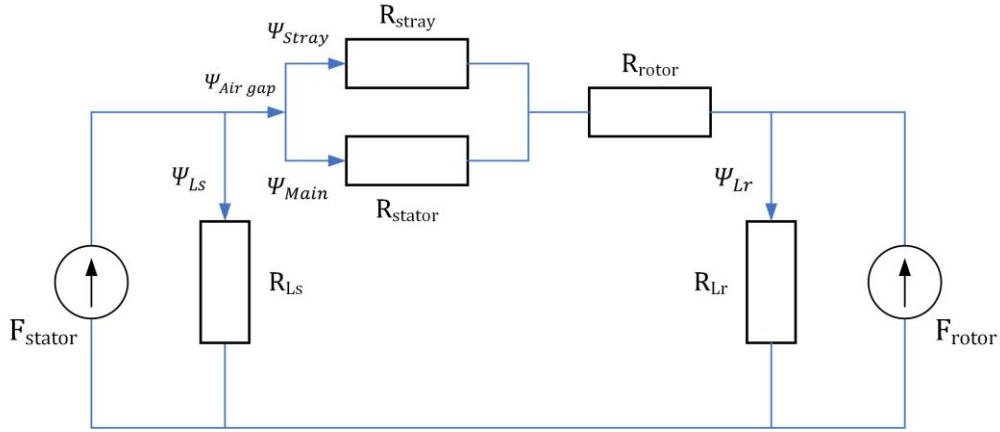
Figure 7. Equivalent magnetic circuit of the simplified cross section of IM.
Source: Koroglu, S., Adam, A.A., Umurkan, N. et al. Leakage magnetic flux density in the vicinity of induction motor during operation. Electr Eng 91, 15–21 (2009). https://doi.org/10.1007/s00202-009-0111-4.

On Figure 7 elements displayed with resistor symbols represent reluctances of the simplified IM geometry and two elements displayed with current source symbols represent stator and rotor magnetomotive forces (MMF). From Figure 7 it can be seen that air gap flux is the sum of the main flux and stray flux. From equivalent magnetic circuit relation of the air gap flux and stray flux can be derived [35]:

$$\Psi_{Stray} = \frac{R_{Stator}}{R_{Stator} + R_{Stray}} \Psi_{Air\ gap} \tag{2}$$

With geometry quantities displayed on Figure 6 reluctances can be expressed:

$$R_{Stator} = \frac{l_{Stator}}{\mu_0 \mu_{Stator} A_{Stator}} = \frac{2e + r_s \theta_p}{\mu_0 \mu_{Stator} r_s \theta_p L_{stack}} \tag{3}$$

$$R_{Stray} = \frac{l_{Stray}}{\mu_0 A_{Stray}} = \frac{2x + (r_s + e + x)\theta_p}{\mu_0 (r_s + e + x)\theta_p L_{stack}} \tag{4}$$

where l is flux path length, A is cross section area at the mean radius of the corresponding section, μ_0 is permeability of the vacuum, μ is relative permeability and L_{stack} is length of active part of induction motor.

Inserting equations (2) and (3) in equation (1) and expressing magnetic flux through magnetic flux density and corresponding surfaces the following expression is obtained [35]:

$$B_{Stray} = \frac{1}{1 + \frac{2x + (r_s + e + x)\theta_p}{r_s + e + x} \frac{\mu_{Stator} r_s}{2e + r_s \theta_p}} \left(\frac{r_s - s}{r_s + e + x} \right) B_{Air\ gap} \tag{5}$$

From equation it is observable that stray magnetic flux density depends on the geometrical and material properties of induction machine, it decreases its vales with increase of x, i.e., increase of distance from stator surface and it is proportional to the magnetic flux density of the air gap.

Because magnetic flux density in the air gap is the superposition of magnetic flux density generated by stator and magnetic flux density generated by rotor for further analysis equation can be written:

$$B_{Stray} = f(x)B_{Air\ gap} = f(x)(B_{Stator} + B_{Rotor}) \tag{6}$$

With absence of current in a broken rotor bar, magnetic flux density generated by rotor will be affected and thus according to equation (5) this change will be reflected in stray magnetic flux. Rotor magnetic flux density can further be expressed:

$$B_{Rotor} = \frac{\mu_0}{g} F_r(\alpha) \tag{7}$$

where g is air gap length and in this analysis, it is considered constant, $F_r(\alpha)$ is rotor MMF.

Rotor MMF can be expressed through current sheet function and spatial current distribution function [39]:

$$F_r(\alpha) = \int J_r(\alpha)D_r(\alpha)\,d\alpha \tag{8}$$

where J_r is current sheet function and D_r is the spatial distribution of the rotor current in the slots.

In this analysis function J_r is assumed to be sinusoidal:

$$J_r(\alpha) = J_R sin(2\pi f_s t - p\alpha - \alpha_r) \tag{9}$$

where J_R is amplitude of current sheet, f_s is frequency of power supply, p is number of pole pairs and α_r is phase angle for rotor current sheet.

For a healthy motor function D_r equals one for whole domain: $D_r(\alpha) = 1$. For the case of one broken rotor bar Figure 8 shows the graph of the function $D_r(\alpha)$.
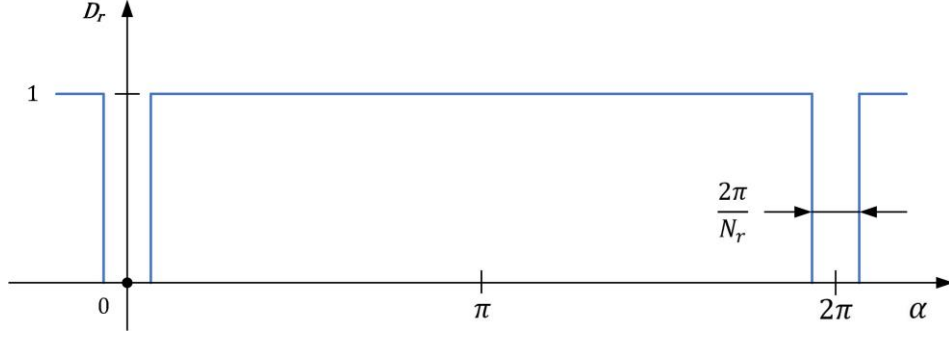
Figure 8. Spatial distribution of the rotor current due to broken rotor bar.
Source: S. B. Lee, J. Shin, Y. Park, H. Kim and J. Kim, "Reliable Flux-Based Detection of Induction Motor Rotor Faults from the Fifth Rotor Rotational Frequency Sideband," in *IEEE Transactions on Industrial Electronics*, vol. 68, no. 9, pp. 7874-7883, Sept. 2021, doi: 10.1109/TIE.2020.3016241.

On the graph displayed on the Figure 8 N_r is the number of rotor slots. The absence of current due to bar breakage is modelled as $D_r(\alpha) = 0$; $\alpha \in \langle 2\pi k - \frac{\pi}{N_r}, 2\pi k + \frac{\pi}{N_r}\rangle$. Fourier series of the function displayed on Figure 8, [39]:

$$D_r = 1 - \frac{1}{N_r} + \sum_{k=1}^{\infty} \frac{2}{k\pi} sin\left(\frac{k\pi}{N_r}\right) sin(2k\pi f_r t - \alpha) \tag{10}$$

where $f_r = n/60$ is rotor rotational frequency.

After inserting equation (8) and equation (9) in equation (7) and performing integration, equation for rotor magnetic flux density is obtained [39]:

$$
\begin{aligned}
B_{Rotor} = \frac{\mu_0}{g}\Bigg\{ & \frac{J_R}{p}\left(1 - \frac{1}{N_r}\right) cos(2\pi f_s t - \alpha_r) + \\
& + \frac{J_R}{p+1}\sum_{k=1}^{\infty} \frac{1}{k\pi} sin\left(\frac{k\pi}{N_r}\right) sin(2\pi(f_s + kf_r)t - \alpha_r) \\
& - \frac{J_R}{p-1}\sum_{k=1}^{\infty} \frac{1}{k\pi} sin\left(\frac{k\pi}{N_r}\right) sin(2\pi(f_s - kf_r)t - \alpha_r)\Bigg\}
\end{aligned}
\tag{11}
$$

According to equation (10) frequencies that appear in rotor magnetic flux density due to one broken rotor bar are:

$$f_{BRB} = f_s \pm kf_r \tag{12}$$

Frequencies given by equation (11) also appear in stray magnetic flux density. In this thesis the sensor for BRB detection is triaxial air coil, i.e., three air coils perpendicular to each other. Each coil encompasses stray magnetic flux that induces electromotive force:

$$e = -\frac{d\Psi_{Stray}}{dt} = -NA_{coil}\frac{dB_{Stray}}{dt} = -f(x)NA_{coil}\left(\frac{dB_{Stator}}{dt} + \frac{dB_{Rotor}}{dt}\right) \qquad (13)$$

where N is number of turns and A_{coil} is surface that is encompassed by the coil.

According to equation (12) frequencies that appear in rotor magnetic flux density will also appear in air coil induced electromotive force.

If induction motor is considered healthy and perfectly manufactured, meaning there is no ecentricty of the rotor, then rotor currents form balanced/symmetrical m phase system. When BRB fault occurs system is no longer symmetrical but according to theory of symmetrical components, newly form system can be mathematically decomposed to two symmetrical systems, direct and inverse system [40]. As the magnetic rotor magnetic field is generated by the rotor currents, same applies to rotor magnetic field. Hence, rotor magnetic field for BRB fault will be decomposed to direct field, one that is rotating in the direction of stator magnetic field and inverse field which is rotating in opposite direction that stator magnetic field. The speed of the direct and inverse system:

$$direct\ system\ \rightarrow\ sf_s$$

$$inverse\ system\ \rightarrow\ -sf_s$$

Direct system or direct magnetic field rotates, relative to stator reference frame, with speed:
$$f_r + sf_s = f_s(1 - s) + sf_s = f_s \qquad (14)$$
Inverse system or inverse magnetic field rotates, relative to stator reference frame, with speed:
$$f_r - sf_s = f_s(1 - s) - sf_s = f_s - 2sf_s = (1 - 2s)f_s \qquad (15)$$

This frequency is induced in stator current by the inverse rotor magnetic field and thus is reflected in the stator magnetic field and furthermore into stray magnetic field.

Induced currents in stator conductors with frequency $(1 - 2s)f_s$ produce magnetic field that interacts with fundamental magnetic field and as a consequence oscillatory torque on rotor is produced with frequency $2sf$. Oscillatory torque gives rise to rotor speed ripples of the same frequency. Furthermore, speed ripples produce angular variations of the rotor which reflects on the phase modulation in the stator flux [36]:

$$\Psi_{M\_S}cos\left\{(\omega_s t - \alpha_s) - \frac{p\Delta T}{J4s^2\omega_s^2}sin\left(2s\omega_s t - (\alpha_s - \alpha_{1-2s})\right)\right\} \qquad (16)$$

where Ψ_{M_S} is amplitude of stator magnetic flux, ω_s is angular frequency ($\omega_s = 2\pi f_s$), p is the number of pole pairs, J is combined rotor-load inertia, ΔT is the amplitude of the torque oscillation, s is the slip, α_s is stator magnetic flux phase angle and α_{1-2s} is phase angle of the induced stator current $i = I\cos((1 - 2s)\omega_s t - \alpha_{1-2s})$.

After applying trigonometric identities and Taylor series expansion and taking only the first term, the expression is obtained:

$$\begin{aligned}\Psi_{M_s}\cos(\omega_s t - \alpha_s) \\ + \frac{\Psi_{M\_S}}{2}\frac{p\Delta T}{J4s^2\omega_s^2}\{\cos((1-2s)\omega_s t - \alpha_{1-2s}) - \cos((1+2s)\omega_s t \\ - (2\alpha_s - \alpha_{1-2s})\}\end{aligned} \tag{17}$$

The frequency that is also present in stator magnetic flux due to BRB fault is $(1 + 2s)f_s$.

The rotating magnetic field created by stator current of frequency $(1 + 2s)f_s$ induce in rotor conductors current of following frequency:

$$f_s(1 - s) + X = (1 + 2s)f_s$$
$$X = f_{BRB} = 3sf_s \tag{18}$$

This frequency is reflected in rotor magnetic flux and consequently in stray magnetic flux. This frequency will also induce new currents in stator conductors which will as a consequence have new induced current in rotor. The diagram that illustrates the process of frequency component appearance is shown in Figure 9.
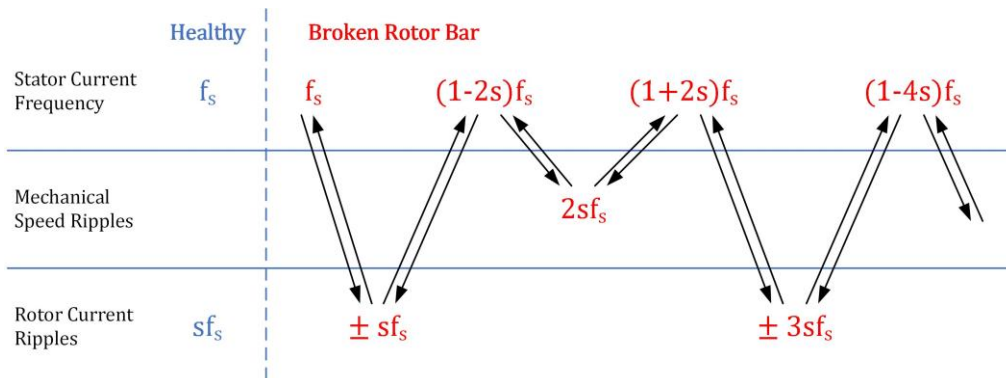

Figure 9. Frequency chain – frequency appearance in stator and rotor magnetic field due to broken rotor bar. Source: Mazaheri-Tehrani, E. , Faiz, J. : Airgap and stray magnetic flux monitoring techniques for fault diagnosis of electrical machines: an overview. IET Electr. Power Appl. 16(3), 277–299 (2022). https://doi.org/10.1049/elp2.12157

3. LITERATURE REVIEW

In this section, a brief description of papers related to SCIM broken bar detection using stray magnetic flux is given. A common feature of all stated papers is the fixed positions of the sensor. The fixed position of the sensor refers to a situation where the sensor is once positioned for measuring, and it is not translated or rotated to a new position for a new measurement during the overall measurement process. The information about the motor state (healthy/BRB) is extracted and processed from the same position of the sensor. There are three standard positions of the sensor: axial, radial, and radial–axial. These three positions are a common feature of all the following articles. Figure 10 shows the standard positions of the sensors and serves as a reference for all articles in this section.
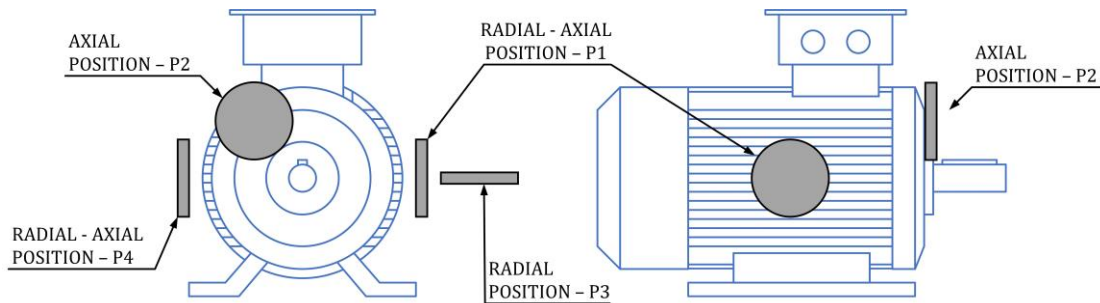
Figure 10. Different fixed sensor positions.

The articles presented in this section emphasize the fixed sensor position and serve as a reference point regarding used methods in this field of research. Together with review articles [8], [32], [33] and [34], they provide insight that random sensor positioning during the measurement process and its potential for motor state information extraction have not been investigated.

In [41], the authors used a laboratory-made air-core coil as a sensor. The analyzed signal was the EMF of the air coil, and the faults were analyzed when the motor was started. Tests were also performed on two induction motors and for three positions of the sensor: radial, axial, and radial–axial. The short-time Fourier Transform (STFT) was applied to transient EMF signals to show the evolution of the fault harmonics. A rotor fault indicator based on the discrete wavelet transform (DWT) was introduced. The authors conclude that misalignment and BRB can be detected with the STFT of the air coil signal. The current analysis shows that the BRB fault can mask the misalignment on the time-frequency map; the rotor fault indicator shows a significant difference compared to the healthy motor; different sensor positions give different rotor fault indicator values, and the largest difference to the healthy condition is reported for the axial position.

In [42], the detection of two adjacent broken bars, two broken bars within half a pole pitch, and two broken bars with one pole pitch is investigated. The sensor used was an air-core coil. The signal was analysed by first performing an STFT with the motor in a steady state and extracting the four frequency trajectories. After the trajectories were extracted, the Fast Fourier Transform (FFT) was applied. The fault detection is based on the observation of the missing frequency component in the frequency spectrum of the healthy motor compared to the fault scenarios. The presented method detects broken bars, adjacent and non-adjacent, with half pole pitch and with one pole pitch. This method can be used as a complement to Motor Current Signal Analysis (MCSA), as the latter provides a false negative misdiagnosis for broken bars with half pole pitch and with one pole pitch.

In [43], authors investigate the of zero-sequence flux method for detection of broken rotor bar using stray flux. For this method three air coils are used. The coils are positioned around the stator and separated by 120 degrees electrical. The sum of the coil signals is analysed and compared to stator current, stray flux and zero-sequance current method. The comparison is made by harmonic signature in frequency spectrum. The amplitude of the signature harmonic is compared for healthy and BRB state. Zero-sequence flux method gives the highest difference in amplitude.

In [44], the authors propose an algorithm based on a sorted spectrum subtraction of healthy and faulty (different spatial combinations of two BRBs) motor states. The algorithm was tested for the following combinations of broken bars: 1-2 (adjacent), 1-3, 1-4, 1-5, and 1-6. To quantify the distinction between healthy and faulty states, a fault indicator based on autocovariance was introduced. For comparison, the authors calculated the ratios of the indicators by dividing each indicator for a faulty condition by the indicator for a healthy motor. The calculation was performed for axial and radial–axial coil position and the results show quantitative differences and different sensitivity depending on the position of the sensor. It is reported that the radial–axial position is more sensitive than the axial position.

In [45], the detection of a broken bar is investigated using two indicators. The first is based on the frequency domain and is calculated as the sum of the average of the absolute values of the bispectrum; the second indicator is based on the time domain and is calculated as the squared value of the median of the autocorrelation function. The tests were carried out during start-up and in a steady state. An air-core coil was used as the sensor. The measurements with the coil were carried out in four positions: radial, axial, and radial–axial (P1 and P4). When analyzing the frequency and time indicators for the steady state, it is noticeable that all faulty values are

lower than in the healthy state, with the exception of sensor position P4 in both cases. The faulty value of the frequency indicator for the start-up regime has a higher value than the value for the healthy state. The values of the time indicator for the start-up process show that all faulty values are lower than the values in the healthy state, with the exception of position P2.

In [46], the authors investigate the two-stage time-frequency analysis for detecting broken bars in a steady state. The authors use STFT with Kaiser–Bessel window function. The expression for the minimum window length is derived in the paper. The two-stage analysis was used to study the 5th and 7th harmonics and their sidebands. The conclusion of the paper is that broken rotor bars can be detected with the SFTF at a steady state and with the minimum window length derived in the paper.

In [47], the authors investigated the influence of the axial air channels of the rotor on the detection of broken rotor bars. The motivation for this research was the misdiagnosis of the MCSA method. If the number of axial channels is equal to the number of poles, the MCSA can generate a false positive or false negative alarm. The motor was tested with 0, 1, and 2 (adjacent) broken bars. The sensor used was an air-core coil placed in a radial position. The stator current and the radial flux (EMF of the coil) were measured for comparison. FFT was used for signal analysis, and the spectral component (1-2s)f was analyzed. The work showed that the detection of rotor fracture is independent of the presence of an axial channel when magnetic stray flux analysis is applied.

In [48], the authors propose a method for automatic detection of a BRB based on a multiple signal classification algorithm (MUSIC) and an artificial neural network (ANN). An air coil was used as the sensor for the measurement of magnetic stray flux. The success rate achieved with the proposed algorithm in detecting BRB faults show the potential for autonomous fault detection based on stray magnetic flux.

In [49], the authors proposed a method for the automatic detection of broken rotor bars, misalignment, and combinations: BRB + misalignment. The proposed method is based on STFT, statistical parameters, feature extraction, linear discriminant analysis (LDA), dimensionality reduction, and feed-forward neural network (FFNN). The sensor used was a triaxial stray flux sensor. The triaxial sensor consists of three Hall sensors whose axes are perpendicular to each other, and which are all installed on one circuit board. They are arranged so that one sensor detects the axial flux, the second the radial flux, and the third the radial–axial flux. The proposed algorithm can automatically detect the healthy state, misalignment, and

Misal. + 1 BRB and Misal. + 2 BRB. For all states, the authors report that the effectiveness is more than 95%.

In [50], the authors investigated the detection of a BRB by monitoring the rotor rotational frequency and the supply frequency sidebands. The authors investigated one BRB, two BRBs (adjacent), and two non-adjacent BRBs separated by 90° (electrically). The faults were investigated using three methods: MCSA, the internal magnetic flux (air gap), and stray magnetic flux. For the stray magnetic flux method, an air-core coil in the radial–axial position was used. The magnetic stray flux in the steady state and the $fs - fr$ frequency component, where fs is supply and fr is the rotor rotational frequency, can be used to identify all faulty conditions. The FFT and STFT analysis of the $fs - fr$ frequency component showed that the internal magnetic flux can detect all faulty states. The authors also showed in experiments that the $fs - fr$ frequency component of the internal and external magnetic flux does not respond to an unbalanced load.

In [51], the authors investigated the effects of a BRB on the mechanical frequencies. An air coil with a square cross-section mounted on the fan cover of the motor in a radial–axial position (P1) is used as a sensor. The motor current was measured for comparison. The measurements were carried out at the rated load of the motor. The analysis of the mechanical frequencies in the steady state to detect rotor faults shows diagnostic potential.

In [39], the authors proposed the fifth harmonic of the rotor rotational frequency as an indicator of rotor faults in induction motors: $fs + 5fr$. The fifth harmonic was chosen because it does not contain sidebands that cause false indications and has a low sensitivity. Stray flux analysis of the $fs + 5fr$ component shows that all faulty states (one BRB and two BRB—adjacent and non-adjacent) are detectable compared to the spectrum of the healthy state and the defined threshold: −66.4 dB. The proposed indicator is immune to the presence of an axial air channel. The indicator is not affected by an unbalanced load and misalignment.

A diagnostic study conducted under real conditions is described in [52]. The diagnosis took place in a pumping station. There was no prior knowledge of the parameters of the mechanical system. The diagnosis was performed with MCSA, stray flux, and vibration analysis with the motors in a steady state. The flux was monitored with two air coils in the radial–axial position (P1). The work shows that the stray flux is not sensitive to mechanical faults originating from the load. A second method was required to localize the fault (the pump system studied is a complex electromechanical system—vertically mounted SCIM, impeller,

15 m shaft, and 6 bearings). In this example, one method alone cannot provide complete screening (fault detection and fault localization).

In [53], fault detection with stray flux in motors with soft starting is investigated. Four soft starters were used. The signals of the air coils were determined for the radial, axial, and radial–axial positions in the steady state and start-up condition. The steady-state signals were analyzed with FFT, and the start-up signals with STFT. The variables in the tests were the time setting and the initial torque/current setting. The faults investigated were as follows: one BRB without load and with load and two BRBs (adjacent) without load and with load. The authors proposed the following fault indicator: the highest value of the sf component from the STFT analysis. Broken rotor bars can be detected when the motor is operated with a soft starter. The transient stray flux, together with the steady-state stray flux, provides reliable information about the rotor fault.

In [54], an automatic diagnostic system based on stray flux and current data is investigated. The diagnostic system consists of the following steps: (1) stray flux and stator current data at start-up, (2) STFT application, (3) division of the STFT map into regions and calculation of a proposed indicator for each region, (4) classification of the condition (healthy, one BRB, two BRB, misalignment) by FFNN, and (5) final diagnosis for the end user via a user interface. The sensor used for stray flux was a triaxial sensor consisting of three Hall sensors on a board arranged perpendicular to each other. The results show 100% effectiveness in detecting two BRBs, 100% effectiveness in detecting one BRB, 95% effectiveness in detecting misalignment, and 100% effectiveness in detecting a healthy motor.

In [55], the possibility of monitoring the tool condition in a CNC machine is investigated. The monitored object was a cutting tool. The idea was to monitor the wear of the cutting tool indirectly by monitoring the stray flux of the spindle motor. The proposed method for tool wear estimation consists of the following steps: (1) Data acquisition from triaxial sensors (3 perpendicular Hall sensors on a board) (2) DWT analysis of each obtained signal (3) Calculation of indicator γDWT (4) Classification of cutting tool wear based on indicator γDWT and depth of cut using FFNN. The proposed method is effective for the automatic classification of tool wear conditions.

In [56], the automatic detection of BRB faults in SCIM with soft start is investigated. The detection is tested with four different soft starters. The detection is based on current and stray flux signals. The proposed method for automatic detection consists of the following steps: (1)

acquiring current and stray flux signals, (2) applying STFT, (3) dividing the STFT map into a grid of m rows by n columns and calculating the proposed indicator for each region of the map, (4) feature reduction by applying LDA, (5) automatic classification based on FFNN. With the proposed method, automatic detection of BRB faults during soft start is possible. An overall efficiency of 94.4% is achieved.

In [57], the automatic detection of BRB faults in SCIM with soft start is investigated. The detection is tested with four different soft starters. The detection is based on stray flux signals obtained from the air coil in the radial–axial position (P1). The proposed method for automatic detection consists of the following steps: (1) acquisition of the transient stray flux signal, (2) addition of white Gaussian noise to the signal, (3) application of the persistence spectrum method, (4) adaptation of the images, (5) application of the convolutional neural network. An accuracy rate of 99.89% was achieved.

In [58], the author proposed a method for detecting multiple faults in IM under periodic low-frequency fluctuating loads. In the study, the following conditions are investigated individually: healthy, partially broken bar, one broken bar, eccentricity due to unbalance, and eccentricity due to misalignment. The proposed method consists of the following steps: (1) data acquisition, (2) feature extraction (time domain), (3) application of Self-Organizing Maps, (4) feature reduction by linear discriminant analysis, (5) application of a neural network classifier. A triaxial sensor was used for data acquisition. The sensor itself is fixed to the frame and consists of Hall-effect transducers that measure axial, radial, and axial–radial flux. The authors report global classification rates of approximately 99.5% and 99% during training and testing, respectively.

Table 1 summarizes the articles from this section.

Table 1. Summary of literature review.

Reference	Sensor Position (Ref. to Figure 10)	Sensor—Type and Dimensions	Fault Detection Method	Analysed Fault	Tested SCIM Rated Power/ Facility/Motor Supply
[36]	P1, P2, P3	Circular coil; N = 1000; Inner φ = 3.9 cm; Outer φ = 8 cm; Height 1 cm	STFT DWT	Misalignment Misal. + 1 BRB Misal. + 2 BRB (adjacent)	M1: 1.1 kW M2: 0.75 kW Lab. Start-up Line supply
[37]	P1	Circular coil; N =1000 Inner φ = 3.9 cm Outer φ = 8 cm Height 1 cm	STFT FFT	2 BRB (adjacent, half pole pitch and one pole pitch)	M: 1.1 kW Lab. Steady state Line supply
[38]	P1,P1,P1 separated by 120 degrees electrical	Square-body; N =1500 Inner body dim. 40x40 mm2 Outer body dim. 55x55 mm2 Height 0.8 cm	FFT	1 BRB	M: 4 kW Lab. Steady state Line supply
[39]	P1, P2	Circular coil; N =1000 Inner φ = 3.9 cm Outer φ = 8 cm Height 1 cm	FFT Spectral subtraction Autocorrelation	2 BRB (5 combinations)	M: 1.1 kW Lab. Steady state Line supply

[40]	P1, P2, P3, P4	Circular coil; N =1000 Inner φ = 3.9 cm Outer φ = 8 cm Height 1 cm	Bispectrum Autocorrelation	1 BRB	M: 1.1 kW Lab. Steady state And Start-up Line supply
[41]	P1	Circular coil Nc =1000 Inner φ = 3.9 cm Outer φ = 8 cm Height 1 cm	STFT	1 BRB 2 BRB (adjacent)	M: 1.1 kW Lab. Steady state Line supply
[42]	P1	Helmholtz coil Nc =320 Inner φ = 121 cm Outer φ = 155 cm	FFT	1 BRB 2 BRB	M1:5.5 kW Lab. Steady state Line supply M2,3: 280 kW, 6.6 kV, Field test Steady state; Line supply
[43]	P1, P2, P3	Circular coil Nc =1000 Inner φ = 3.9 cm Outer φ = 8 cm Height 1 cm	MUSIC FFNN	1 BRB 2 BRB	M1: 1.1 kW M2: 7.5 kW Lab. Start-up Line supply
[44]	P1, P2	Triaxial stray flux sensor Three hall sensors perpendicular axis to each other Allegro—A1325	STFT Statistical parameters LDA dimensionality reduction FFNN	Misalignment Misal. + 1 BRB Misal. + 2 BRB (adjacent)	M:0.74 kW Lab. Start-up Line supply
[45]	P1	Circular coil Nc = 320	FFT STFT	1 BRB 2 BRB (adjacent) 2 BRB (non-adjacent; 90° el. apart)	M: 7.5 hp Lab. Start-up and steady state Line supply
[46]	P1	Square body Nc = 1500 copper wire φ = 0.1 mm Inner square length 40 mm Outer square length 50 mm Height 4.5 mm	FFT	1 BRB	M:4 kW Lab. Steady state Line supply
[47]	P1	Circular coil Nc =300 (as stated in text)	FFT	1 BRB 2 BRB adjacent 2 BRB non-adjacent Load unbalance Misalignment Eccentricity	M1:7.5 kW M2: 5.5 kW M3: 2.0 kW M4: 5.5 kW Lab. Steady state Line supply
[48]	P1	Square body Nc = 3500 Inner square length 40 mm Outer square length 50 mm Height 4.5 mm	FFT	Misalignment Eccentricity Bearing fault	M1:750 kW M2: 750 kW M3: 240 kW M4: 240 kW Field testing Steady state Line supply
[49]	P1, P2, P3	Circular coil Nc =1000 Inner φ = 65 mm Outer φ = 80 mm Height 15 mm	FFT STFT	1 BRB 2 BRB (adjacent)	M: 1.1 kW Lab. Start-up and steady state 4 soft-starters
[50]	P1	Triaxial stray flux sensor Three perpendicular hall-effect sensors	STFT FFNN	1 BRB 2 BRB (adjacent) Misalignment	M1: 1 hp M2: 1.47 hp Lab. Start-up Line supply
[51]	P1	Triaxial stray flux sensor Three hall sensors mounted perpendicular on a PCB board	DWT FFNN	Cutting tool wear evaluation	M1: 3.7 kW Line supply
[52]	P1	The text description of the coil does not match the coil presented in the paper	STFT LDA FFNN	1 BRB 2 BRB (adjacent)	M: 1.1 kW Lab. Start-up and steady-state 4 soft-starters
[53]	P1	Circular coil Nc =1000 Inner φ = 6.5 cm Outer φ = 8 cm Height 1.5 cm	Persistence spectrum CNN	1 BRB 2 BRB (adjacent)	M: 1.1 kW Lab. Start-up and steady-state 4 soft-starters
[53]	P1	Triaxial stray flux sensor Three perpendicular hall-effect sensors	Self-Organizing Maps NN	1/2 BRB 1 BRB Unbalance Misalignment	M: 1.5 kW Lab. Fluctuating load VFD supply

4. THESIS SCIENTIFIC CONTRIBUTION AND RESEARCH PLAN

The development of a portable triaxial air coil for magnetic stray flux is expected to enable measurement of a broken rotor bar by placing sensors on random position across induction motor surface. Furthermore, the dissertation reasearch plan is:

- Research on the technical aspects of the triaxial air coil sensor

- Research on the development of a triaxial air coil sensor and definition of a test bench

- Use of a triaxial air coil for flexible stray flux measurement on a three-phase induction motor in steady state condition

- Analysis of the obtained data for stray flux detection

Therefore, based on a reasearch object the working hypotesis is:

A portable triaxial air core stray flux sensor can be developed to reliably detect broken rotor bars of a squirrel cage induction motor at steady state.

From the defined hypothesis, the main dissertation scientific contribution is:

- Reliable measurement and detection of a broken rotor bar based on stray flux measurement in three axes
- Flexible detection of broken rotor bar of a three-phase induction motor in a steady state

5. MATERIALS AND METHODS

This section describes the triaxial air coil, the test objects, the test setup and the research methodology. The geometry, materials and dimensions of the triaxial air-core coil are presented. The test objects and their technical parameters are presented. The simulation of a broken rotor bar and the experimental setup (position of the test objects in the laboratory, power supply and measuring equipment) are also presented. The methodology for three approaches, the statistical, the characteristic and the FFT analysis, is presented.

5.1. Triaxial air coil

The reason why triaxial air coil is chosen instead of single air coil sensor is that triaxial coil at the same time encompasses a portion of each stray flux component: radial, axial and radial-axial component. Another view is that for the same number of positions on the motor, with triaxial sensor 3 times more signals can be logged at the same time.

The triaxial air coil consists of three copper coils that are perpendicular to each other. Each coil was wound up by hand and has 500 turns. The nominal diameter of the single-coated enamelled wire was 0.2 mm. The body for the triaxial coils was designed in Autodesk Inventor Professional and 3D printed using UltiMaker S5. The material used for the body was PLA (infill density 100 %). Copper wire data is shown in Figure 11a and PLA filament data is shown in Figure 11b.

| (a) | (b) |

Figure 11. (a) Copper wire data; **(b)** PLA filament data.

Resistance and inductance of each coil were measured with HAMEG Milliohm-Meter HM 8014 and HAMEG LC-Meter 8018. The results are as follows: Coil 1: 43.3 Ω, 14.5 mH, Coil 2: 42.0 Ω, 13.3 mH, Coil 3: 44.1 Ω, 15.5 mH. The model with the dimensions of the body, cross-section of the model and the finished triaxial sensor is shown in Figure 12.
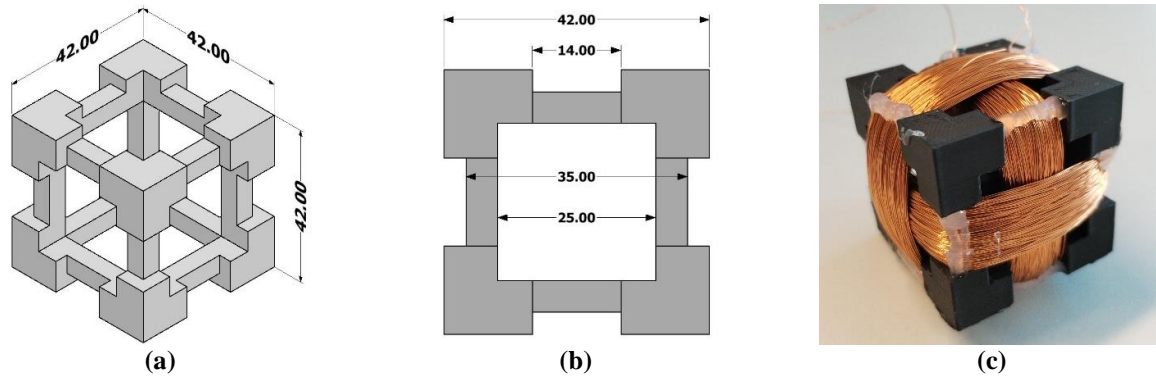
Figure 12. Triaxial sensor: **(a)** Technical drawing of the sensor body; **(b)** cross section of the sensor body; **(c)** photograph of the finished sensor.

5.2. Test objects – Induction motors

The test objects are four, three-phase, totally enclosed, fan-cooled (TEFC) SCIMs. Figure 13 shows the photograph of the test objects. They are divided into two groups, Siemens motors and Končar motors. Within each group the motors have the same characteristics. Technical characteristics of the motors are shown in Table 2.
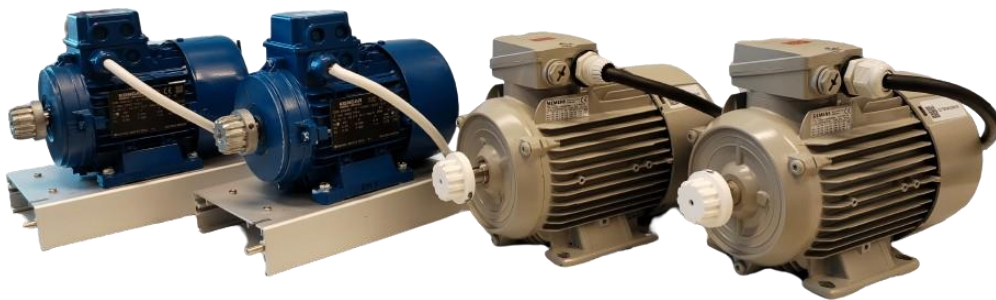
Figure 13. Test objects: two Končar motors and two Siemens motors.

Table 2. Technical characteristics of Siemens and Končar motors.

Manufacturer		Siemens	Končar
Type		1AV3082B	H5AZ 71B-2
Voltage (Y)	[V]	400	400
Frequency	[Hz]	50	50
Power	[kW]	0.55	0.55
Current	[A]	1.26	1.4
Power factor	[ ]	0.78	0.72
Speed	[rpm]	1440	2790
Efficiency class		IE3	IE3
Efficiency	[%]	80.8	77.8
Mounting position		B3	B3
Mass	[kg]	11	5.9

5.3. Experimental setup

Experimental setup consists of a triaxial sensor, a data logger, a laptop, a servo machine test system (control module and servo-motor), power supply module and test objects. Figure 14 shows the experimental setup.
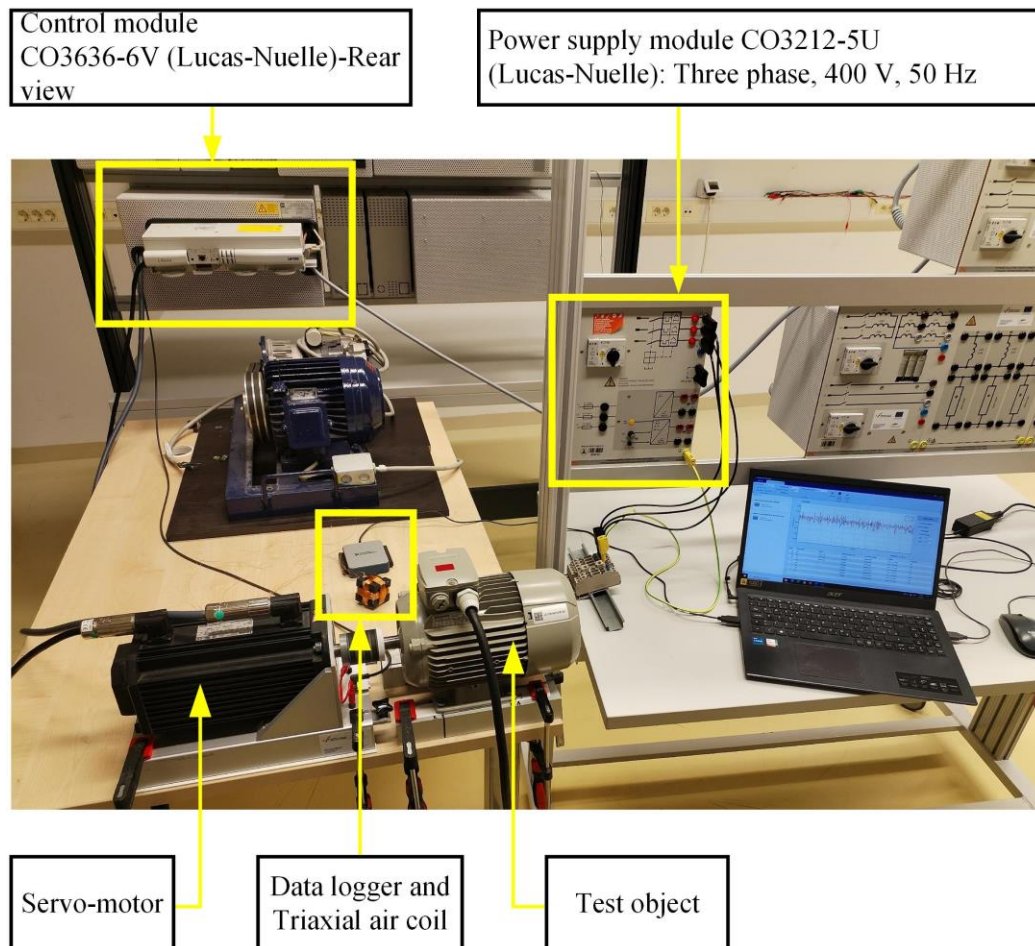
Figure 14. Experimental setup – power supply module, control module, servo motor, test object, laptop, data logger and triaxial sensor.

The data logger used was National Instruments, model USB-6003, and the laptop was Acer Aspire 5, model N20C5 - (11th Gen Intel(R) Core (TM) i5-1135G7 @ 2.40 GHz; 2.42 GHz. Data was recorded using the MATLAB (R2020b) Analog Input Recorder application. The duration of measurement was set to 20 s, and the sampling frequency to 5 kHz. Three channels were used: ai0, ai1, and ai2. After setting the duration, sampling frequency and selecting three channels, the application automatically resets the sampling frequency to 5000.3125 Hz and the number of samples per measurement to 100006.

The servo machine test system from the manufacturer Lucas-Nuelle consists of the control module and the servo motor (manufacturer Lenze; type MCA13l41). The type of the test system

is CO3636-6V. The servo motor was used as a brake/load, and the control module was used to set the load torque to a constant value for each measurement. Control module displays the torque value and the rotational speed.

Končar motors throughout the experiment had metal couplings. Siemens motors throughout the experiment had plastic couplings designed in Autodesk Inventor Professional and 3D printed using UltiMaker S5. The material used for plastic coupling was ABS (ϕ 2.85 mm, infill density 100%). Throughout the experiment Siemens motors were mounted on hollow metal supports and fixed to the table with three clamps. Clamps were positioned approximately on the same positions for each Siemens motor. When the first Siemens IM was placed, the position of the hollow beams was marked on the table. Figure 15a shows the mounting and the positioning of the servo and Siemens motor during experiment, Figures 15b and 15c show the up-close view of the clamps and their position.

| (a) | (b) | (c) |
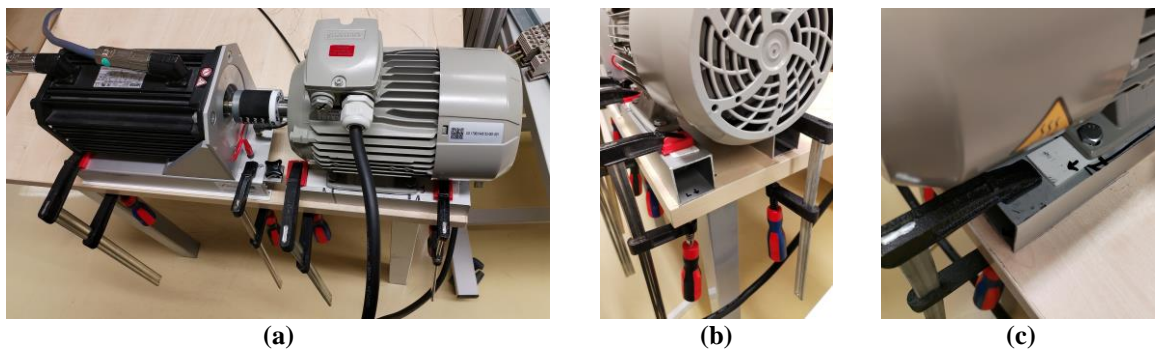
Figure 15. (a) Mounting and positioning of servo and Siemens motor; **(b)** Up-close view from the non-drive end; **(c)** Up-close view from non-drive end, right side.

Končar motors due to their size and shaft height were mounted on platforms that are compatible with servo motor platform. Two clamps were used for Končar motor table fixation. Figure 16a shows the mounting and positioning of servo and Končar motor and Figure 16b shows the view from non-drive end.
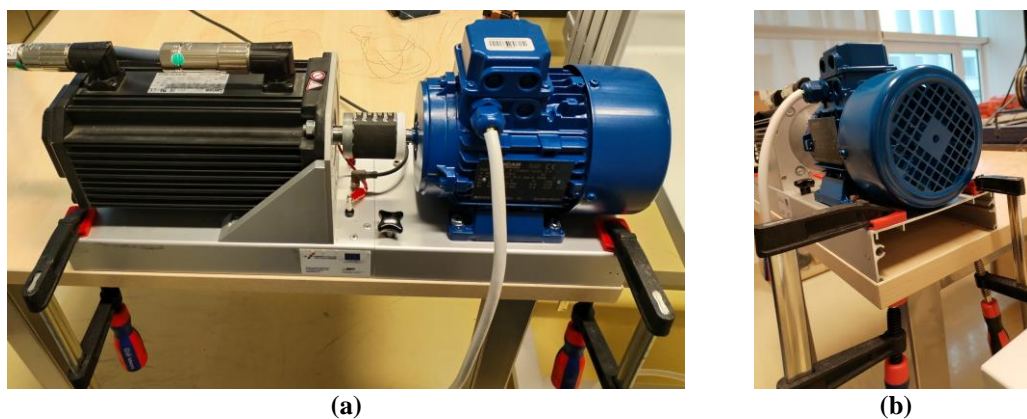

| (a) | (b) |

Figure 16. (a) Mounting and positioning of servo and Končar motor; **(b)** View from the non-drive end.

Broken rotor bar fault is created by drilling a hole into a rotor bar. The diameter of the hole for Siemens motor is 4 mm, and for Končar motor is 3 mm. Due to lack of information about rotor bar shape and dimensions the drilling was first conducted with 2 mm diameter drill bit. The criterium for hole diameter was visual conformation of rotor bar breakage which resulted in 4 mm and 3 mm for Siemens and Končar respectively. Figure 17a shows Siemens rotor with drilled rotor bar and Figure 17b show Končar rotor with drilled rotor bar.

| (a) | (b) |
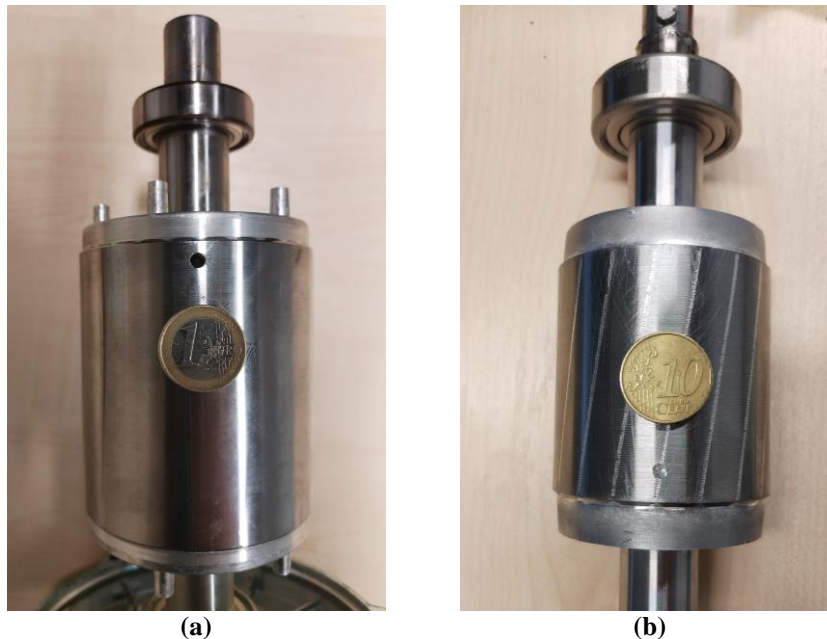
Figure 17. Artificially generated broken rotor bar fault: **(a)** Siemens rotor – 4 mm in diameter; **(b)** Končar rotor – 3 mm in diameter.

The hypothesis of the dissertation states that random positioning approach can be used to extract the information about motor health state. Random positioning implies the random position of the sensor center and random orientation of the sensor near motor surface. With random position approach, the sensor can be placed in infinitely many positions. One could, e.g., fix the center of the sensor in one point of space and rotate it arbitrarily in infinitely many ways or one could, e.g., fix the orientation of sensor (coordinated system of the senor relative to some referent coordinate system) and translate it in infinitely many ways. This means that every experimenter can have finite and unique set of measurements. To make the experiment repeatable as much as possible, four guidelines for sensor positioning are given:

1. At least one vertex of the sensor must always be in contact with the IM,
2. Divide the IM into 5 areas—left, right and upper area, drive end and non-drive end (plastic fan cap)
3. Change the area after each measurement
4. Position the sensor randomly in the given area.

Division of the motor into 5 area is shown in Figure 18. Because of the mounting type (B3), bottom part, between the mounting feet is excluded from the measurement. Also placing the sensor on the terminal box (on the cap) is excluded.
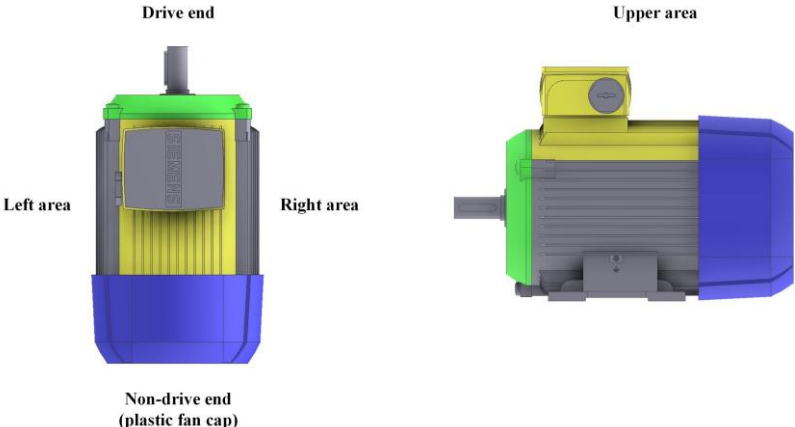
Figure 18. One of four guidelines for sensor positioning - division of the motor in 5 areas: left, right, upper (yellow), drive end (green) and non-drive end (blue) area.
IM 3D model source: *https://mall.industry.siemens.com/mall/en/mx/Catalog/Product/1LE10030DB222AA4*

An examples of random sensor positions are shown in Figure 19.
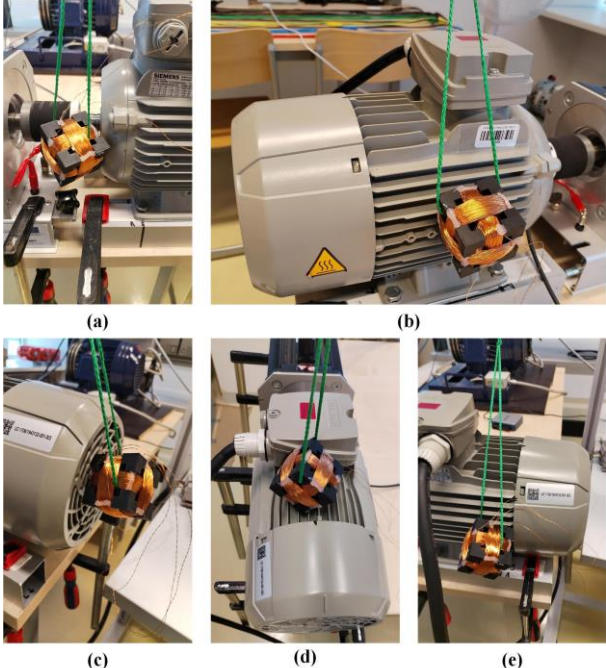
Figure 19. Examples of sensor positions: **(a)** drive end; **(b)** left area; **(c)** non-drive end; **(d)** upper area; **(e)** left area.

The labeling of the motors was done in the following way: one of the motors from the group that was kept healthy throughout the experiment was labeled as IM1; second motor while it was kept healthy, was labeled IM2_H and after the artificialy generated broken bar fault it was labeled IM2_BRB1.

5.4. Methods

Experiment consists of two parts. First part is validation of the measurement process and second part is detection of broken rotor fault.

Validation of measurement process implies consistent information extraction with traixial coil using random positioning approach. Consistent information extraction means that when series of measurements is conducted, e.g., on healthy motor, then obtained data, quantitatively must provide information that there is no difference within series of measurements. If experiment shows that there is quantitavly difference within series of measurement conducted on the motor with unchanged motor health state, then information extraction with triaxial coil and random positioning approach is not valid since it would give different information for the same (unchanged) motor state.

Detection of broken rotor fault implies that analysis of two data sets, one obtained for healthy and other for faulty motor, must quantitatively show difference between two data sets.

One measurement implies one random position of the sensor and data logging of the signals at that position. The physical quantity measured is the induced electromotive force (emf) of each coil. All measurements were taken after the motors have reached a steady state, while being line-fed without control applied to startup.

To prove the hypothesis of this dissertation, i.e, to prove that triaxial air core stray flux sensor can be developed to reliably detect broken rotor bars of a squirrel cage induction motor at steady state, three approaches are applied to obtained data: raw data analysis, feature analysis and FFT analysis. Since hypothesis does not state the method, the criterium for positive outcome is that any of mentioned approaches provide reliable BRB detection.

Validation of measurement process based on raw data was design in the following way, for each motor and motor state 100 measurements per day were taken during period of 10 days. First set of measurements was conducted on healthy Siemens motor labeled as IM1. Second set was conducted on healthy Siemens motor labeled as IM2_H and third set was conducted on faulty Siemens motor labeled the IM2_BRB1. Same procedure of measurement apply to Končar motors. Overall, 3000 measurements for Siemens group and 3000 measuremetns for Končar group.

5.4.1. Statistical Analysis

The method for validation of measurement process based on raw data is statistical analysis.

First step of the analysis is to determine whether data follows parametric or non-parametric distribution. This is performed with quantitative statistical tests for normality available in MATLAB (R2020b) and graphical test, quanatile-quantile plot. Based on the outcome of the normality test, appropriate statistical tests are applied to the series of data grouped by variable „day": day1, day2, day3,..., day10. After the statistical test is conducted, for the purpose of validation of measurement process, multiple comparison analysis is applied. If the multiple comparison analysis shows that there is no statistical significant difference between each day combination (day 1 – day 2, day 1 – day 3, ..., day 9 – day 10) then measurement process is considered valid.

The method for broken rotor detection based on raw data is statistical analysis. Data for this analysis is grouped by the variable "motor": IM1, IM2_H, IM2_BRB1.

For validation of measurement process each "day" variable contains 100 measurements. For broken rotor detection each "day" variable contains 300 measurements. Taking into account the number of data logging samples per measurement (100006 samples) data table for validation of measurement has dimensions 10000600 x 10. Data table for broken rotor bar detection has dimensions 30001800 x 10. Organization of data within data table is shown in Figure 20.
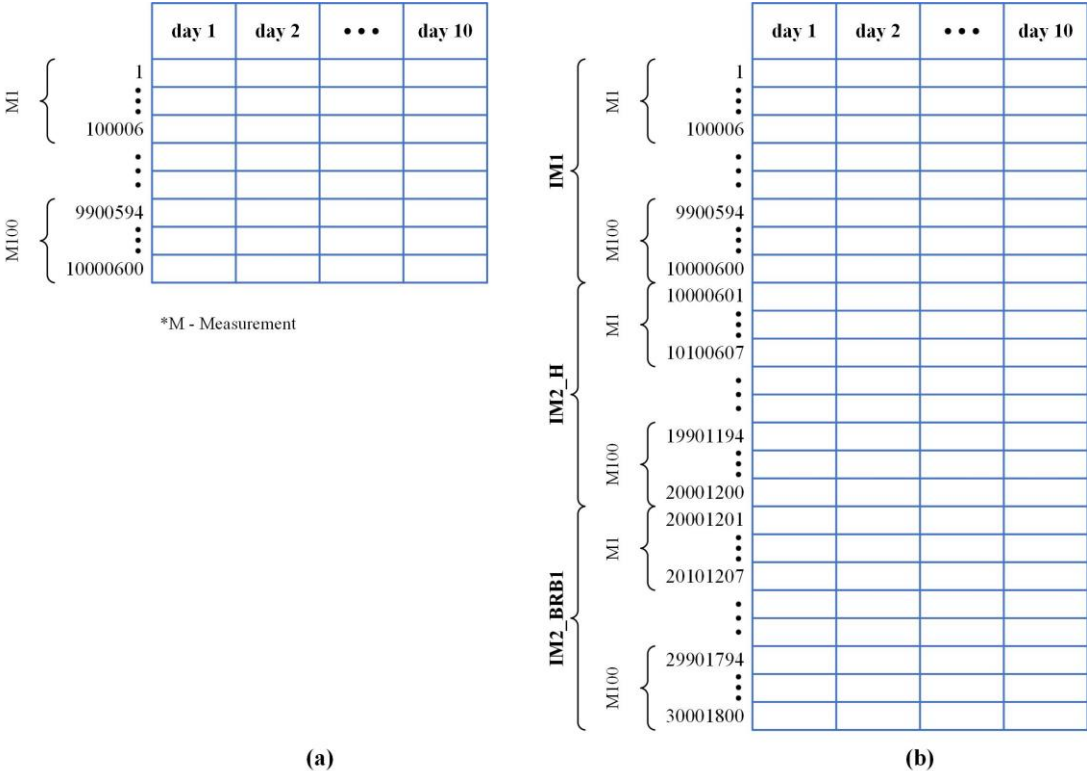

Figure 20. Data organization for raw data analysis: **(a)** validation of measurement process; **(b)** detection of broken rotor bar.

5.4.2. Feature Analysis

Feature analysis is performed with time-domain features. There are many time-domain features that can be chosen. Based on the articles that investigate fault detection in IMs [59], [60], [61], [62], [49] and [63] in this research 19 time-domain features have been chosen for BRB detection investigation. Chosen time-domain features and their equations are shown in Table 3.

Table 3. Time-domain features.

No.	Feature	Equation	No.	Feature	Equation
1	Energy	$\sum_{i=1}^{N}\lvert x_i\rvert^2$	11	Peak-to-peak	$\max_i(x_i) - \min_i(x_i)$
2	Mean	$\mu = \frac{1}{N}\sum_{i=1}^{N} x_i$	12	Peak-to-rms	$\frac{\max_i(x_i)}{rms}$
3	Standard deviation	$\sigma = \sqrt{\frac{1}{N-1}\sum_{i=1}^{N}\lvert x_i - \mu\rvert^2}$	13	Shape factor	$\frac{rms}{\frac{1}{N}\sum_{i=1}^{N}\lvert x_i\rvert}$
4	Variance	$\frac{1}{N-1}\sum_{i=1}^{N}\lvert x_i - \mu\rvert^2$	14	Impulse factor	$\frac{\max_i\lvert x_i\rvert}{\frac{1}{N}\sum_{i=1}^{N}\lvert x_i\rvert}$
5	Median	$\frac{1}{2}\left(X\left[\frac{N}{2}\right] + X\left[\frac{N}{2}+1\right]\right)$	15	Clearance factor	$\frac{\max_i\lvert x_i\rvert}{\left(\frac{1}{N}\sum_{i=1}^{N}\sqrt{\lvert x_i\rvert}\right)^2}$
6	Kurtosis	$\frac{1}{N}\sum_{i=1}^{N}\left(\frac{x_i - \mu}{\sigma}\right)^4$	16	Harmonic mean	$\frac{N}{\sum_{i=1}^{N}\frac{1}{x_i}}$
7	Skewness	$\frac{1}{N}\sum_{i=1}^{N}\left(\frac{x_i - \mu}{\sigma}\right)^3$	17	Fifth central moment	$\frac{1}{N}\sum_{i=1}^{N}(x_i - \mu)^5$
8	Root mean square	$rms = \sqrt{\frac{1}{N}\sum_{i=1}^{N}\lvert x_i\rvert^2}$	18	Sixth central moment	$\frac{1}{N}\sum_{i=1}^{N}(x_i - \mu)^6$
9	Root sum of squares	$rssq = \sqrt{\sum_{i=1}^{N}\lvert x_i\rvert^2}$	19	Waveform length	$\sum_{i=1}^{N-1}\lvert x_{i+1} - x_i\rvert$
10	Interquartile range	$X\left[\frac{3}{4}(N+1)\right] - X\left[\frac{1}{4}(N+1)\right]$			
$X -$ sorted values of data samples(measurement) $N -$ number of data samples					

For each measurement all three emf signals from triaxial coil were added to form one single measurement matrix with dimensions 100006 x 1000. This matrix is the input for two nested loops. Inner for-loop has 100 iterations and outer for-loop has 30 iterations. Numbers 100 and 30 are chosen empirically. At each beginning of the inner for-loop measurement matrix columns are randomly shuffled. The reason for shuffling is to avoid any bias during measurement since the measurement itself was done by one person. Afterwards, for each column of the matrix all time-domain features were calculated. For each feature, matrix was formed such that columns

of the matrix represent motors IM1, IM2_H and IM2_BRB1 respectively and rows represent calculated features. Dimensions of the matrix are 1000 x 3. Newly formed matrix is an input for Friedman test. The assumption is that each calculated series of features come from non-parametric distribution, i.e., data distribution is not tested for normality. After Friedman test, multiple compare function was used to calculate p-value for each motor combination. This procedure was repeated in „for" loop 100 times and the results of the loop is the number of appearances of the feature that satisfies the condition: $p_{IM1-IM2\_H} > 0.05$, $p_{IM1-IM2\_BRB1} < 0.05$, $p_{IM2\_H-IM2\_BRB1} < 0.05$. The whole procedure, from column shuffling is repeated 30 times. At the end of each iteration, number of appearances of the features is saved and thus forming result matrix with dimensions 20 x 30. From this matrix mean value and standard deviation is calculated for each feature.

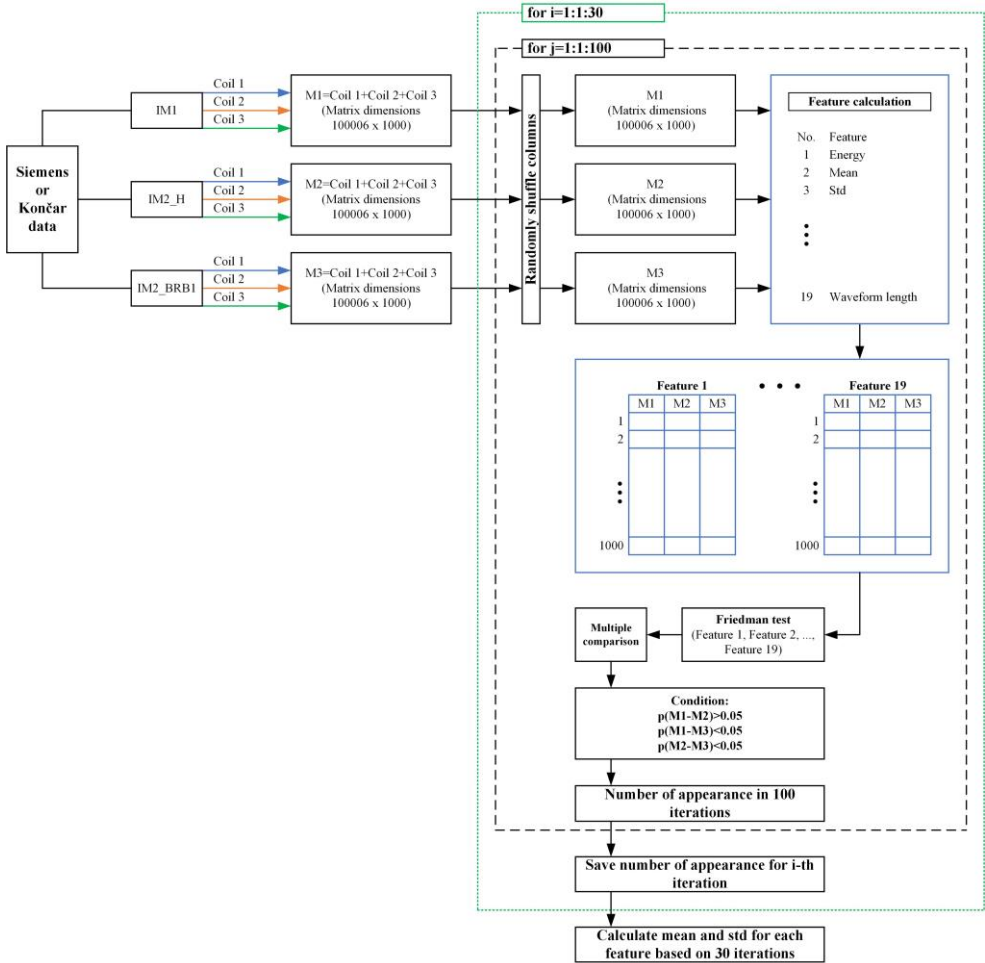Described procedure is show in the form of flowchart in Figure 21.

Figure 21. Flowchart for BRB feature analysis based on 1000 measurements.

After feature analysis based on 1000 measurements is conducted, broken rotor bar detection is investigated for different number of measurements. The analysis for different number of

measurements is conducted as follows: all three emf signals from triaxial coil were added to form one single measurement matrix with dimensions 100006 x 1000; this matrix is the input for two nested loops; inner for-loop has 100 iterations and outer for-loop has 50 iterations; fifty iterations of outer loop correspond to vector length of chosen number of measurements (nm), nm=20, 40 , 60, …, 980, 1000; for each nm 100 iterations is executed; in each iteration of the inner loop number of measurements, nm, is randomly taken from measurement matrix; randomization is achieved by random shuffling of the measurement matrix columns at the beginning of the each iteration of the inner loop; after randomly taken number of measurements, calculation of feature follows and the formation of feature matrix (nm x 3); feature matrix is input for Friedman test after which multiple comparison is applied; as a result for each feature it is counted how many times (out of 100) the condition $p_{IM1\text{-}IM2\_H} > 0.05$, $p_{IM1\text{-}IM2\_BRB1} < 0.05$, $p_{IM2\_H\text{-}IM2\_BRB1} < 0.05$ is meet.

The flowchart of feature analysis for different number of measurements is shown in Figure 22.
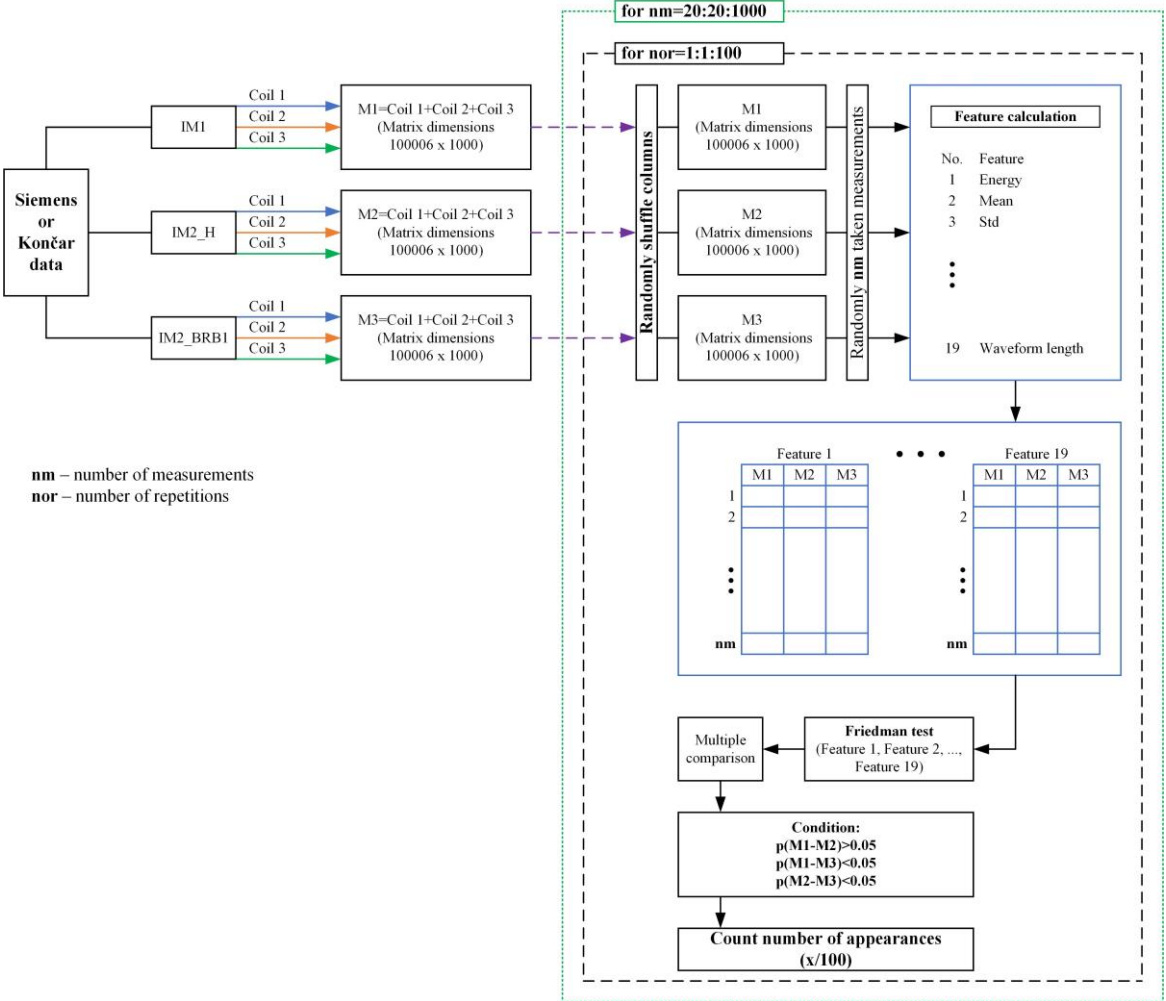

Figure 22. Flowchart of feature analysis for different number of measurements.

5.4.3. FFT Analysis

Classical approach to broken rotor bar detection is application of Fast Fourier Transform (FFT) to measured signals, whether they are electrical current, vibration, sound or stray magnetic flux signals. When dealing with stray magnetic flux signal standard indicators of the BRB fault are following frequency components [38][64]:

$$sf_s \tag{19}$$

$$3sf_s \tag{20}$$

$$(1 \pm 2ks)f_s \tag{21}$$

$$\left(\frac{k}{p}(1-s) \pm s\right)f_s \tag{22}$$

where s is the slip of IM, f_s is supply frequency, p is the number of pole pairs and k is the integer k=1, 2, 3, …

Broken rotor bar detection based on FFT requires the knowledge of healthy motor frequency spectrum. Then amplitudes of the frequency components and their frequency shift due to change in speed are compared to motor under test. If the motor under test has broken rotor bar it is expected that amplitudes of components defined by Eq.19, 20 and 21 have higher values that for the healthy motor.

After FFT analysis based on 1000 measurements is conducted, the influence of number of measurements is investigated. For each frequency component that is identified as BRB indicator following procedure is conducted: determine the frequency interval that encompasses frequency component of interest, measurement matrix for each motor is formed by adding frequency spectrum of each coil, set the number of measurements, 100 times randomly take the chosen number of measurements of each motor, for each iteration save the value of amplitude for each motor, count the how many time amplitude of IM2_BRB1 has higher value than IM1 and IM2_H, save count, repeat whole process 30 times, calculated the mean and standard deviation of count based on 30 iterations, execute the process from beginning for new frequency component. Flowchart of the process is shown in Figure 23.
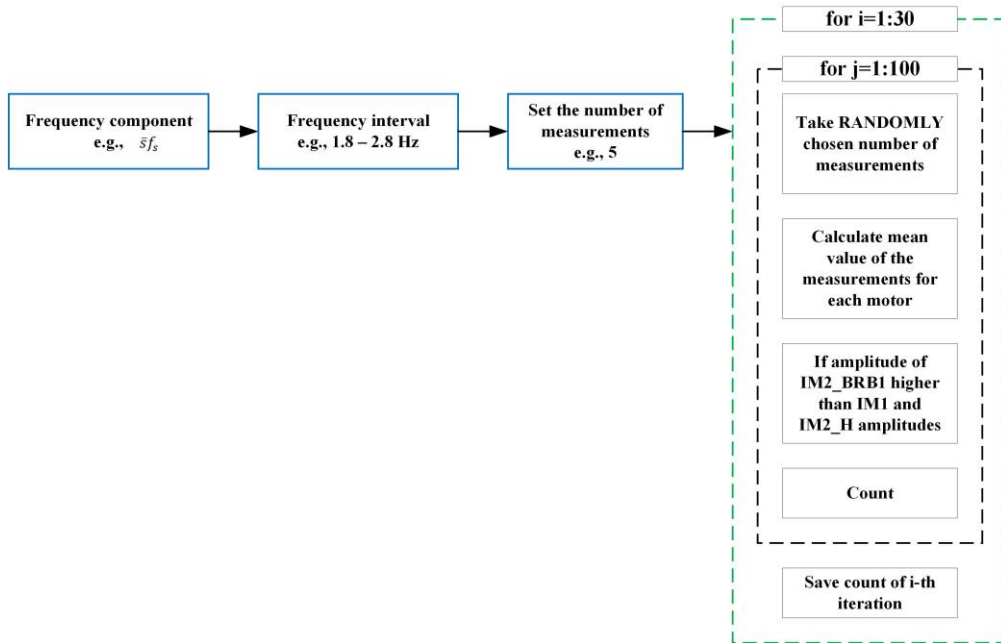
Figure 23. Flowchart for the number of measurements influence based on BRB indicator frequency components.

The final number of measurements in research is set based on results of Siemens or Končar group. Which group achieves positive results with smaller number of measurement, that group will be regarded as referent group.

In this dissertation, data analysis will first be conducted and presented for Siemens group. After, the whole process will be repeated and presented for Končar group.

6. RESULTS

In this section the results of the applied methods are first shown for Siemens group and then for Končar group. The order of the presented results is statistical analysis, feature analysis and FFT analysis, respectively. After all results are presented for both motor groups, comparison of the Siemens and Končar results by the method is presented.

6.1. Siemens – Statistical Analysis

The raw data visualization for each motor, each motor state and each day is shown with histograms in Figure 24. The histogram of each day contains all data values obtained with the data logger for all three coils. The number of bins chosen to represent the histogram is 100. This number of bins was chosen for visualization purposes only, i.e., to show 10 histograms in one figure that can be visually distinguished. The visualization is not intended to draw conclusions about the data distribution.

Figure 24. Siemens group - raw data visualization for each day: **(a)** IM1; **(b)** IM2_H; **(c)** IM2_BRB1; Number of bins for all histograms is 100.

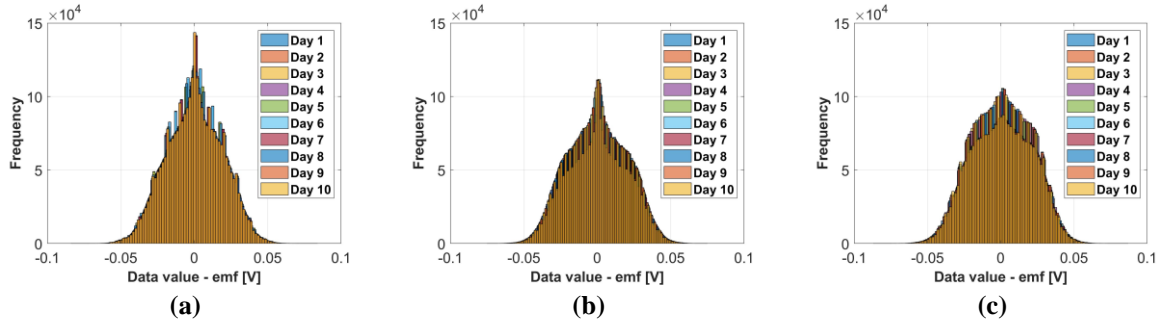To determine the statistical method for daily data comparison, i.e., which tests to use, parametric or non-parametric, the data must be examined for normality. There are two approaches to data testing, numerical tests, and graphical interpretation [65]. As stated in [66], there are 55 tests for normality, but in this study, only the tests implemented in MATLAB R2020b are used, i.e., One-sample Kolmogorov–Smirnov, Anderson–Darling, and Jarque–Bera and Lilliefors test.

When dealing with a large number of samples, normality tests may detect minimal deviations from normality as significant. Therefore, graphical methods can be a helpful tool for normality decisions [65]. In this paper, a graphical method, the quantile-quantile (Q-Q) plot, is used. The results of the normality tests obtained from MATLAB R2020b are shown in Table 4.

Table 4. Siemens group - results of the normality tests.

Test	Motor	p-value									
		day 1	day 2	day 3	day 4	day 5	day 6	day 7	day 8	day 9	day 10
One-sample Kolmogorov–Smirnov	IM1	<0.001	<0.001	<0.001	<0.001	<0.001	<0.001	<0.001	<0.001	<0.001	<0.001
	IM2_H	<0.001	<0.001	<0.001	<0.001	<0.001	<0.001	<0.001	<0.001	<0.001	<0.001
	IM2_BRB1	<0.001	<0.001	<0.001	<0.001	<0.001	<0.001	<0.001	<0.001	<0.001	<0.001
Anderson-Darling	IM1	<0.001	<0.001	<0.001	<0.001	<0.001	<0.001	<0.001	<0.001	<0.001	<0.001
	IM2_H	<0.001	<0.001	<0.001	<0.001	<0.001	<0.001	<0.001	<0.001	<0.001	<0.001
	IM2_BRB1	<0.001	<0.001	<0.001	<0.001	<0.001	<0.001	<0.001	<0.001	<0.001	<0.001
Jarque-Bera	IM1	<0.001	<0.001	<0.001	<0.001	<0.001	<0.001	<0.001	<0.001	<0.001	<0.001
	IM2_H	<0.001	<0.001	<0.001	<0.001	<0.001	<0.001	<0.001	<0.001	<0.001	<0.001
	IM2_BRB1	<0.001	<0.001	<0.001	<0.001	<0.001	<0.001	<0.001	<0.001	<0.001	<0.001
Lilliefors	IM1	<0.001	<0.001	<0.001	<0.001	<0.001	<0.001	<0.001	<0.001	<0.001	<0.001
	IM2_H	<0.001	<0.001	<0.001	<0.001	<0.001	<0.001	<0.001	<0.001	<0.001	<0.001
	IM2_BRB1	<0.001	<0.001	<0.001	<0.001	<0.001	<0.001	<0.001	<0.001	<0.001	<0.001

The results from Table 4 show that the p-value for every motor, motor state and day is less than 0.001, which means the rejection of the null hypothesis that the data come from a normal distribution.

The Q-Q plot for each motor, motor state, and day is shown in Figure 25.

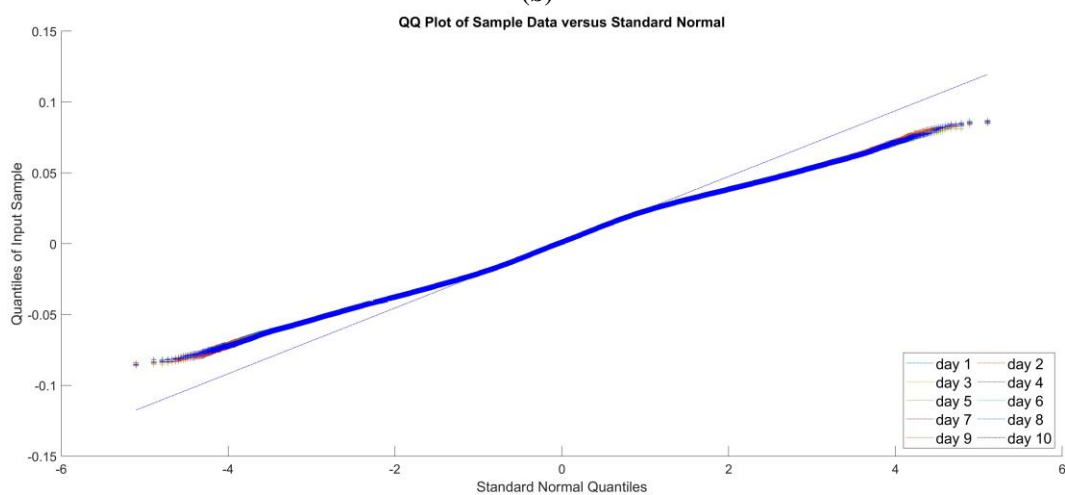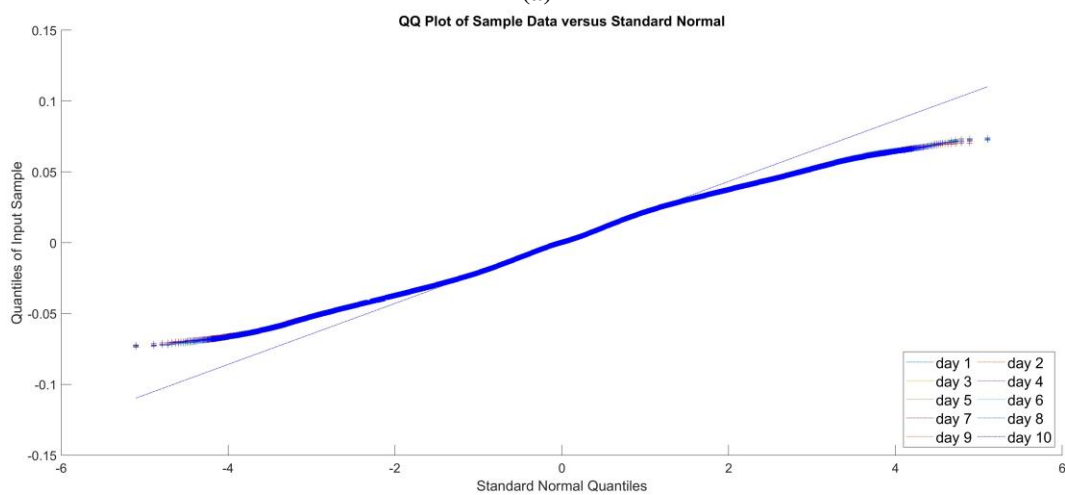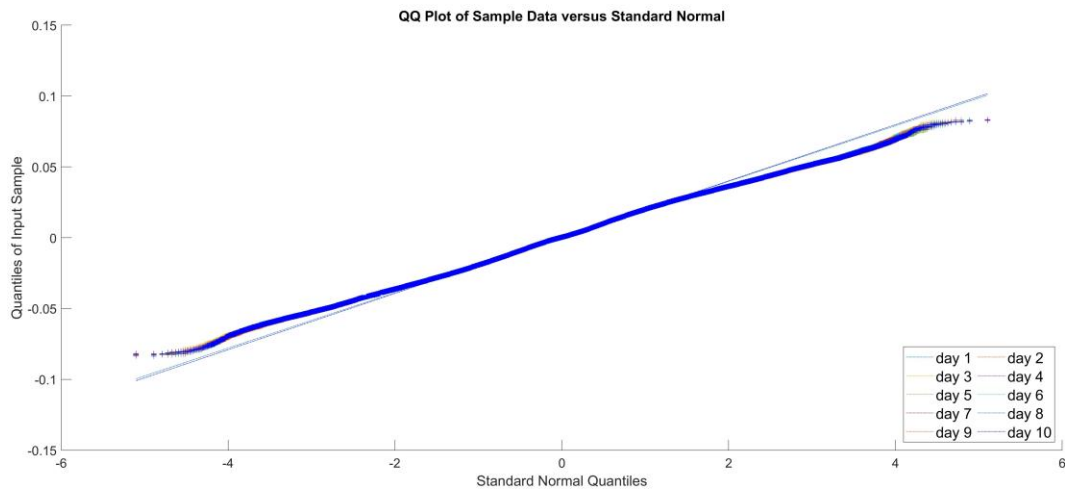**Figure 25.** Siemens group - Quantile-Quantile plot for each day: **(a)** IM1; **(b)** IM2_H; **(c)** IM2_BRB1.

The Q-Q plot in Figure 25a shows deviations from the normality line, but not to the extent that suggests non-normal data, leading the author to conclude that the data from IM1 are subject to a normal distribution; the Q-Q plots in Figure 25b and 25c show deviations from the normality

line, leading the author to conclude that the data from IM2_H and IM2_BRB1 are subject to non-normal distribution.

The inconsistency between the results from Table 4 and the visual interpretation of the Q-Q plot in Figure 25a, due to both the large sample size and the awareness that the interpretation of Q-Q plots can be subjective [67], led to the decision to apply parametric and non-parametric tests for the validation of measurement process and the distinction between healthy state and broken bar state.

6.1.1. Siemens – Normality Assumption

Because the measurements were conducted on SCIMs over 10 consecutive days (100 measurements per day), meaning that measurements were repeated on the same objects at more than two time points, repeated measures analysis of variance (RM-ANOVA) as a method for determining the independence of the daily measurements was chosen. RM-ANOVA is a statistical method used when differences between three or more correlated groups are investigated [68]. The assumptions of the RM-ANOVA are approximately normally distributed dependent variable, no outliers in any of the repeated measurements, and sphericity [69]. The studies conducted in [70] have shown that RM-ANOVA is a valid statistical method even in the case of non-normal distribution if the sphericity assumption is met. The sphericity of the data is examined using the Mauchly test [71]. The results of the Mauchly test for each motor and motor condition are shown in Table 5. The Mauchly test is performed with the implemented MATLAB functions "rm = fitrm()" and "mauchly(rm)".

Table 5. Siemens group - results of the Mauchly test for each motor and motor state.

Motor	W	ChiStat	DF	p-value
IM1	0.99999	41.49	44	0.5798
IM2_H	0.99999	33.811	44	0.86671
IM2_BRB1	0.99999	36.867	44	0.76842

The results from Table 5 show that the p-value for each motor is greater than 0.05, which means that the differences in all daily combinations have equal variances, i.e., the sphericity assumption is met.

Statement of the null and alternative hypothesis for the daily measurement of each motor and motor condition:

$H_0 : \mu_1 = \mu_2 = \ldots = \mu_{10}$

$H_1: at\ least\ on\ measurement\ \mu\ differs\ from\ another$

where μ_n is the population mean of n-th day.

The results of the RM-ANOVA analysis are shown in Table 6. The RM-ANOVA is performed with the implemented MATLAB function "ranova(rm)".

Table 6. Siemens group - results of RM-ANOVA analysis for each motor separately.

Motor		SumSq	DF	MeanSq	F	p-value
IM1	(Intercept): day	0.0032546	9	0.00036162	1.0344	0.40934
	Error(day)	9439.4	2.7×10^7	0.00034961		
IM2_H	(Intercept): day	0.0037357	9	0.00041508	1.0644	0.38553
	Error(day)	10529	2.7×10^7	0.00038995		
IM2_BRB1	(Intercept): day	0.0015375	9	0.00017084	0.41369	0.92853
	Error(day)	11150	2.7×10^7	0.00041296		

Results from Table 6 show that the p-value for each motor is greater than 0.05, which means that there is not enough evidence to reject the null hypothesis at a 5% significance level, i.e., all mean values of the 10-day measurements are the same for a given motor. The p-values for day-to-day comparison are determined using the MATLAB function "multcompare(rm)". The results of the multiple comparison with uncorrected p-values are shown in Figure 26.

(a)

(b)

(c)
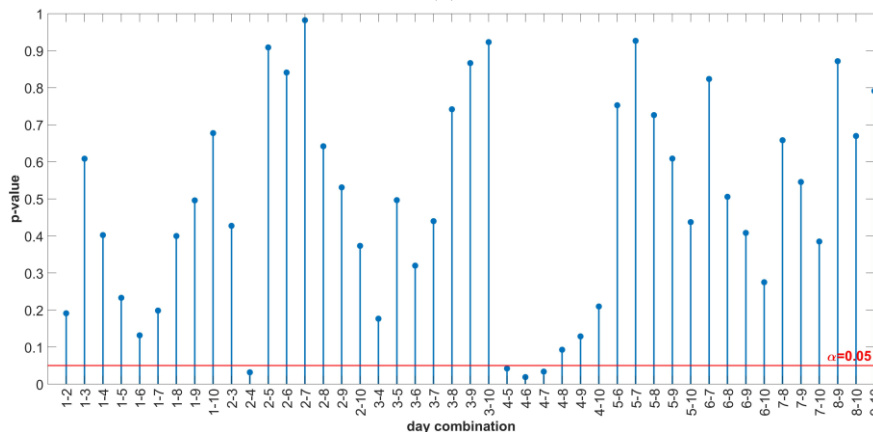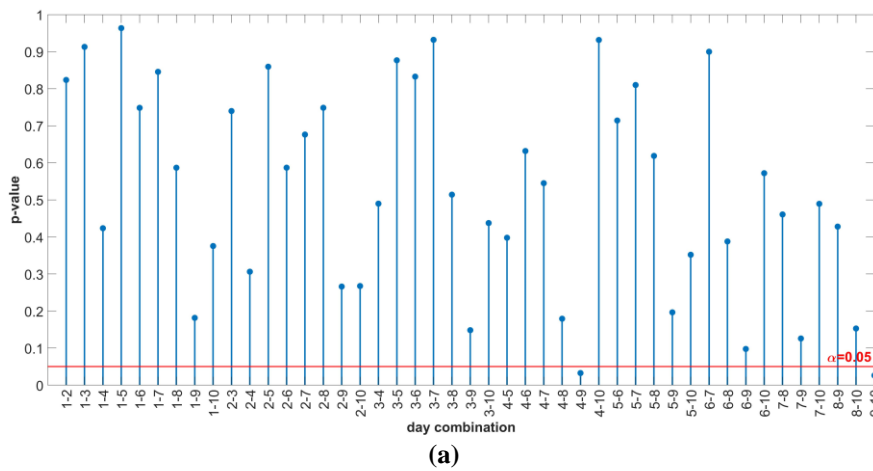
Figure 26. Siemens group - multiple comparison results of RM-ANOVA—uncorrected p-values: **(a)** IM1; **(b)** IM2_H; **(c)** IM2_BRB1.

Figure 26 shows that not all day-to-day combinations have p-values of more than 0.05.

For multiple hypothesis tests, the probability that the null hypothesis is rejected, even though it is true, increases with the number of tests (Type I error—false positive) [72]. The Type I error is controlled by adjusting the p-value. Two general methods for p-value adjustment are the familywise error rate (FWER) and the f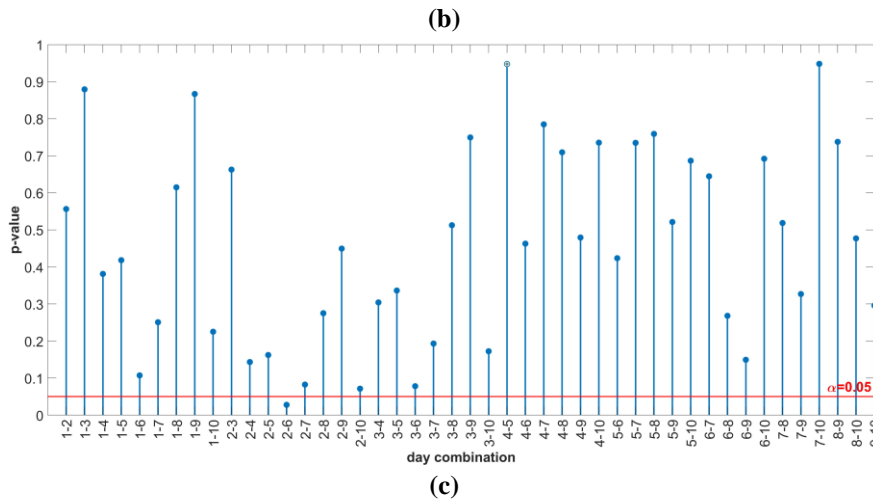alse discovery rate (FDR) [73]. The FWER is the probability of one or more type I errors occurring in a family of tests under the null hypothesis, and the FDR is the expected proportion of the ratio: number of false-positive tests to the number of tests with the null hypothesis rejected [74]. There are a variety of methods for controlling FWER (Bonferroni, Holm, Hochberg, Hommel, and adaptive Bonferroni) and FDR (two-stage linear set-up procedure of Benjamini, Krieger and Yekutieli, Benjamini and Hochberg, and Storey Tibshirani) [75], [76], [77]. The most representative methods for FWER and FDR are Bonferroni and Benjamini–Hochberg, respectively. Since the Bonferroni correction is conservative and less powerful compared to the Benjamini–Hochberg (BH) correction [78], p-value adjustment for the multiple comparison results is performed using the BH correction.

BH correction method: Sorting the p-values in ascending order, ranking the p-values (the smallest p-value has rank 1), calculating the critical BH value for each p-value using the formula *(i/m)Q*, where *i* is the rank of a particular p-value, *m* is the total number of tests, and *Q* is the false discovery rate chosen by the user. After sorting the p-values and calculating the critical value, the largest p-value whose value is less than the critical value sets the cut-off for rejecting the null hypothesis. All null hypotheses with p-values smaller than the largest p-value found, including the largest p-value, are rejected [79], [80]. The results of the BH correction are shown in Figure 27.
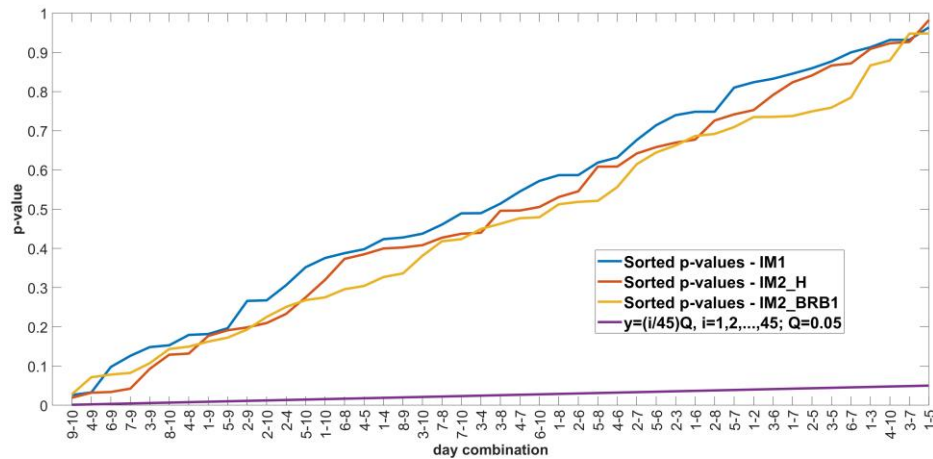
Figure 27. Siemens group - results of Benjamini-Hochberg procedure.

Results from Figure 27 show that there is no intersection of the sorted p-values with the line $y = (i/m)Q$, which means that all day-to-day combinations with p-values below 0.05 are false positives, i.e., there is no statistically significant difference between all day-to-day combinations for each motor.

To comprehend more clearly the overall measurement and validation process flow chart is shown in Figure 28.

To investigate whether the approach with a triaxial sensor, random positions over the motors, and raw data makes a difference between the motor conditions, a two-way RM-ANOVA was used. The two-way RM-ANOVA is performed using the MATLAB function "ranova(rm)". Before performing the two-way RMANOVA, the Mauchly test is performed to check whether the sphericity is met. The result of the Mauchly test is shown in Table 7, and the result of the analysis is shown in Table 8.

Table 7. Siemens group - results of the Mauchly test of data prepared for two-way RM-ANOVA.

W	ChiStat	DF	p-value
1	36.631	44	0.77698

Table 8. Siemens group - results of the two-way RM-ANOVA.

	SumSq	DF	MeanSq	F	p-value
(Intercept): day	0.0013094	9	0.00014549	0.37871	0.94548
Motor	8.6033	2	4.3017	10413	0
Motor: day	0.0072185	18	0.00040103	1.0439	0.40485
Error(day)	31,118	8.1×10^7	0.00038417	1	0.5
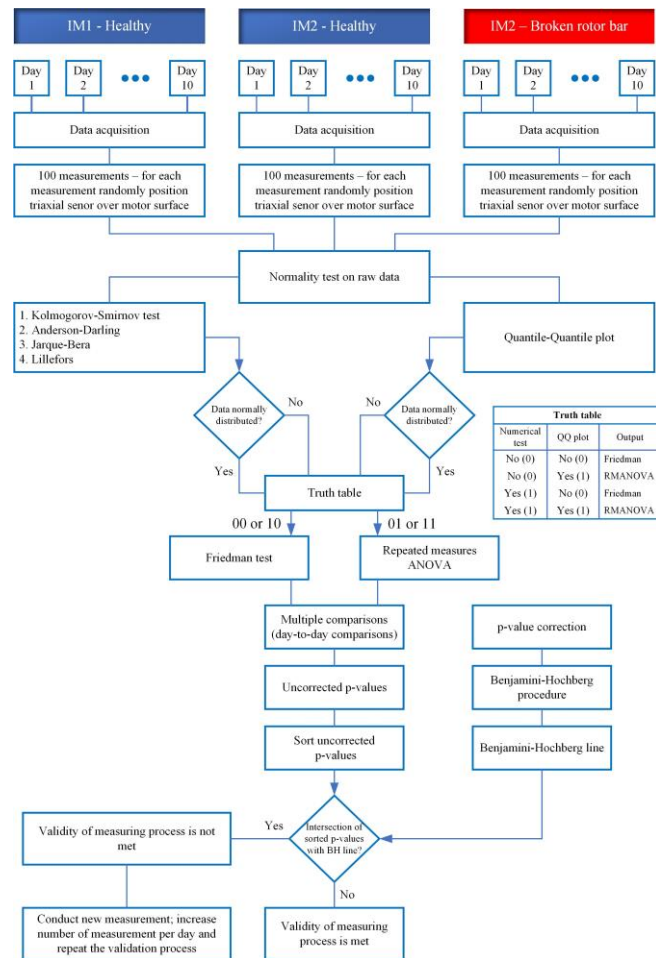
Figure 28. Flowchart of validation process based on raw data

Results from Table 7 show that sphericity is met ($p > 0.05$). The results from Table 8 show that there is not enough evidence for the variable "day" to reject the null hypothesis with a significance level of 5%, i.e., there is no significant difference in the mean values between the days. This is already evident in the analysis, which was carried out separately for each motor. Table 8 also shows that there is strong evidence ($p = 0$) for the variable "Motor" to reject the null hypothesis at a significance level of 5%, i.e., there is a statistically significant difference between the motors. The multiple comparison test according to the variable "Motor" is shown in Table 9, and the estimated difference in means (with 95% confidence intervals) is shown in Figure 29.

Table 9. Siemens group - results of multiple comparison test by variable "Motor" - uncorrected p-values.

Motor 1	Motor 2	Difference	StdErr	p-value	Lower	Upper
IM1	IM2_H	9.0766×10^{-5}	5.2479×10^{-6}	5.0809×10^{-67}	8.048e-05	0.00010105
IM1	IM2_BRB1	-0.00060576	5.2479×10^{-6}	0	-0.00061605	-0.00059548
IM2_H	IM2_BRB1	-0.00069653	5.2479×10^{-6}	5.0809×10^{-67}	-0.00070681	-0.00068624

Figure 29. Siemens group - estimated difference in means of variable "Motor" with 95% confidence interval.

The results from Table 9 show that there is a statistically significant difference between the individual motors. Figure 29 shows the graphical representation of the results from Table 9. 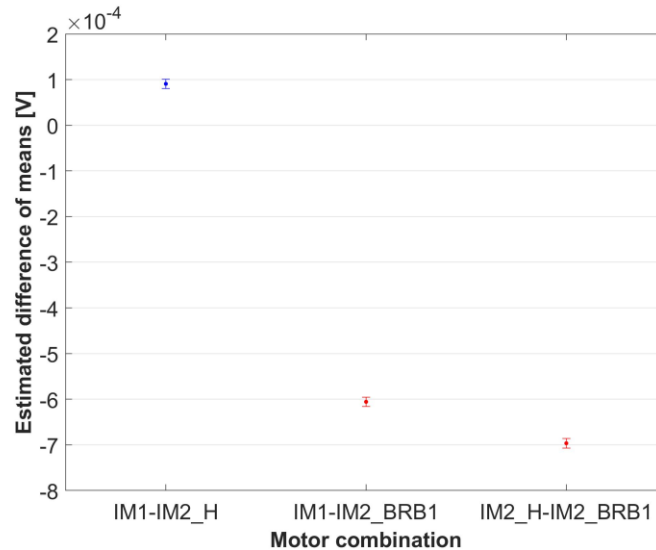The estimated difference in means with a 95 % confidence interval for healthy–healthy motor combinations is represented in blue colour, and healthy–BRB combinations are represented in red color in Figure 29. The non-overlapping intervals of healthy-healthy combination with any healthy–BRB1 combinations graphically indicate a statistically significant difference. From Figure 29, it is observable that healthy–BRB1 combinations differ significantly in value from healthy–healthy combination. To quantify the differences, the percentage difference between values of estimated differences in means is calculated, and the results are shown in Table 10.

Table 10. Siemens group - percentage difference in estimated differences in means relative to the healthy–healthy motor combination.

Reference	Motor Combination	Percentage Difference of Estimated Differences in Means
IM1–IM2_H	IM1–IM2_BRB1	767.40%
	IM2_H–IM2_BRB1	867.40%

6.1.2. Siemens – Non parametric Assumption

The assumption of a non-normal data distribution implies the use of a non-parametric test. In non-parametric analysis, the data are transformed into ranks or signs [81]. The power of non-parametric tests is generally lower than that of parametric tests, but they are more powerful for non-normally distributed data [81], [82]. The non-parametric alternative to the RM-ANOVA test is the Friedman test [83]. The null hypothesis of the Friedman test states that the compared groups come from the same population or the population with the same median [84]. The null hypothesis for this study is that the data obtained from the measurements taken over a 10-day

period for a particular motor come from the same population. The test is performed using the MATLAB function "friedman(x)", where "x" represents the data table shown in Figure 20b. The results of the Friedman test for each motor are shown in Table 11.

Table 11. Siemens group - results of the Friedman test for each motor.

Motor		SS	df	MS	Chi-sq	Prob>Chi-sq
	Columns	92.7364	9	10.304	10.13	0.34
IM1	Error	247,166,451.7636	26,999,991	9.1543		
	Total	247,166,544.5	29,999,999			
	Columns	104.678	9	11.6309	11.43	0.2471
IM2_H	Error	247,189,783.322	26,999,991	9.1552		
	Total	247,189,888	29,999,999			
	Columns	62.6033	9	6.95593	6.84	0.654
IM2_BRB1	Error	247,200,721.8967	26,999,991	9.15559		
	Total	247,200,784.5	29,999,999			

The results from Table 11 show that all p-values are greater than 0.05, i.e., for each motor/motor condition, there is insufficient evidence to reject the null hypothesis at a 5% significance level, meaning that all measurements for a given motor come from the same distribution. The results of the multiple comparison with uncorrected p-values for each motor are shown in Figure 30.

(a)

(b)
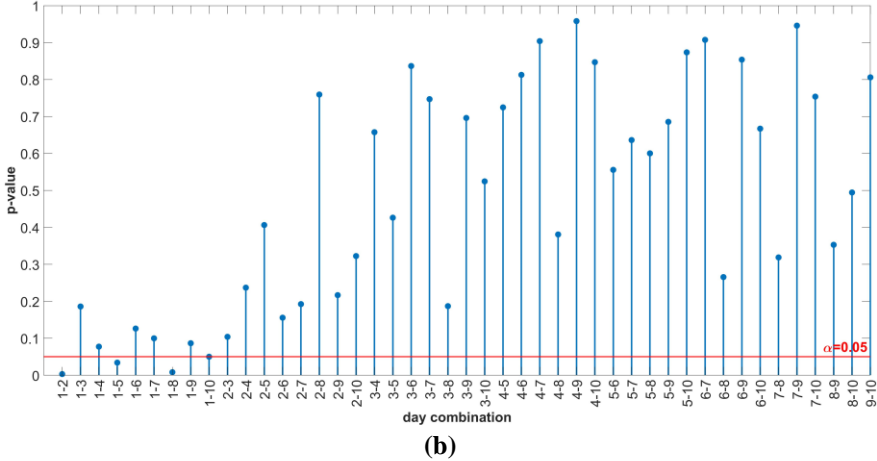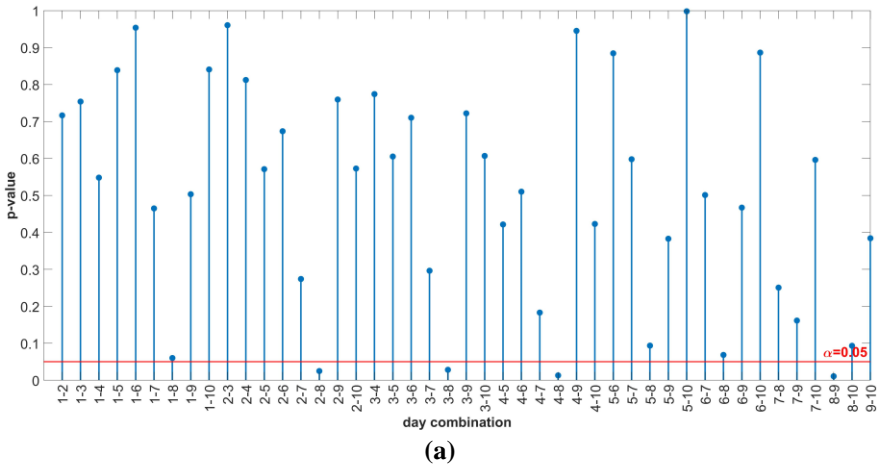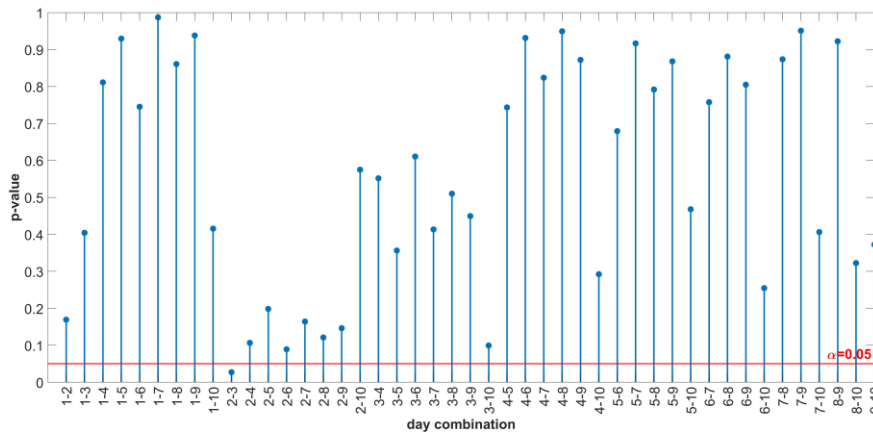
(c)

Figure 30. Siemens group - multiple comparison results of Friedman test—uncorrected p-values: **(a)** IM1; **(b)** IM2_H; **(c)** IM2_BRB1.

Figure 30 shows that not all p-values are above the significance level of 0.05. To check whether the significant p-values are false-positive, the BH correction is applied. The results of the BH correction are shown in Figure 31.
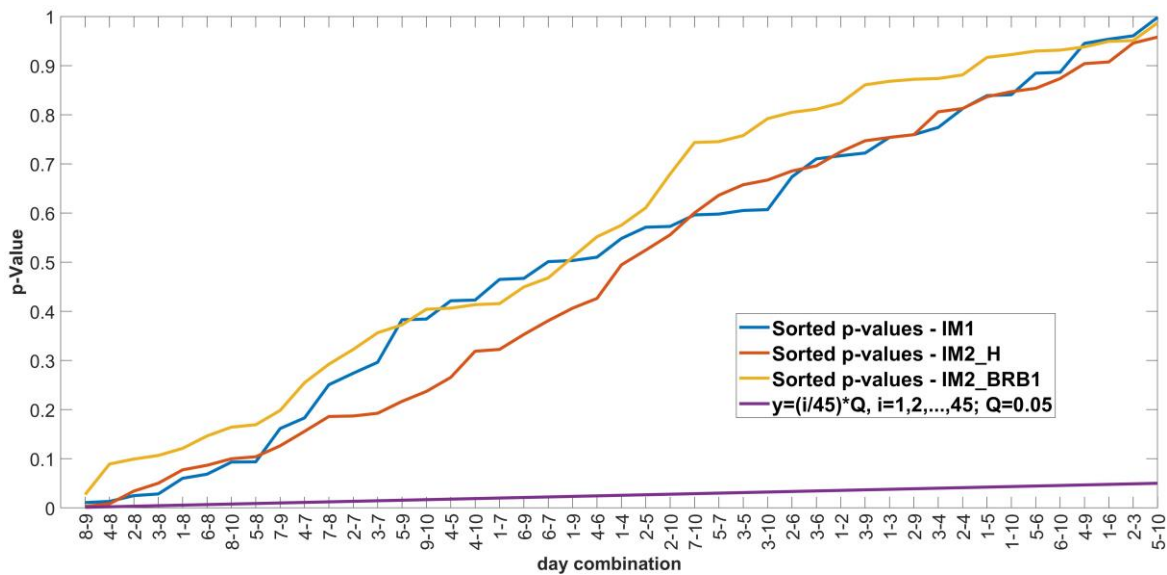
Figure 31. Siemens group - correction of p-values with BH after multiple comparison of the Friedman test.

The results from Figure 31 show that there is no intersection of the sorted p-values with the line $y=(i/m)Q$, which means that all day-to-day combinations with p-values below 0.05 are false positives, i.e., there is no statistically significant difference between all day-to-day combinations for each motor.

To examine the differentiation between motor conditions assuming a non-normal distribution, the Friedman test was used. The data for the analysis are organized in a table consisting of columns representing the variable "Motor" and rows representing the variable "day". The null

hypothesis for this analysis is as follows: the data obtained for each motor with the measurements over a 10-day period come from the same population. The results of the Friedman test are shown in Table 12.

Table 12. Siemens group - results of the Friedman test for motor comparison.

	SS	df	MS	Chi-sq	Prob>Chi-sq
Columns	1.8583×10^4	2	9.2914×10^3	1.8647×10^4	0
Error	5.9776×10^7	59,999,998	0.9963		
Total	5.9795×10^7	89,999,999	0.00038417		

The results from Table 12 show that there is a significant difference between the motors ($p = 0$), i.e., that the data obtained for each motor does not come from the same population. The multiple comparison by the variable "Motor" is shown in Table 13 and the estimated difference in mean ranks (with 95% confidence intervals) is shown in Figure 32.

Table 13. Siemens group - results of the multiple comparison by variable "Motor"—uncorrected p-values.

Motor 1	Motor 2	Difference	p-value	Lower	Upper
IM1	IM2_H	0.0042759	8.3828×10^{-62}	0.0037707	0.0047811
IM1	IM2_BRB1	−0.028118	0	−0.028623	−0.027613
IM2_H	IM2_BRB1	−0.032394	0	−0.032899	−0.031889
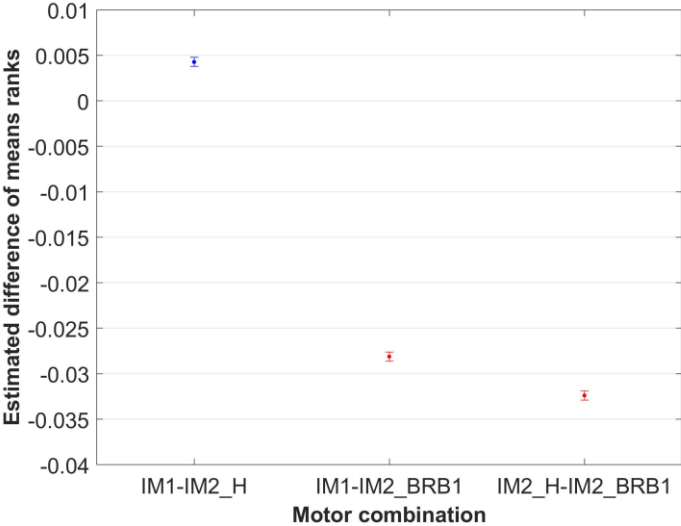
Figure 32. Siemens group - estimated difference in mean ranks of variable "Motor" with 95% confidence interval.

The results from Table 13 show that there is a statistically significant difference between the individual motors. Figure 32 shows the graphical representation of the results from Table 13. The percentage difference of estimated mean ranks for the motor combinations with BRB fault compared to the healthy motor combinations is shown in Table 14.

Table 14. Siemens group - percentage difference in estimated differences in mean ranks relative to the healthy–healthy motor combination.

Reference	Motor Combination	Percentage Difference in Estimated Differences in Mean Ranks
IM1–IM2_H	IM1–IM2_BRB1	757.60%
	IM2_H–IM2_BRB1	857.60%

6.2. Siemens – Feature Analysis

Results of feature analysis based on 1000 measurements for the Siemens group are shown in Figure 33.
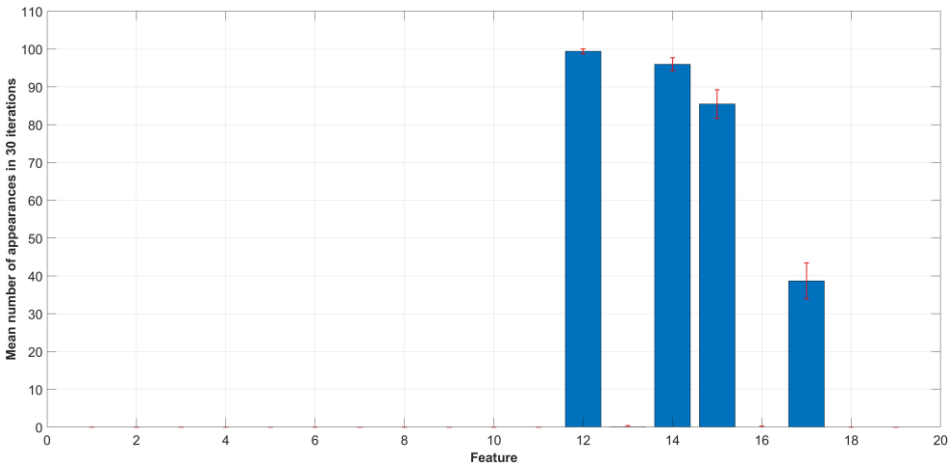
Figure 33. Mean number of appearances in 30 iterations for Siemens group.

Figure 33 shows mean number of appearances of features in 30 iterations, according to flowchart on Figure 16, and corresponding standard deviation interval displayed with red bars. From Figure 28 it is observable that 4 out of 19 features appear with different mean values. Features No. 12 has highest mean value: 99.4 %. Feature No. 14 has second highest value, 96.0 %. Feature No. 15 has third highest value, 85.46 %, and Feature No. 17 has fourth highest value, 38.66 %.

Results of feature analysis for different number of measurements are shown in Figure 34 (3D bar graph), Figure 35 (view 1), Figure 36 (view 2) and Figure 37 (view 3).
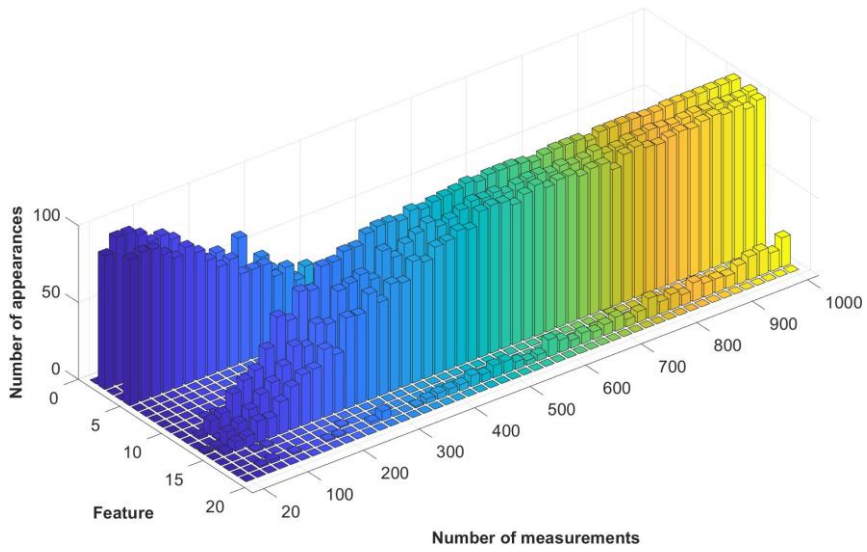
Figure 34. Siemens group – Feature appearance as a function of number of measurements – 3D bar graph.
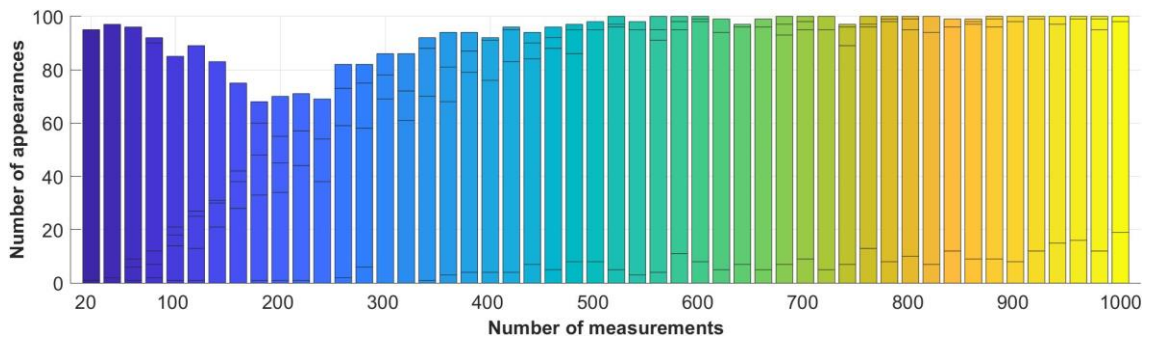
Figure 35. Siemens group – Feature appearance as a function of number of measurements – view 1.
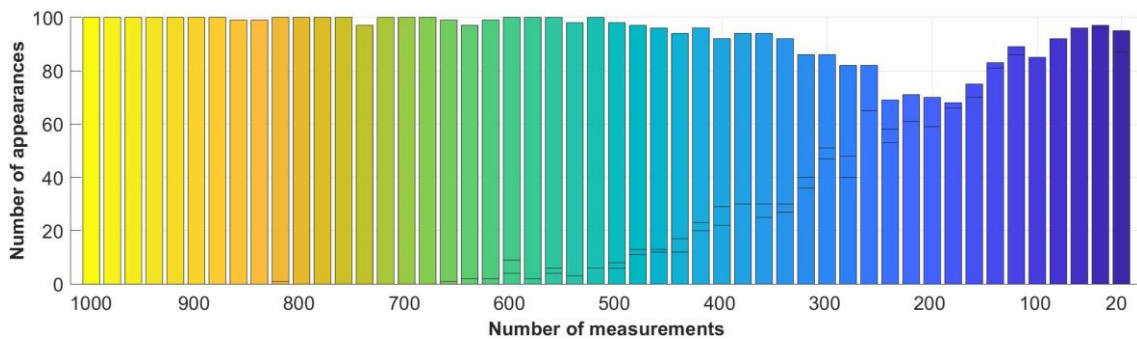
Figure 36. Siemens group – Feature appearance as a function of number of measurements – view 2.
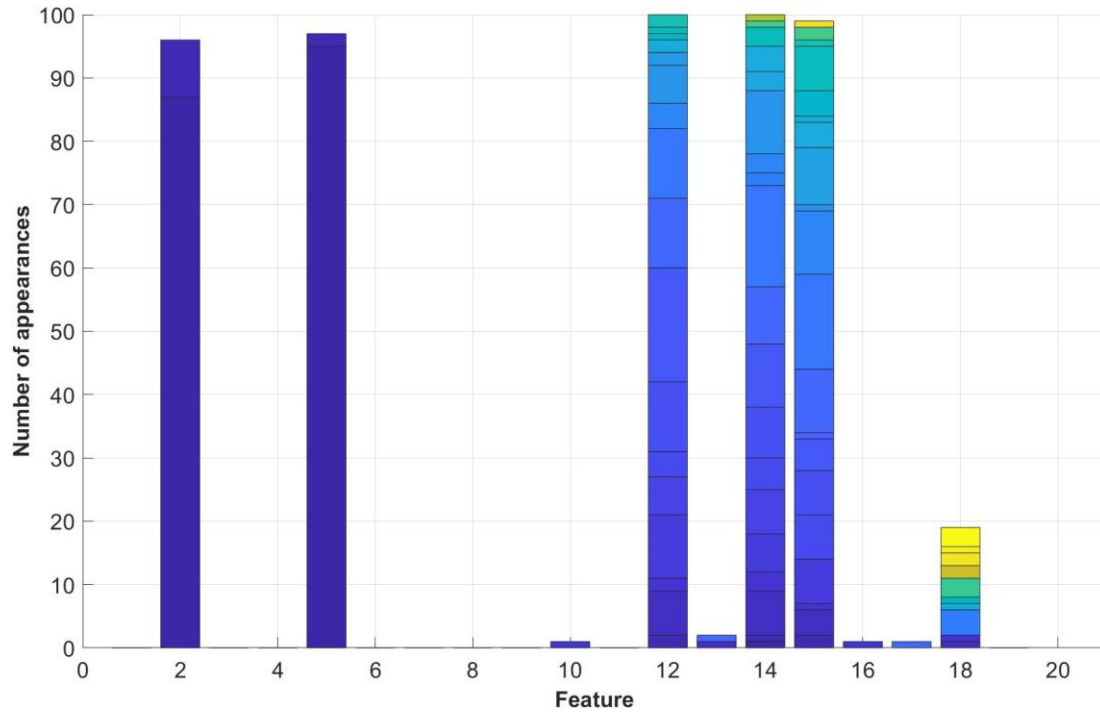
Figure 37. Siemens group – Feature appearance as a function of number of measurements – view 3.

Analysing results through Figures 34 and 37 one can observe that there are features that do not appear at all in broken rotor bar detection analysis for Siemens group. Features that do not appear at all for Siemens group are shown in Table 15.

Table 15. Features that do not appear at all in the analysis for Siemens group.

No.	Feature	No.	Feature
1	Energy	8	Root mean square
3	Standard deviation	9	Root sum of squares
4	Variance	11	Peak-to-peak
6	Kurtosis	19	Waveform length
7	Skewness		

From Figure 34 it is observable that different features have different dependency on number of measurements. Features with high number of appearances in the interval nm=20, …, 120 are features mean (No. 2) and median (No. 5). With the increase of the number of measurements, the number of appearances for features 2 and 5, decreases and reaches zero at nm=640 for feature 2 and at nm=680 for feature 5. Maximum values that feature 2 and 5 achieve are 96 % for nm=40,60 and 97 % for nm=40 respectively. Appearance of feature interquartile range (No. 10), shape factor (No. 13), harmonic mean (No. 16) and fifth central moment (No. 17) is considered negligible since their maximum values do not have values more than 2 %. Feature sixth central moment (No. 18) has overall increasing trend on the interval nm=340, …, 1000.

Maximum value that feature No. 18 achieves is 19 % at nm=1000. Features peak-to-rms (No. 12), impulse factor (No. 14) and clearance factor (No. 15) exhibit increase and decrease in appearance but with overall trend of increase. Feature 12 reaches 100 % at nm=520 and for interval nm=540, …, 1000 has average value 99.5 % with standard deviation value 0.93 %. Feature 14 reaches 97 % at nm=520 and for interval nm=540, …, 1000 has average value 98.5 % with standard deviation value 1.31 %. Feature 15 reaches 96 % at nm=520 and for interval nm=540, …, 1000 has average value 95.62 % with standard deviation value 2.37 %.

Higher value of „Number of appearances" for a given feature means that the condition $p_{IM1-IM2\_H}$ > 0.05, $p_{IM1-IM2\_BRB1}$ < 0.05, $p_{IM2\_H-IM2\_BRB1}$ < 0.05 is meet more times then in comparison with another feature, i.e., given feature differentiates healthy from faulty state more times that other feature. For example, if all 1000 measurement are considered, then for feature No. 12 (Peak-to-rms) it can observed from Figure 28 that mentioned condition is meet 99.4 times on average in 30 iterations, whereas feature No. 17 has meet the condition 38.66 times on average in 30 iterations. Feature No. 12 more reliably diffirentiates healthy from faulty state then feature No. 17.

Analysis for different number of measurements is conducted without iterations. The reason for this was execution time of MATLAB script. Code execution time for case of all 1000 measurements (MATLAB script shown in Appendix B) was approximately 9 hours. For each number of measurement only one time random measurements were taken and analysed for the mentioned condition. This was carried out for series nm=20, 40, 60, ..., 1000, in total 50 times. Code execution time for generating Figure 29 was approximately 14 h. If 30 iteration were conducted execution time would approximately be 17.5 days.

6.3. Siemens – FFT Analysis

FFT analysis is based on 1000 measurements. First, all signals for each motor/motor state are added as shown in Figure 16 (e.g., M1=Coil 1+Coil 2+Coil 3). On each measurement of each motor/motor state FFT is applied. Afterwards, for each frequency component mean value is calculated. FFT for each motor/motor state of the Siemens group is shown in Figure 38.
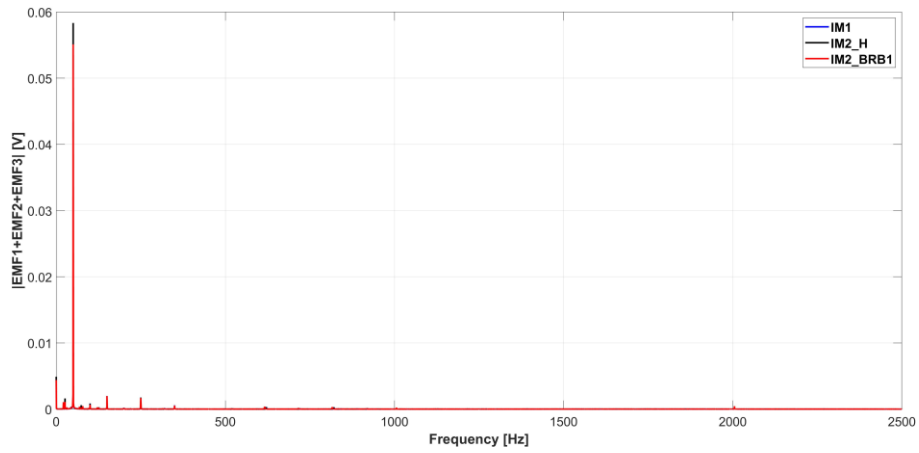
Figure 38. Siemens group - FFT of IM1, IM2_H and IM2_BRB1.

For comparison of healthy motors and faulty motor the slip value is needed. Because analysis is conducted on 1000 measurements the average speed value $\bar{n}$ is calculated for each motor based on the logging described in APPENDIX A. Based on $\bar{n}$ average slip $\bar{s}$ is calculated. In Table 16 average speed value ($\bar{n}$), standard deviation (σ) and average slip ($\bar{s}$) is presented for Siemens group. Also, for Siemens group, calculated frequency components according to Eq.1 and 2 are show in Table 16.

Table 16. Siemens group - frequency components according to Eq. 1 and 2.

		IM1	**IM2_H**	**IM2_BRB1**
$\bar{n}$	[rpm]	1437.35	1435.5	1427.40
σ	[rpm]	1.08	1.10	0.75
$\bar{s}$	[ ]	0.0418	0.043	0.0484
$\bar{s}f_s$	[Hz]	2.08	2.15	2.42
$3\bar{s}f_s$	[Hz]	6.26	6.45	7.26

Figure 39 shows the FFT of the frequency interval 0 – 8 Hz for Siemens group.
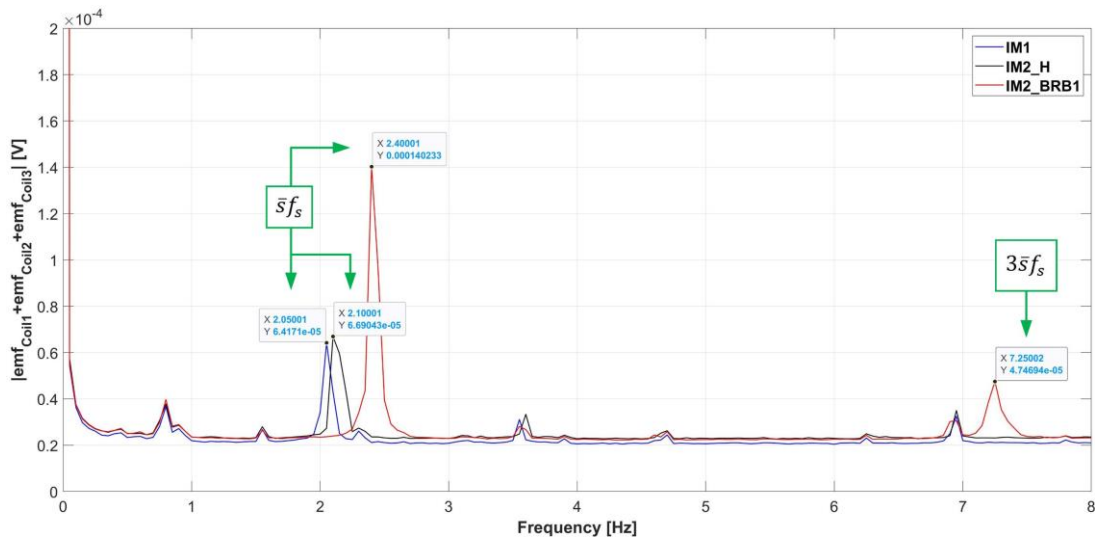
Figure 39. Siemens group - frequency spectrum of the interval 0 - 8 Hz.

From Figure 39 it can be observed that frequency component $\bar{s}f_s$ of healthy motors have small difference in amplitude and that big difference in amplitude compared to faulty motor. Percentage difference of the amplitudes for healthy motors, relative to IM1, is 4.26 %. Percentage difference of the amplitudes for IM1 and IM_BRB1 is, relative to IM1, is 118.53 %. Percentage difference of the amplitudes for IM2_H and IM_BRB1 is, relative to IM2_H, is 109.60 %. Amplitudes of frequency components $3\bar{s}f_s$ for healthy motors are negligible when compared to $3\bar{s}f_s$ component amplitude of faulty motor. Amplitude of $3\bar{s}f_s$ component for faulty motor is $4.74 \cdot 10^{-5}$ [V]. For Simens group frequency components defined by Eq. 3 and 4 are show in Table 17. For each motor components are calculated for k=1, 2, …, 10.

Table 17. Siemens group – frequency components defined by Eq. 3 and 4. for k=1, 2, …, 10.

k	$(1-2k\bar{s})f_s$	$(1+2k\bar{s})f_s$	$\left(\frac{k}{p}(1-\bar{s})-\bar{s}\right)f_s$	$\left(\frac{k}{p}(1-\bar{s})+\bar{s}\right)f_s$
IM1				
1	45.82	54.17	21.87	26.04
2	41.64	58.35	45.83	50.00
3	37.47	62.53	69.78	73.96
4	33.29	66.71	93.73	97.91
5	29.12	70.88	117.69	121.86
6	24.94	75.06	141.64	145.82
7	20.76	79.24	165.60	169.78
8	16.58	83.41	189.59	193.73
9	12.41	87.59	213.51	217.69
10	8.24	91.76	237.47	241.65
IM2_H				
1	45.70	54.30	21.77	26.07
2	41.40	58.60	45.70	50.00
3	37.10	62.90	69.62	73.92
4	32.80	67.20	93.55	97.85
5	28.50	71.50	117.47	121.77
6	24.20	75.80	141.40	145.70
7	19.90	80.10	165.32	169.62
8	15.60	84.40	189.25	193.55
9	11.30	88.70	213.17	217.47
10	7.00	93.00	237.10	241.40
IM2_BRB1				
1	45.16	54.84	21.37	26.21
2	40.32	59.68	45.16	50.00
3	35.48	64.52	68.95	73.79
4	30.64	69.36	92.74	97.58
5	25.80	74.20	116.53	121.37
6	20.96	79.04	140.32	145.16

7	16.12	83.88	164.11	168.95
8	11.28	88.72	187.90	192.74
9	6.44	93.56	211.69	216.53
10	1.60	98.40	235.48	240.32

Figure 40 shows the FFT of the frequency interval 8 – 19 Hz for Siemens group.
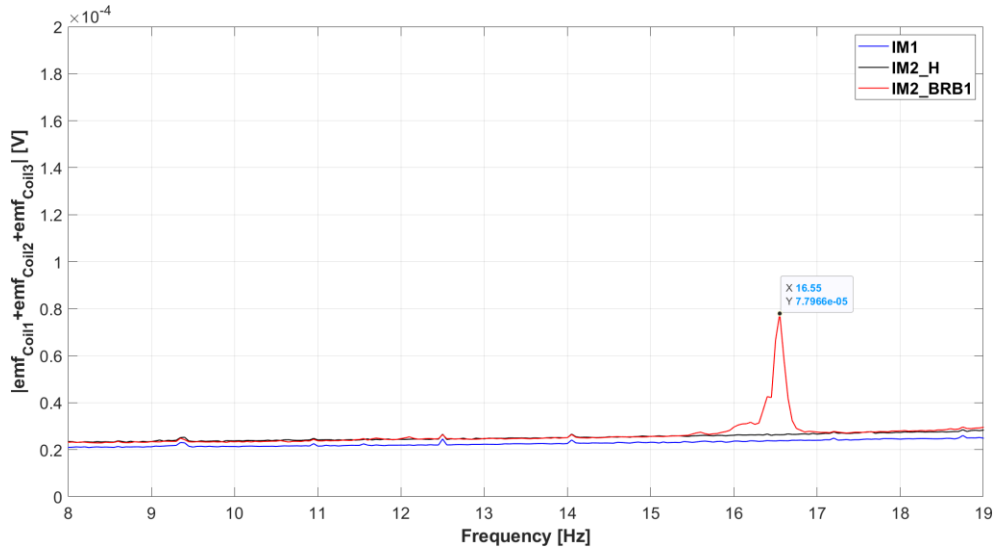
Figure 40. Siemens group - frequency spectrum of the interval 8 - 19 Hz.

In Figure 40 only one frequency component of the faulty motor stands out. At the frequency 16.55 Hz faulty motor has a peak whose value is $7.79 \cdot 10^{-5}$ [V]. All amplitudes of the healthy motors on the interval 8 – 19 Hz are negligible when compared to the frequency components of the faulty motor at 16.55 Hz. Looking at the frequencies from Table 17 one can observe that frequency 16.55 Hz does not match any of values for IM2_BRB1.

Figure 41 shows the FFT of the frequency interval 19 – 38 Hz for Siemens group.
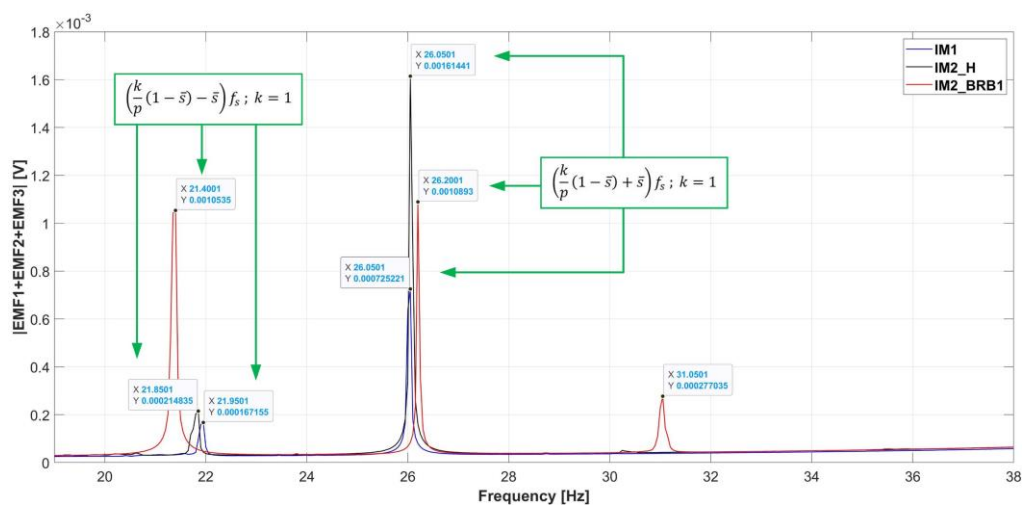
Figure 41. Siemens group - frequency spectrum of the interval 19 - 38 Hz.

From Figure 41 it can be observed that all frequency components that appear in range 20-28 Hz are predicted with Eq. 4. Frequencies that appear in the interval 21–22 Hz are defined with equation $\left(\frac{k}{p}(1-\bar{s})-\bar{s}\right)f_s$ and frequencies from the interval 26–26.3 Hz are defined with equation $\left(\frac{k}{p}(1-\bar{s})+\bar{s}\right)f_s$. Frequency components of healthy motors that appear at 21.8501 Hz (IM2_H) and 21.9501 Hz (IM1) have percentage difference in amplitudes, relative to IM1, 28.52 %. Percentage difference between healthy IM1 (21.9501 Hz) and faulty IM2_BRB1 (21.4001 Hz), relative to IM1, is 530.25 %. Percentage difference between healthy IM2_H (21.8501 Hz) and faulty IM2_BRB1 (21.4001 Hz), relative to IM2_H, is 390.37 %. Percentage difference between healthy IM1 and faulty IM2_BRB1 motor from the interval 26–26.3 Hz, relative to IM1, is 50.20 %. Percentage difference between healthy IM2_H and faulty IM2_BRB1 motor from the interval 26–26.3 Hz, relative to IM2_H, is -32.52 %. Percentage difference between healthy IM1and healthy IM2_H motor from the interval 26–26.3 Hz, relative to IM1, is 122.61 %. Figure 36 also show that when two intervals are compared, components of the healthy motor exhibit increase in amplitude while components of the faulty motor have negligible difference in amplitudes. Frequency component at 31.05 Hz that appears for faulty motor does not match any of values for IM2_BRB1 from Table 17.

Figure 42 shows the FFT of the frequency interval 38 – 50 Hz for Siemens group.

Figure 42. Siemens group - frequency spectrum of the interval 38 - 50 Hz.

From Figure 37 it can be observed that frequency components $(1-2\bar{s})f_s$ and $(1-4\bar{s})f_s$ appear only for faulty motor. Frequency components that appear for all motors/motor states in the interval 44.0001 – 44.4001 Hz do not match any of values from Table 17.

Figure 43 shows the FFT of the frequency interval 50 – 75 Hz for Siemens group.
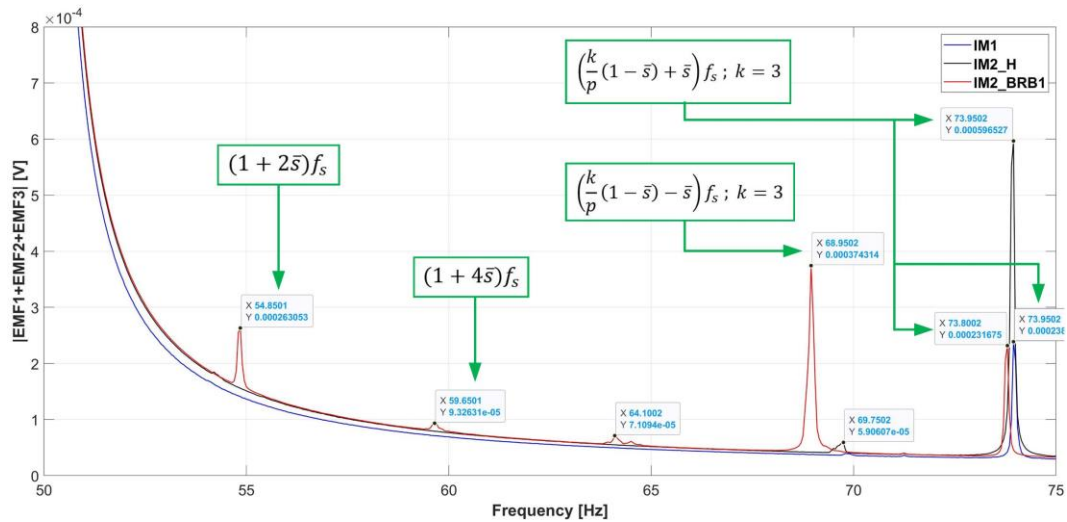
Figure 43. Siemens group - frequency spectrum of the interval 38 - 50 Hz.

From Figure 43 it can be observed that frequency components $(1 + 2\bar{s})f_s$ and $(1 + 4\bar{s})f_s$ appear only for faulty motor. Frequency components $\left(\frac{k}{p}(1 - \bar{s}) - \bar{s}\right)f_s$; $k = 3$ of the faulty motor stands out compared to the healthy motors. Percentage difference between healthy IM2_H and faulty IM2_BRB1 motor, relative to IM2_H, is 533.77 %. Frequency component $\left(\frac{k}{p}(1 - \bar{s}) + \bar{s}\right)f_s$; $k = 3$ is present for each motor/motor state and has highest amplitude for IM2_H. Percentage difference between healthy IM2_H and IM2_BRB1, relative to IM2_H, is -61.16 %. Percentage difference between healthy IM1 and IM2_BRB1, relative to IM1, is -2.91 %.

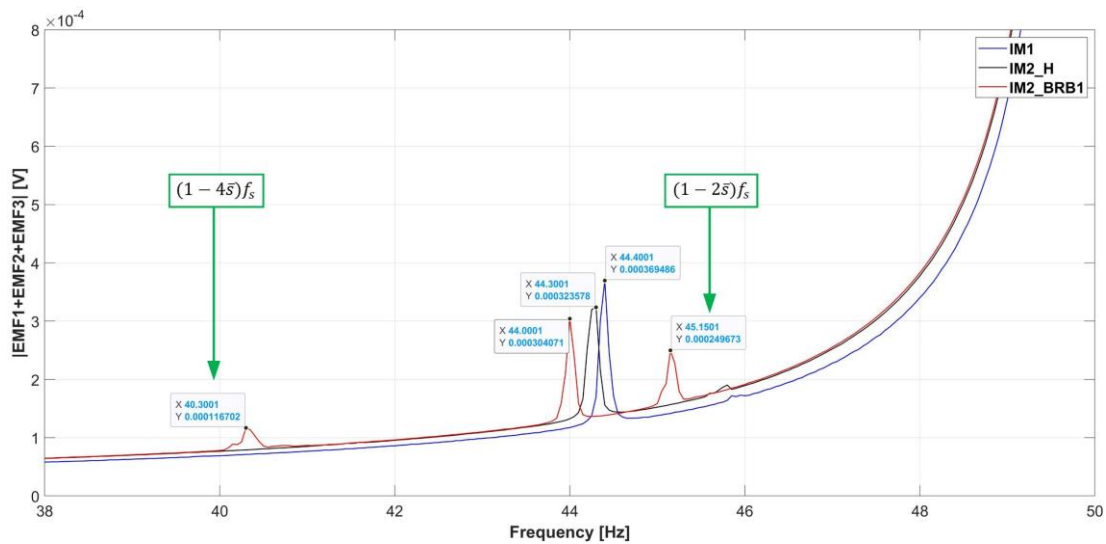Figure 44 shows the FFT of the frequency interval 75 – 100 Hz for Siemens group.
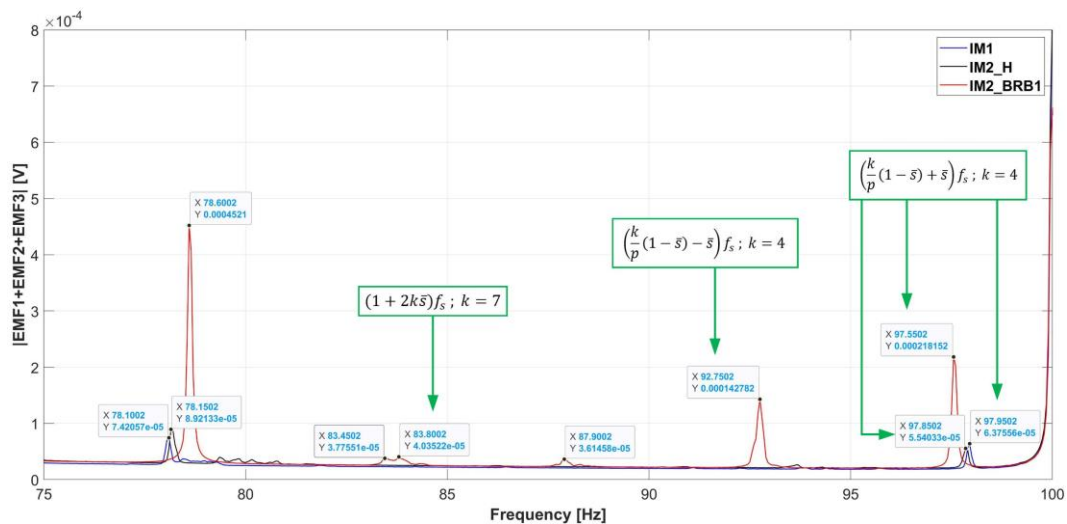
Figure 44. Siemens group - frequency spectrum of the interval 38 - 50 Hz.

From Figure 44 it can be observed that three frequency components from the interval 78.1-78.6002 Hz do not match any value from Table 17. Same applies for frequency component at 83.4502 Hz and at 87.9002 Hz. Frequency components that appear only for faulty motor are

54

$(1 + 2\bar{s})f_s$; $k = 7$ and $\left(\frac{k}{p}(1 - \bar{s}) - \bar{s}\right)f_s$; $k = 4$. Frequency component that appears for all motor/motor state is $\left(\frac{k}{p}(1 - \bar{s}) + \bar{s}\right)f_s$; $k = 4$ and it has highest amplitude value for faulty motor. Percentage difference between healthy IM1 and faulty IM2_BRB1 motor, relative to IM1, is 242.17 %.

Frequency components on interval 0 – 100 Hz that only appear for IM2_BRB1 or have higher IM2_BRB1 amplitude value compared to healthy motors, are listed in Table 18.

Table 18. Frequency components for Siemens group that indicate the presence of broken rotor bar.

No.	Frequency component	f [Hz]	Frequency interval [Hz]
1	$\bar{s}f_s$	2.4	1.8-2.8
2	$3\bar{s}f_s$	7.25	7-8
3	$\left(\frac{1}{p}(1 - \bar{s}) - \bar{s}\right)f_s$	21.4	20-23
4	$(1 - 4\bar{s})f_s$	40.3	40-41
5	$(1 - 2\bar{s})f_s$	45.15	44.6-46
6	$(1 + 2\bar{s})f_s$	54.85	54-56
7	$(1 + 4\bar{s})f_s$	59.65	58-60
8	$\left(\frac{3}{p}(1 - \bar{s}) - \bar{s}\right)f_s$	68.95	68-71
9	$(1 + 8\bar{s})f_s$		
10	$(1 + 14\bar{s})f_s$	83.80	82-85
11	$\left(\frac{2}{p}(1 - \bar{s}) - \bar{s}\right)f_s$		
12	$\left(\frac{4}{p}(1 - \bar{s}) - \bar{s}\right)f_s$	92.75	91-95
13	$\left(\frac{2}{p}(1 - \bar{s}) + \bar{s}\right)f_s$		
14	$\left(\frac{4}{p}(1 - \bar{s}) + \bar{s}\right)f_s$	97.55	96-98

Corresponding frequency intervals that are chosen for number of measurements analysis are show in Table 18.

Randomly taken number of measurements that have been investigated are 1, 2, 3, 4, 5 and 10. This series is chosen based on the dynamics of the results. Results based on flowchart from Figure 18 for Siemens group are shown in Figure 45 and Figure 46.
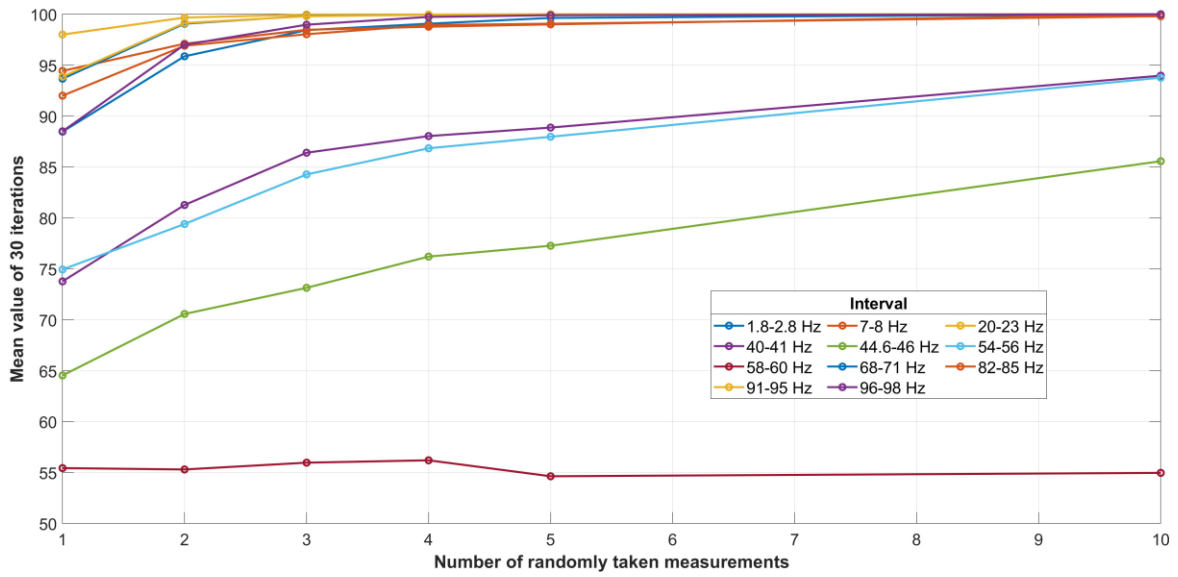
Figure 45. Dependence of mean value of 30 iterations on number of randomly taken measurements.
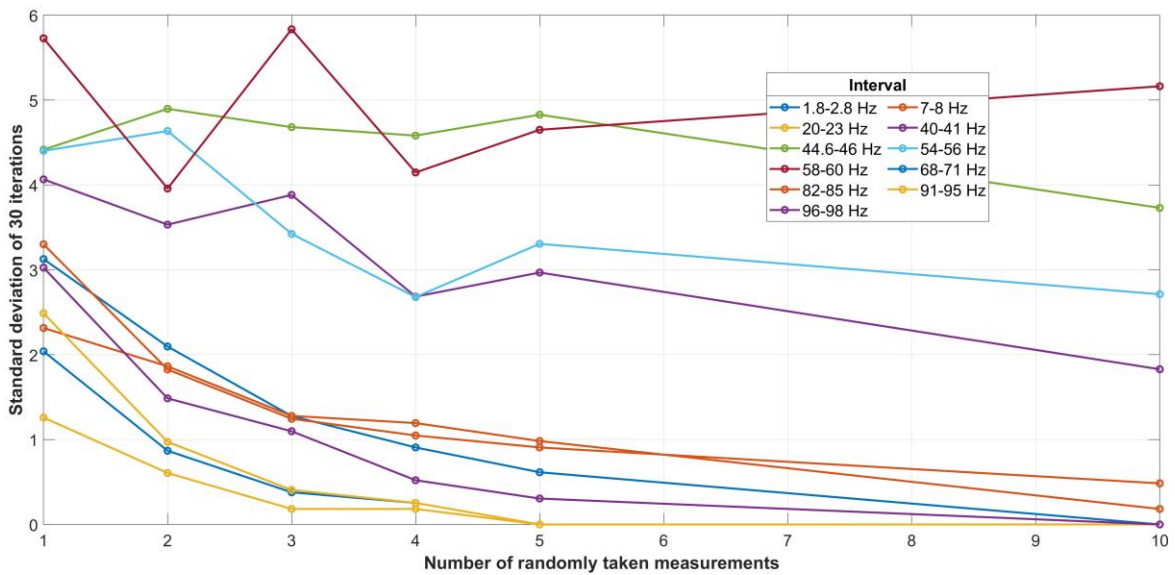
Figure 46. Dependence of standard deviation of 30 iterations on number of randomly taken measurements.

On Figure 45 it is observable that different frequency components have different response to randomly taken number of measurements. For 1 randomly taken measurement highest value has 20-23 Hz interval with corresponding frequency component $\left(\frac{1}{p}(1-\bar{s})-\bar{s}\right)f_s$. Lowest value has 58-60 Hz interval with corresponding frequency component $(1+4\bar{s})f_s$. Frequency components that have maximum mean value of 30 iterations for 5 randomly taken measurements are $\left(\frac{1}{p}(1-\bar{s})-\bar{s}\right)f_s$, $\left(\frac{3}{p}(1-\bar{s})-\bar{s}\right)f_s$ and $\left(\frac{4}{p}(1-\bar{s})-\bar{s}\right)f_s$. At 10 randomly taken measurements frequency components $\bar{s}f_s$, $\left(\frac{1}{p}(1-\bar{s})-\bar{s}\right)f_s$, $\left(\frac{4}{p}(1-\bar{s})-\bar{s}\right)f_s$, $\left(\frac{3}{p}(1-\bar{s})-\bar{s}\right)f_s$ and $\left(\frac{4}{p}(1-\bar{s})+\bar{s}\right)f_s$ have maximum mean value of 30 iterations. At 10 randomly taken

measurements frequency components $3\bar{s}f_s$, $(1 + 14\bar{s})f_s$, $(1 - 4\bar{s})f_s$, $(1 + 2\bar{s})f_s$, $(1 - 2\bar{s})f_s$ and $(1 + 4\bar{s})f_s$ have values 99.96 %, 99.80 %, 93.96 %, 93.76 %, 85.86 % and 54.96 % respectively.

On Figure 46 it is observable that different frequency components have different standard deviation response to randomly taken number of measurements. Frequency component that for 1 randomly taken measurement has lowest value is $\left(\frac{1}{p}(1 - \bar{s}) - \bar{s}\right)f_s$. Frequency component that for 1 randomly taken measurement has highest value is $(1 + 4\bar{s})f_s$. Frequency components that have minimum value of standard deviation of 30 iterations for 5 randomly taken measurements are $\left(\frac{1}{p}(1 - \bar{s}) - \bar{s}\right)f_s$, $\left(\frac{3}{p}(1 - \bar{s}) - \bar{s}\right)f_s$ and $\left(\frac{4}{p}(1 - \bar{s}) - \bar{s}\right)f_s$. At 10 randomly taken measurements frequency components $\bar{s}f_s$, $\left(\frac{1}{p}(1 - \bar{s}) - \bar{s}\right)f_s$, $\left(\frac{4}{p}(1 - \bar{s}) - \bar{s}\right)f_s$, $\left(\frac{3}{p}(1 - \bar{s}) - \bar{s}\right)f_s$ and $\left(\frac{4}{p}(1 - \bar{s}) + \bar{s}\right)f_s$ have minimum value of standard deviation of 30 iterations. At 10 randomly taken measurements frequency components $3\bar{s}f_s$, $(1 + 14\bar{s})f_s$, $(1 - 4\bar{s})f_s$, $(1 + 2\bar{s})f_s$, $(1 - 2\bar{s})f_s$ and $(1 + 4\bar{s})f_s$ have standard deviation values 0.18 %, 0.48 %, 1.82 %, 2.71 %, 3.72 % and 5.16 % respectively.

6.4. Končar – Statistical Analysis

The raw data visualization for each motor, each motor state and each day is shown with histograms in Figure 47. The histogram of each day contains all data values obtained with the data logger for all three coils. The number of bins chosen to represent the histogram is 100. This number of bins was chosen for visualization purposes only, i.e., to show 10 histograms in one figure that can be visually distinguished. The visualization is not intended to draw conclusions about the data distribution.
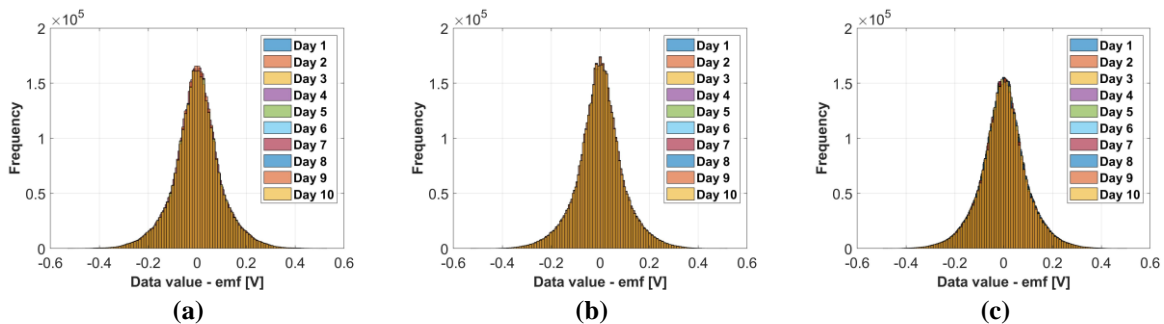
Figure 47. Končar group - raw data visualization for each day: **(a)** IM1; **(b)** IM2_H; **(c)** IM2_BRB1; Number of bins for all histograms is 100.

The results of the numerical normality tests, same test applied for Siemens group, are shown in Table 19.

Table 19. Končar group - results of the normality tests.

Test	Motor	p-value									
		day 1	day 2	day 3	day 4	day 5	day 6	day 7	day 8	day 9	day 10
One-sample Kolmogorov–Smirnov	IM1	0	0	0	0	0	0	0	0	0	0
	IM2_H	0	0	0	0	0	0	0	0	0	0
	IM2_BRB1	0	0	0	0	0	0	0	0	0	0
Anderson-Darling	IM1	$<5\cdot10^{-4}$	$<5\cdot10^{-4}$	$<5\cdot10^{-4}$	$<5\cdot10^{-4}$	$<5\cdot10^{-4}$	$<5\cdot10^{-4}$	$<5\cdot10^{-4}$	$<5\cdot10^{-4}$	$<5\cdot10^{-4}$	$<5\cdot10^{-4}$
	IM2_H	$<5\cdot10^{-4}$	$<5\cdot10^{-4}$	$<5\cdot10^{-4}$	$<5\cdot10^{-4}$	$<5\cdot10^{-4}$	$<5\cdot10^{-4}$	$<5\cdot10^{-4}$	$<5\cdot10^{-4}$	$<5\cdot10^{-4}$	$<5\cdot10^{-4}$
	IM2_BRB1	$<5\cdot10^{-4}$	$<5\cdot10^{-4}$	$<5\cdot10^{-4}$	$<5\cdot10^{-4}$	$<5\cdot10^{-4}$	$<5\cdot10^{-4}$	$<5\cdot10^{-4}$	$<5\cdot10^{-4}$	$<5\cdot10^{-4}$	$<5\cdot10^{-4}$
Jarque-Bera	IM1	<0.001	<0.001	<0.001	<0.001	<0.001	<0.001	<0.001	<0.001	<0.001	<0.001
	IM2_H	<0.001	<0.001	<0.001	<0.001	<0.001	<0.001	<0.001	<0.001	<0.001	<0.001
	IM2_BRB1	<0.001	<0.001	<0.001	<0.001	<0.001	<0.001	<0.001	<0.001	<0.001	<0.001
Lilliefors	IM1	<0.001	<0.001	<0.001	<0.001	<0.001	<0.001	<0.001	<0.001	<0.001	<0.001
	IM2_H	<0.001	<0.001	<0.001	<0.001	<0.001	<0.001	<0.001	<0.001	<0.001	<0.001
	IM2_BRB1	<0.001	<0.001	<0.001	<0.001	<0.001	<0.001	<0.001	<0.001	<0.001	<0.001

The results from Table 19 show that the p-value for every motor, motor state and day is less than 0.001, which means the rejection of the null hypothesis that the data come from a normal distribution. The Q-Q plot for each motor, motor state, and day is shown in Figure 48.

(a)

(b)

(c)
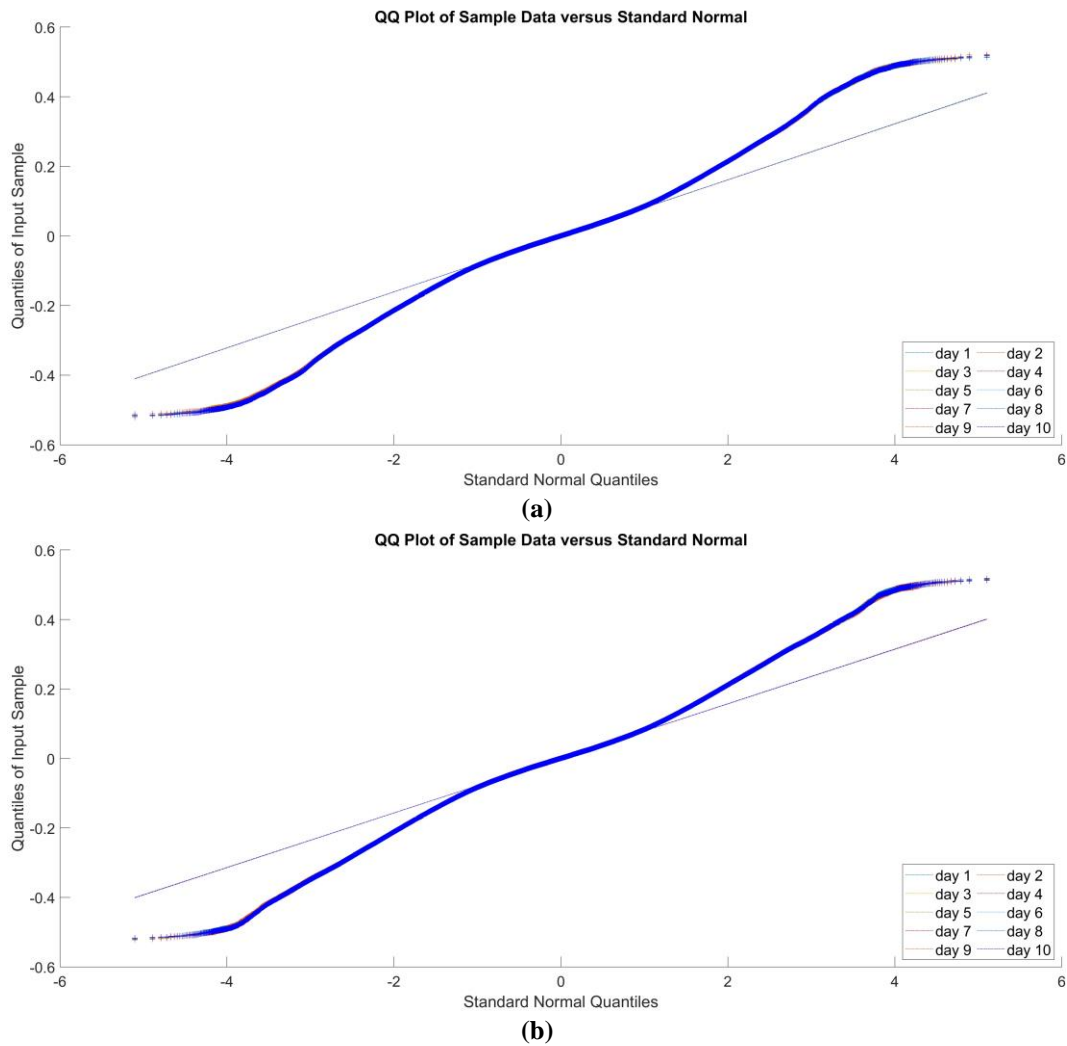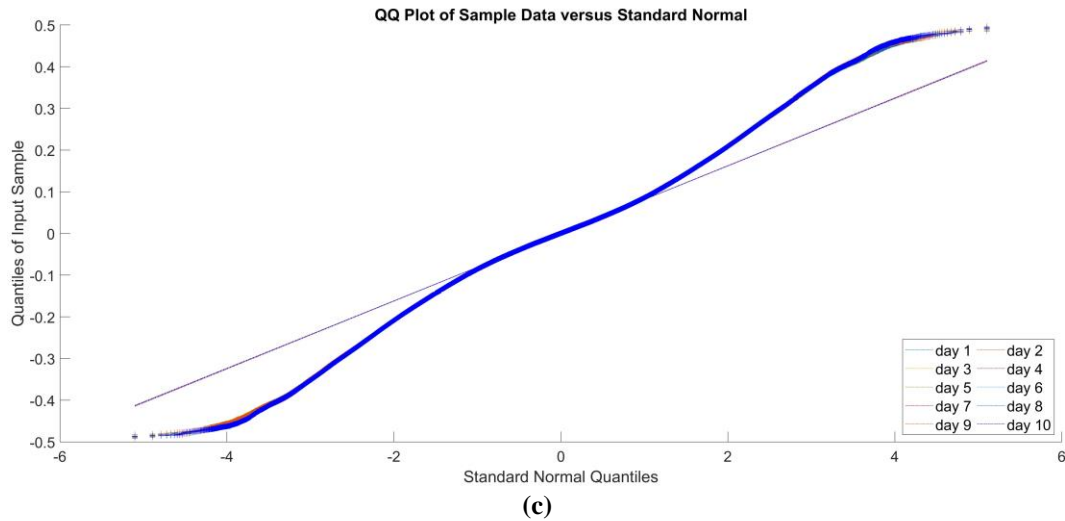
Figure 48. Končar group - Quantile-Quantile plot for each day: **(a)** IM1; **(b)** IM2_H; **(c)** IM2_BRB1.

Q-Q plots on Figure 48 show that data for all motors and all days is non-normally distributed. For Končar group there is no inconsistency between numerical tests and Q-Q plots. This conclusion leads to the application of Friedman test, according to flowchart on Figure 28.

6.4.1. Končar – Non-parametric Assumption

The results of the Friedman test for each motor are shown in Table 20.

Table 20. Končar group - results of the Friedman test for each motor.

Motor		SS	df	MS	Chi-sq	Prob>Chi-sq
	Columns	104.05	9	11.5611	11.35	0.2522
IM1	Error	247,428,043.95	26,999,991	9.164		
	Total	247,428,148	29,999,999			
	Columns	60.2422	9	6.69358	6.57	0.6814
IM2_H	Error	247,426,124.2578	26,999,991	9.16393		
	Total	247,426,184.5	29,999,999			
	Columns	34.0362	9	3.7818	3.71	0.9292
IM2_BRB1	Error	247,427,684.4638	26,999,991	9.16399		
	Total	247,427,718.5	29,999,999			

The results from Table 20 show that all p-values are greater than 0.05, i.e., for each motor/motor condition, there is insufficient evidence to reject the null hypothesis at a 5% significance level, meaning that all measurements for a given motor come from the same distribution. The results of the multiple comparison with uncorrected p-values for each motor are shown in Figure 49.
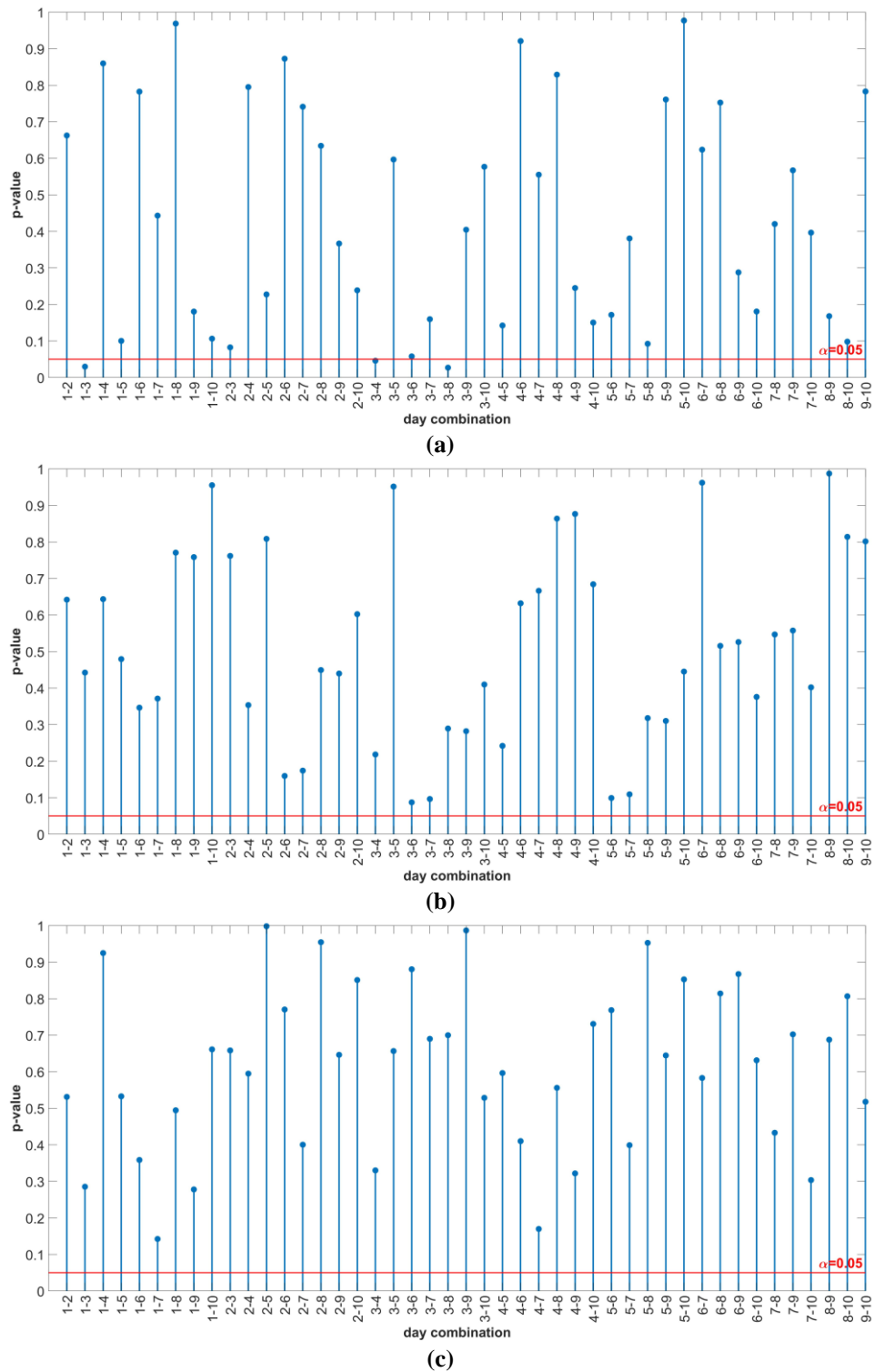
Figure 49. Končar group - multiple comparison results of Friedman test—uncorrected p-values: **(a)** IM1;
(b) IM2_H; **(c)** IM2_BRB1.

Figure 49 shows that not all p-values are above the significance level of 0.05. To check whether
the significant p-values are false-positive, the BH correction is applied. The results of the BH
correction are shown in Figure 50.
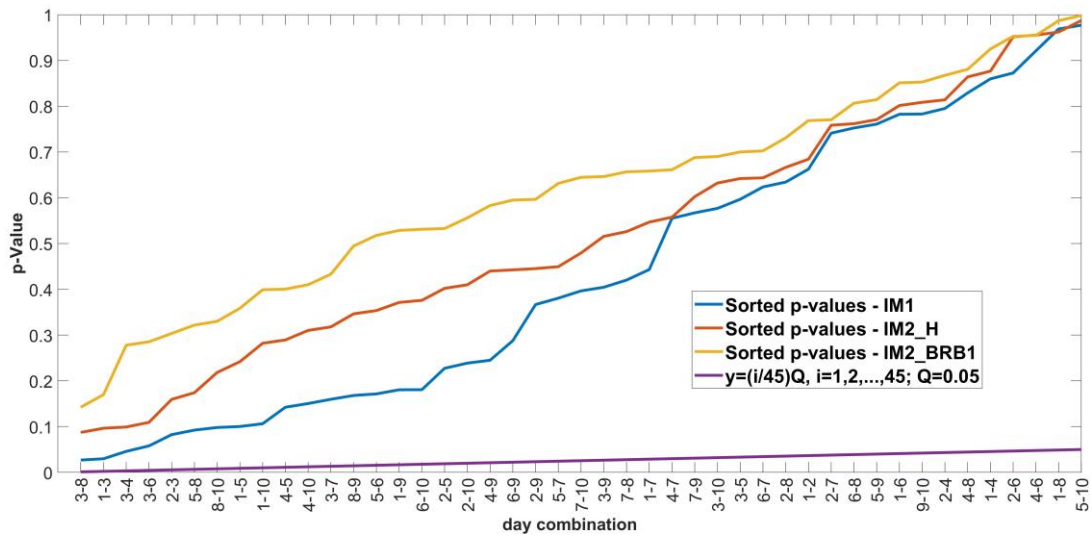
Figure 50. Končar group - correction of p-values with BH after multiple comparison of the Friedman test.

The results from Figure 50 show that there is no intersection of the sorted p-values with the line $y=(i/m)Q$, which means that all day-to-day combinations with p-values below 0.05 are false positives, i.e., there is no statistically significant difference between all day-to-day combinations for each motor.

Results of Friedman test for healthy-BRB1 discrimination are shown in Table 21.

Table 21. Končar group - results of the Friedman test for motor comparison.

	SS	df	MS	Chi-sq	Prob>Chi-sq
Columns	5.24513	2	2.62256	5.25	0.0725
Error	59,951,939.25487	59,999,998	0.9992		
Total	59,951,944.5	89,999,999			

Results from Table 21 show that there is not enough evidence to reject the null hypothesis at a 5% significance level. The null hypothesis states that data from all motors and motor states come from the same distribution. The multiple comparison by the variable "Motor" is shown in Table 22 and the estimated difference in mean ranks (with 95% confidence intervals) is shown in Figure 51.

Table 22. Končar group - results of the multiple comparison by variable "Motor"—uncorrected p-values.

Motor 1	Motor 2	Difference	p-Value	Lower	Upper
IM1	IM2_H	0.00011313	0.66114	-0.00039272	0.00061899
IM1	IM2_BRB1	0.00055922	0.030257	5.3359e-05	0.0010651
IM2_H	IM2_BRB1	0.00044608	0.083923	-5.9774e-05	0.00095194
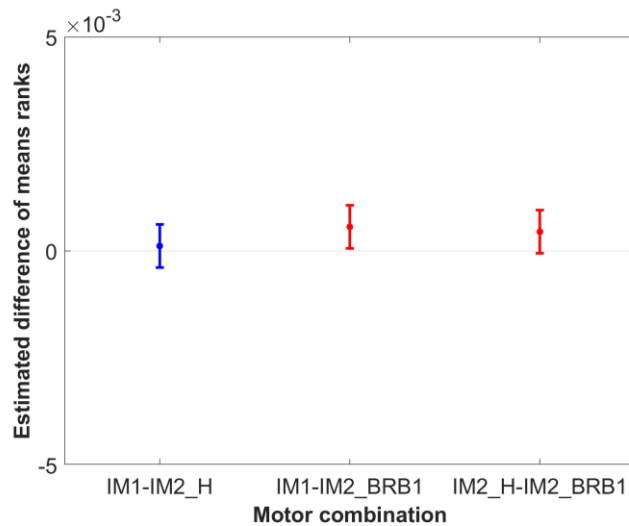
Figure 51. Končar group - estimated difference in mean ranks of variable "Motor" with 95% confidence interval.

The results from Table 22 show that there is not enough evidence to reject the null hypothesis at a 5% significance level for IM1 and IM2_H combination, there is a statistically significant difference between IM1 and IM2_BRB1 combination and that there is not enough evidence to reject the null hypothesis at a 5% significance level for IM2_H and IM2_BRB1 combination. Figure 46 shows the graphical representation of the results from Table 22. The percentage difference of estimated mean ranks for the motor combinations with BRB fault compared to the healthy motor combinations is shown in Table 23.

Table 23. Končar group - percentage difference in estimated differences in mean ranks relative to the healthy–healthy motor combination.

Reference	Motor Combination	Percentage Difference in Estimated Differences in Mean Ranks
IM1–IM2_H	IM1–IM2_BRB1	394.31 %
	IM2_H–IM2_BRB1	294.30 %

6.5. Končar – Feature Analysis

Results of feature analysis based on 1000 measurements for the Končar group are shown in Figure 52.
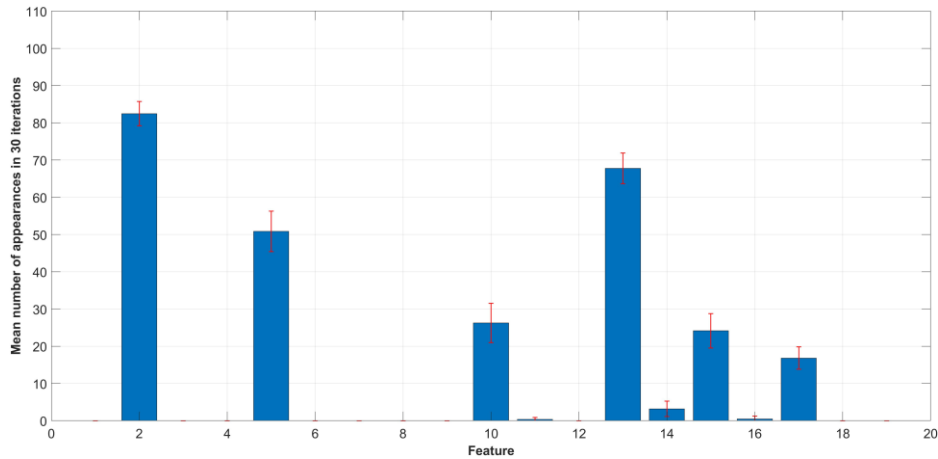
Figure 52. Mean number of appearances in 30 iterations for Končar group.

Figure 52 shows mean number of appearances of features in 30 iterations, according to flowchart on Figure 16 and corresponding standard deviation interval displayed with red bars. From Figure 52 it is observable that 9 out of 19 features appear with different mean values. Feature 11, 14 and 16 have mean values that is lower than 10 %. Highest value, 82.46 %, has feature 2. Second highest value, 67.76 %, has feature 13. Third highest value, 50.83 %, has feature 5. Feature 10 has mean value 26.23 %, feature 15 24.13 % and feature 17 has mean value 16.8 %.

Results of feature analysis for different number of measurements are shown in Figure 53 (3D bar graph), Figure 54 (view 1), Figure 55 (view 2) and Figure 56 (view 3).
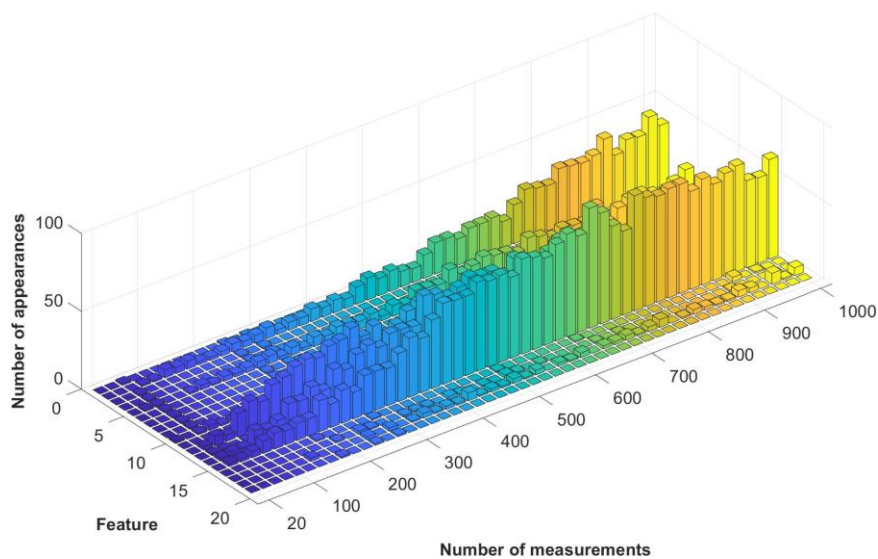
Figure 53. Končar group – Feature appearance as a function of number of measurements – 3D bar graph.
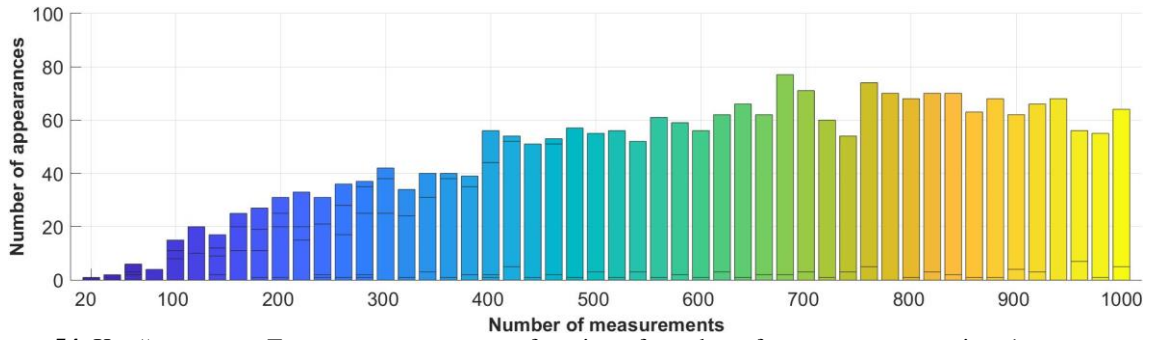
Figure 54. Končar group – Feature appearance as a function of number of measurements – view 1.
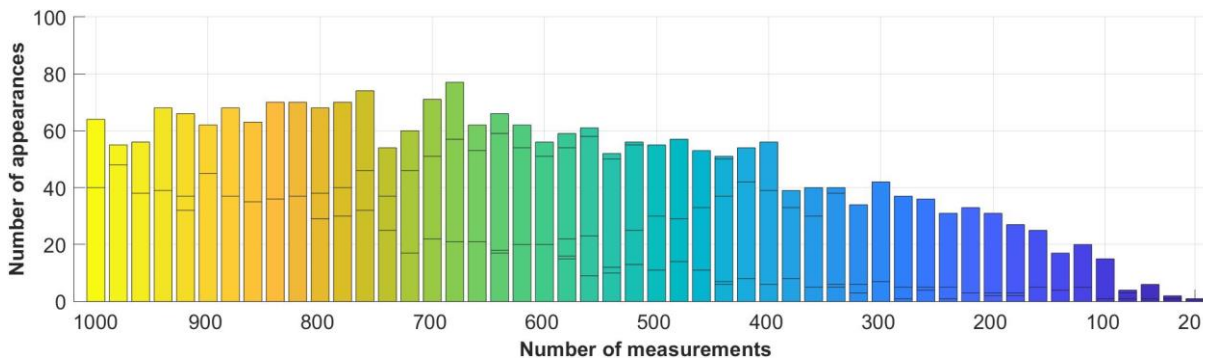
Figure 55. Končar group – Feature appearance as a function of number of measurements – view 2.
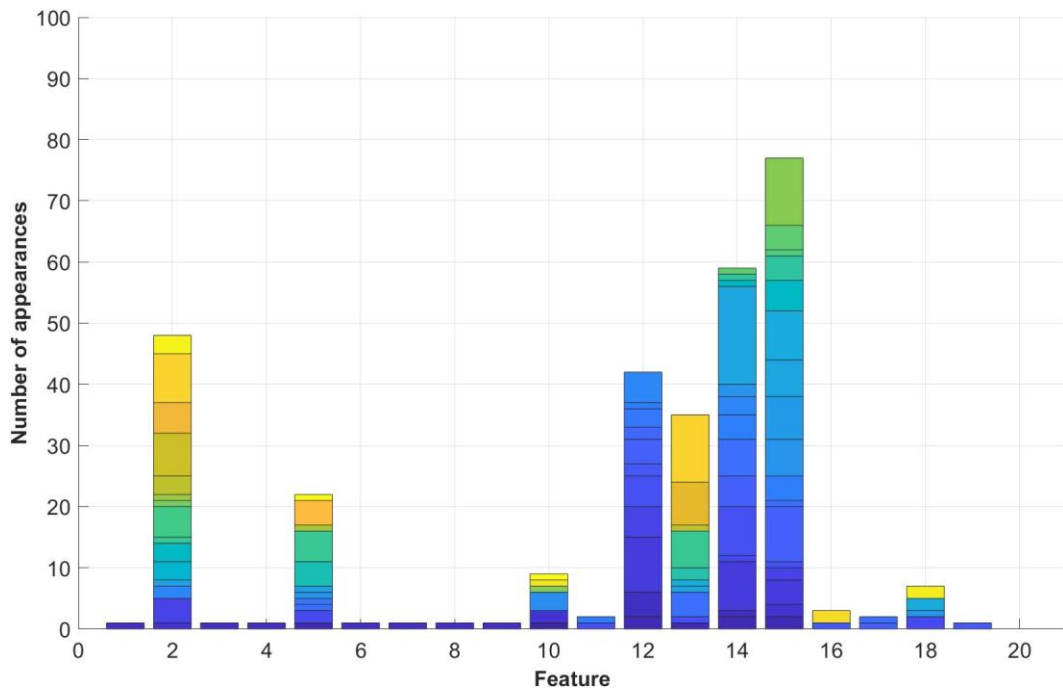
Figure 56. Končar group – Feature appearance as a function of number of measurements – view 3.

Based on Figure 56 features 1, 3, 4, 6, 7, 8, 9, 10, 11, 16, 17, 18 and 19 are considered negligible since their maximum values are all below 10 %. Feature 2 has overall increase trend over whole interval with maximum value of 48 % at nm=980. Feature 5 has overall increase trend over whole interval with maximum value of 22 % at nm=1000. Feature 12 has overall increase trend

on the interval nm=20, …, 300 and overall decreasing trend on the interval nm=320, …, 1000. Maximum value for feature 12 is 42 % at nm=320. Feature 13 has overall increase trend over whole interval with maximum value of 35 % at nm=900. Feature 14 has overall increasing trend on the interval nm=20, …, 640 and overall decreasing trend on interval nm=660, …, 1000. Maximum value for feature 14 is 59 % at nm=640. Feature 15 has overall increasing trend on the interval nm=20, …, 680 and overall decreasing trend on interval nm=700, …, 1000. Maximum value for feature 16 is 77 % at nm=680.

6.6. Končar – FFT Analysis

FFT analysis for Siemens and Končar group is based on 1000 measurements. First, all signals for each motor/motor state are added as shown in Figure 16 (e.g., M1=Coil 1+Coil 2+Coil 3). On each measurement of each motor/motor state FFT is applied. Afterwards, for each frequency component mean value is calculated. FFT for each motor/motor state of the is shown i for Končar group is shown in Figure 57.
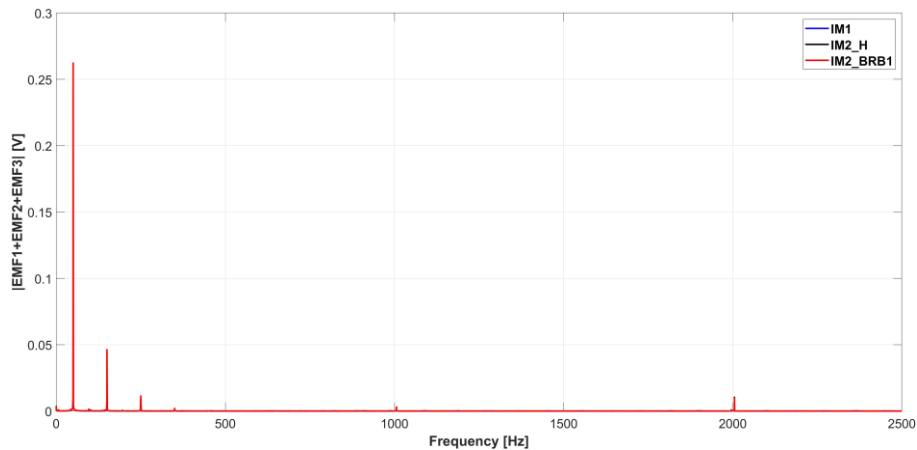
Figure 57. Končar group - FFT of IM1, IM2_H and IM2_BRB1

In Table 24 average speed value, standard deviation and average slip is presented for Končar group. Also, for Končar group, calculated frequency components according to Eq.1 and 2 are show in Table 24.

Table 24. Končar group - frequency components according to Eq. 1 and 2.

		IM1	IM2_H	IM2_BRB1
$\bar{n}$	[rpm]	2807.65	2795.45	2786.5
σ	[rpm]	1.04	0.88	0.75
$\bar{s}$	[ ]	0.0641	0.0681	0.0711
$\bar{s}f_s$	[Hz]	3.20	3.40	3.55
$3\bar{s}f_s$	[Hz]	9.61	10.22	10.65

For Končar group frequency components defined by Eq. 3 and 4 are show in Table 25. For each motor, components are calculated for k=1, 2, …, 10.

Table 25. Končar group – frequency components defined by Eq. 3 and 4. for k=1, 2, …, 10.

k	$(1-2k\overline{s})f_s$	$(1+2k\overline{s})f_s$	$\left(\frac{k}{p}(1-\overline{s})-\overline{s}\right)f_s$	$\left(\frac{k}{p}(1-\overline{s})+\overline{s}\right)f_s$
IM1				
1	43.58	56.41	43.58	50.00
2	37.17	62.82	90.38	96.79
3	30.76	69.23	137.17	143.58
4	24.35	75.64	183.97	190.38
5	17.94	82.06	230.76	237.17
6	11.53	88.47	277.56	283.97
7	5.12	94.88	324.35	330.76
8	-1.29	101.29	371.14	377.56
9	-7.70	107.70	417.94	424.35
10	-14.11	114.11	464.73	471.14
IM2_H				
1	43.18	56.81	43.18	50.00
2	36.36	63.63	89.77	97.00
3	29.54	70.45	136.36	143.18
4	22.72	77.27	182.95	189.77
5	15.90	84.09	229.54	236.36
6	9.09	90.91	276.13	282.95
7	2.27	97.72	322.72	329.54
8	-4.54	104.54	369.31	376.13
9	-11.36	111.36	415.90	422.72
10	-18.18	118.18	462.49	469.31
IM2_BRB1				
1	42.88	57.11	42.88	50.00
2	35.76	64.23	89.32	96.44
3	28.65	71.35	135.76	142.88
4	21.53	78.46	182.20	189.32
5	14.41	85.58	228.65	235.76
6	7.30	92.70	275.09	282.20
7	0.18	99.81	321.53	328.65
8	-6.93	106.93	367.97	375.09
9	-14.05	114.05	414.41	421.53
10	-21.16	121.16	460.85	467.97

Figure 58 shows the FFT of the frequency interval 0 – 8 Hz for Končar group.
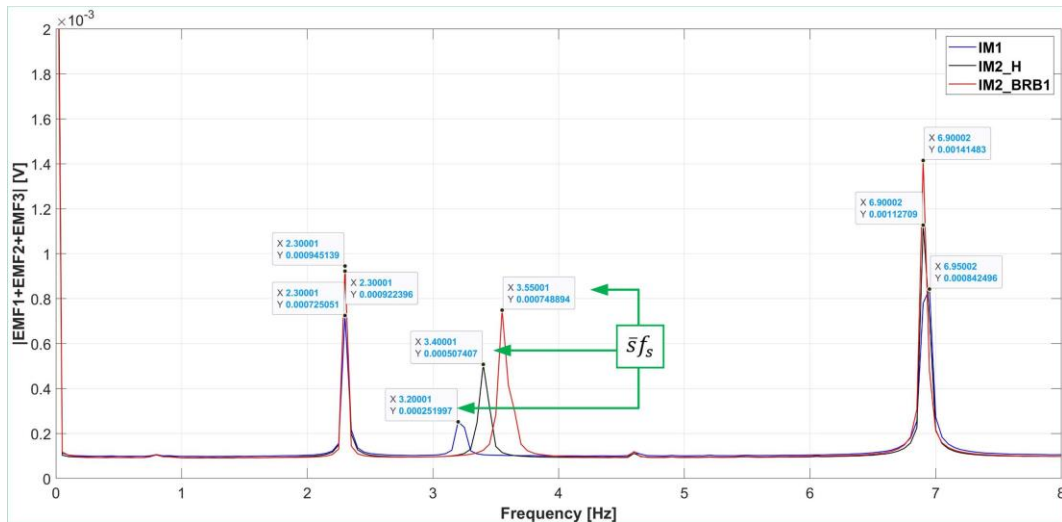
Figure 58. Končar group - frequency spectrum of the interval 0 - 8 Hz.

From Figure 58 frequency components at 2.3 Hz and 6.9 Hz that appear for all motors/motor states do not match any value from the Table 25. Each motor/motor state has component $\bar{s}f_s$. The lowest amplitude value appears for IM1 and the highest amplitude value appears for IM2_BRB1. Percentage difference between healthy IM1 and faulty IM2_BRB1 motor, relative to IM1, is 197.18 %. Percentage difference between healthy IM2_H and faulty IM2_BRB1 motor, relative to IM2_H, is 47.59 %.

Figure 59 shows the FFT of the frequency interval 8 – 14 Hz for Končar group.

Figure 59. Končar group - frequency spectrum of the interval 8 - 14 Hz.

From Figure 59 frequency components at 11.5 Hz that appears for all motors/motor states matches only for IM1 and frequency component $(1 - 2k\bar{s})f_s$; $k = 6$. Frequency component $3\bar{s}f_s$ has the highest amplitude value for the IM2_BRB1 and lowest amplitude value for IM2_H.

Percentage difference between IM1 and IM2_BRB1 motor, relative to IM1, is 8.54 %. Percentage difference between IM2_H and IM2_BRB1 motor, relative to IM2_H, is 29.50 %.

Figure 60 shows the FFT of the frequency interval 14 – 26 Hz for Končar group.
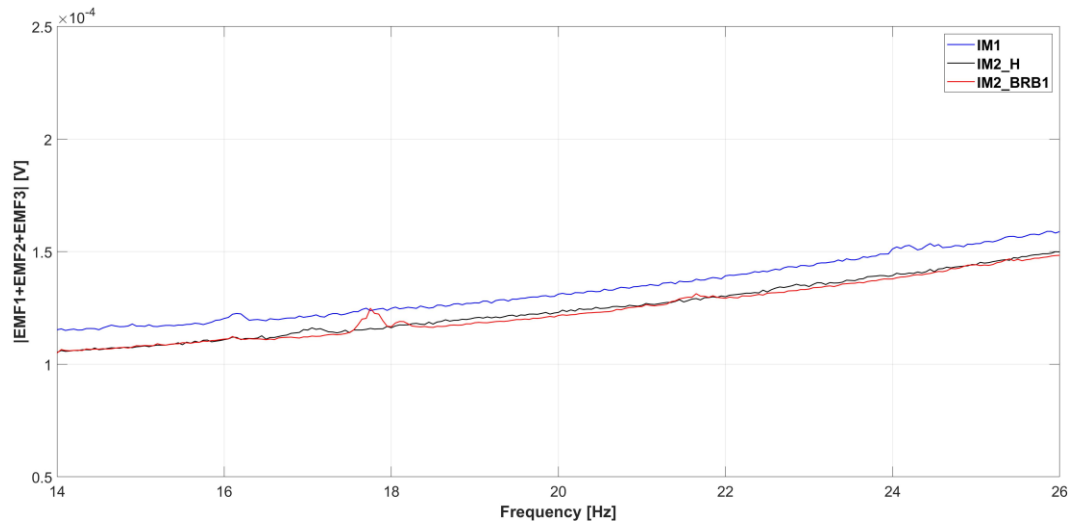
Figure 60. Končar group - frequency spectrum of the interval 14 - 26 Hz.

From Figure 60 it observable that for interval 14-26 Hz there are no interesting peaks except for IM2_BRB1 at 17.9 Hz but as its amplitude has negligible difference when compared to IM1amplitude, no attention is given to this frequency component.

Figure 61 shows the FFT of the frequency interval 26 – 34 Hz for Končar group.
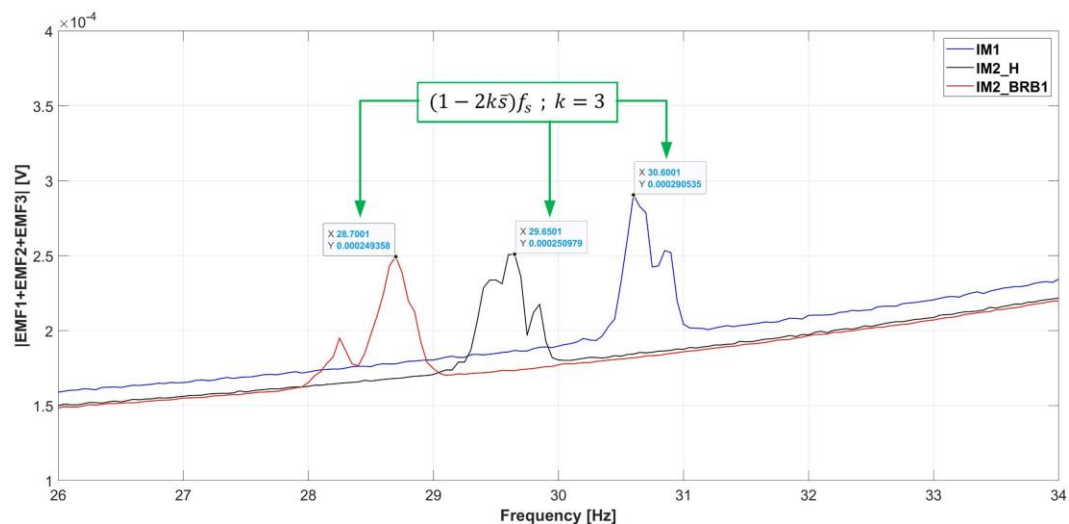
Figure 61. Končar group - frequency spectrum of the interval 26 - 34 Hz.

From Figure 61 it observable that for the interval 26-34 Hz frequency component $(1 - 2k\bar{s})f_s$; $k = 3$ is present for all motors/motor states. Percentage difference between IM1 and IM2_BRB1 motor, relative to IM1, is -14.17 %. Percentage difference between IM1 and IM2_H motor, relative to IM1, is -13.61 %.

Figure 62 shows the FFT of the frequency interval 34 – 50 Hz for Končar group.
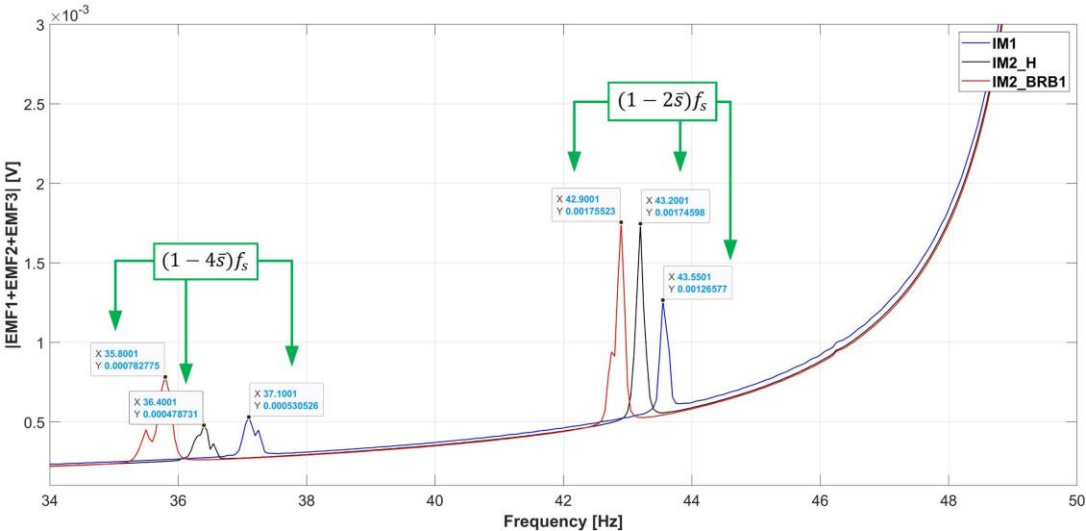
Figure 62. Končar group - frequency spectrum of the interval 34 - 50 Hz.

From Figure 62 it observable that for the interval 35-38 Hz frequency component $(1 - 4\bar{s})f_s$ is present for all motors/motor states. Percentage difference between IM1 and IM2_BRB1 motor, relative to IM1, is 47.54 %. Percentage difference between IM1 and IM2_H motor, relative to IM1, is -9.76 %. For the interval 42-44 Hz frequency component $(1 - 2\bar{s})f_s$ is present for all motors/motor states. Percentage difference between IM1 and IM2_BRB1 motor, relative to IM1, is 38.66 %. Percentage difference between IM1 and IM2_H motor, relative to IM1, is 37.93 %. Percentage difference between IM2_H and IM2_BRB1 motor, relative to IM2_H, is 0.53 %.

Figure 63 shows the FFT of the frequency interval 50 – 68 Hz for Končar group.
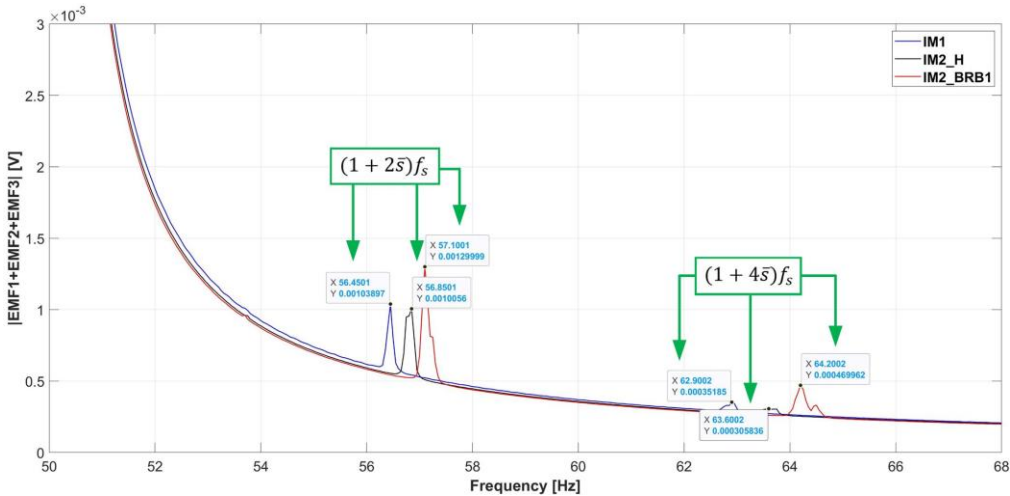
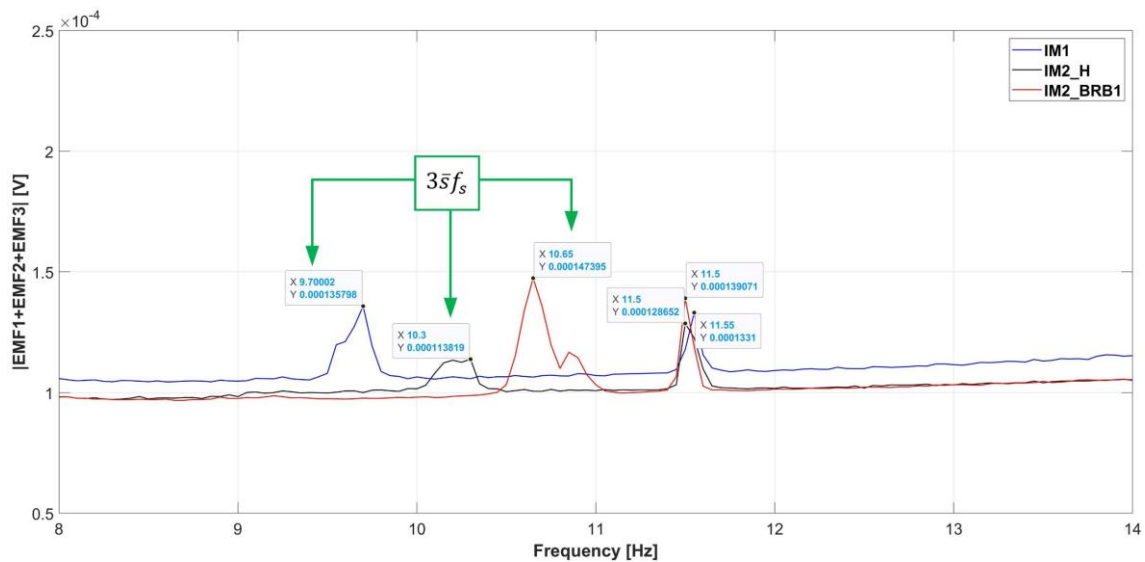**Figure 63.** Končar group - frequency spectrum of the interval 50 - 68 Hz.

From Figure 63 it observable that for the interval 56-58 Hz frequency component $(1 + 2\bar{s})f_s$ is present for all motors/motor states. Percentage difference between IM1 and

IM2_BRB1 motor, relative to IM1, is 25.12 %. Percentage difference between IM1 and IM2_H motor, relative to IM1, is -3.21 %. For the interval 62-64 Hz frequency component $(1 + 4\bar{s})f_s$ is present for all motors/motor states. Percentage difference between IM1 and IM2_BRB1 motor, relative to IM1, is 33.56 %. Percentage difference between IM1 and IM2_H motor, relative to IM1, is -13.07 %.

Figure 64 shows the FFT of the frequency interval 50 – 68 Hz for Končar group.
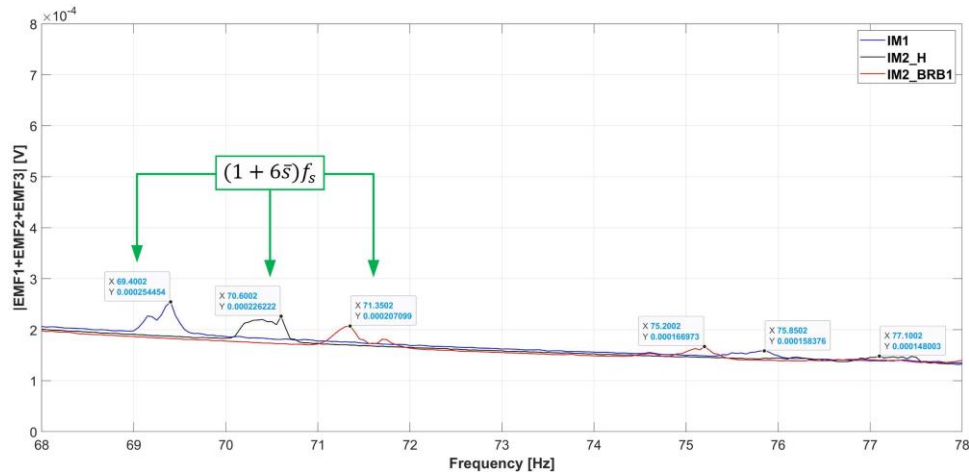
Figure 64. Končar group - frequency spectrum of the interval 68 - 78 Hz.

From Figure 64 it observable that for the interval 69-72 Hz frequency component $(1 + 6\bar{s})f_s$ is present for all motors/motor states. Percentage difference between IM1 and IM2_BRB1 motor, relative to IM1, is -18.61 %. Percentage difference between IM1 and IM2_H motor, relative to IM1, is -11.09 %. Frequency components from interval 75-78 Hz do not match any value from the Table 25.

Figure 65 shows the FFT of the frequency interval 78 – 100 Hz for Končar group.
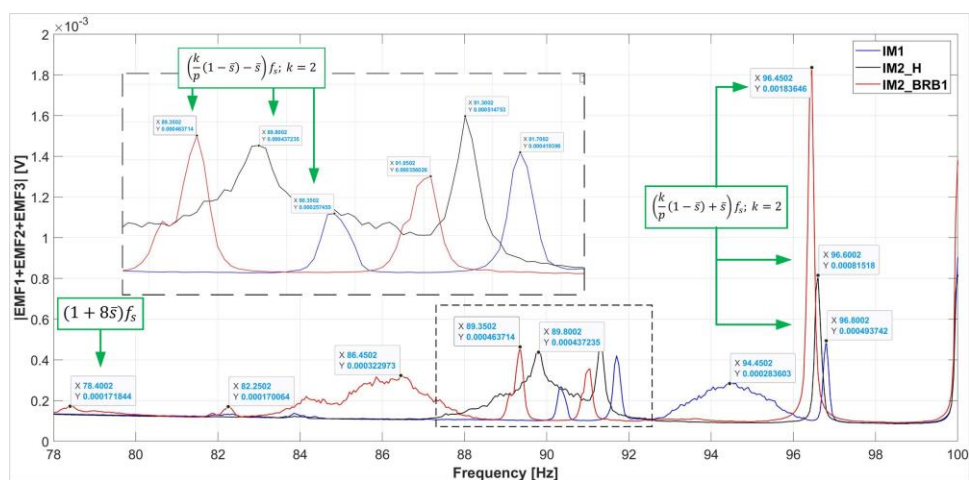
Figure 65. Končar group - frequency spectrum of the interval 78 - 100 Hz.

From Figure 65 it observable that frequency component $(1 + 8\bar{s})f_s$ is present only for IM2_BRB1. Frequency components that appear at f=82.25, 86.45, 91.05, 91.30, 91.70 and 94.45 Hz do not match any value from Table 25. Frequency component $\left(\frac{k}{p}(1 - \bar{s}) - \bar{s}\right)f_s$; k=2 in interval 89-90.4 Hz is present for all motors/motor states. Percentage difference between IM1 and IM2_BRB1 motor, relative to IM1, is 80.11 %. Percentage difference between IM1 and IM2_H motor, relative to IM1, is 69.82 %. Frequency component $\left(\frac{k}{p}(1 - \bar{s}) + \bar{s}\right)f_s$; k=2 in interval 96-97 Hz is present for all motors/motor states. Percentage difference between IM1 and IM2_BRB1 motor, relative to IM1, is 271.94 %. Percentage difference between IM1 and IM2_H motor, relative to IM1, is 65.10 %. Percentage difference between IM2_H and IM2_BRB1 motor, relative to IM2_H, is 125.28 %.

Frequency components on interval 0 – 100 Hz that only appear for IM2_BRB1 or have higher IM2_BRB1 amplitude value compared to healthy motors, are listed in Table 26.

Table 26. Frequency components for Končar group that indicate the presence of broken rotor bar and their corresponding frequency intervals.

No.	Frequency component	f [Hz]	Frequency interval [Hz]
1	$\bar{s}f_s$	3.55	3-4
2	$3\bar{s}f_s$	10.65	9-11
3	$\left(\frac{1}{p}(1 - \bar{s}) - \bar{s}\right)f_s$		
4	$(1 - 4\bar{s})f_s$	35.8	35-38
5	$(1 - 2\bar{s})f_s$		
6	$(1 + 2\bar{s})f_s$	57.10	56-58
7	$(1 + 4\bar{s})f_s$	64.20	62-65
8	$\left(\frac{3}{p}(1 - \bar{s}) - \bar{s}\right)f_s$		
9	$(1 + 8\bar{s})f_s$	78.40	78-80
10	$(1 + 14\bar{s})f_s$		
11	$\left(\frac{2}{p}(1 - \bar{s}) - \bar{s}\right)f_s$	89.35	88-90.6
12	$\left(\frac{4}{p}(1 - \bar{s}) - \bar{s}\right)f_s$		
13	$\left(\frac{2}{p}(1 - \bar{s}) + \bar{s}\right)f_s$	96.45	96-97
14	$\left(\frac{4}{p}(1 - \bar{s}) + \bar{s}\right)f_s$		

Corresponding frequency intervals that are chosen for number of measurements analysis are show in Table 26.

Randomly taken number of measurements that have been investigated are also 1, 2, 3, 4, 5 and 10. This series for Končar group has been chosen for purposes of comparison to Siemens group. Results based on flowchart from Figure 18 for Končar group are shown in Figure 66 and Figure 67.
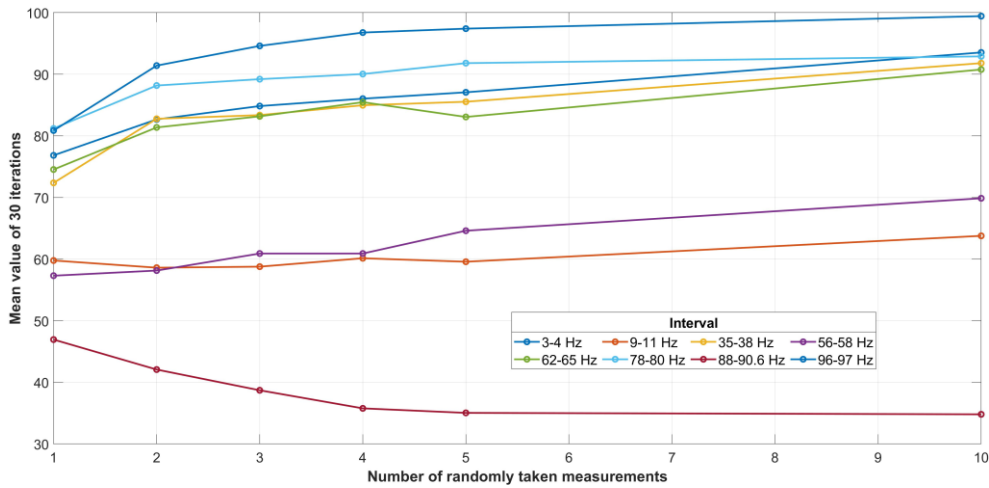
Figure 66. Dependence of mean value of 30 iterations on number of randomly taken measurements for Končar group.
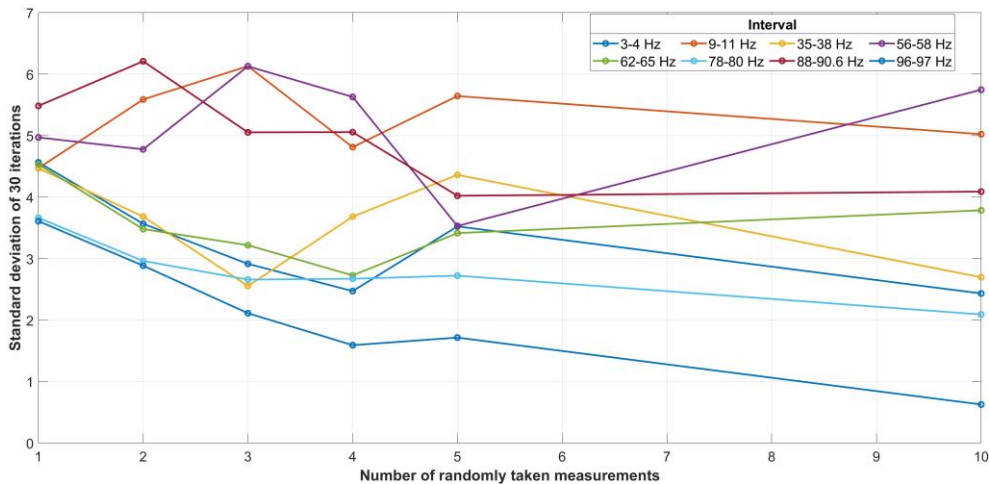
Figure 67. Dependence of standard deviation of 30 iterations on number of randomly taken measurements.

From Figure 66 it is observable that different frequency components have different response to randomly taken number of measurements. For 1 randomly taken measurement highest value has 78-80 Hz interval with corresponding frequency component $(1 + 8\bar{s})f_s$. Lowest value has 88-90.6 Hz interval with corresponding frequency component $\left(\frac{2}{p}(1 - \bar{s}) - \bar{s}\right)f_s$. At 5 randomly taken measurements the highest value, 97.4 %, has component $\left(\frac{2}{p}(1 - \bar{s}) + \bar{s}\right)f_s$ that corresponds to 96-97 Hz interval. The lowest value, 35.03 %, at 5 randomly taken measurements has

component $\left(\frac{2}{p}(1-\bar{s})-\bar{s}\right)f_s$ that corresponds to 88-90.6 Hz interval. At 10 randomly taken measurements the frequency component with highest value, 99.43 %, is $\left(\frac{2}{p}(1-\bar{s})+\bar{s}\right)f_s$. At 10 randomly taken measurements the mean values of frequency components $\bar{s}f_s$, $(1+8\bar{s})f_s$, $(1-4\bar{s})f_s$ and $(1+4\bar{s})f_s$ with corresponding intervals, 3-4 Hz, 78-80 Hz, 35-38 Hz and 62-65 Hz, respectively have mean values 93.53 %, 92.9 %, 91.8 % and 90.76 %, respectively. Frequency components $(1+2\bar{s})f_s$, $3\bar{s}f_s$ and $\left(\frac{2}{p}(1-\bar{s})-\bar{s}\right)f_s$ with corresponding intervals, 56-58 Hz, 9-11 Hz and 88-90.6 Hz, respectively have mean values 69.86 %, 63.76 % and 34.8 % respectively.

On Figure 67 it is observable that different frequency components have different standard deviation response to randomly taken number of measurements. For 1 randomly taken measurement frequency component that has lowest value of standard deviation is $\left(\frac{2}{p}(1-\bar{s})+\bar{s}\right)f_s$. Frequency component that has highest standard deviation value for 1 randomly taken measurement is $\left(\frac{2}{p}(1-\bar{s})-\bar{s}\right)f_s$. At 5 randomly taken measurements the highest standard deviation value, 5.64 %, has component $3\bar{s}f_s$. The lowest value, 1.71 %, at 5 randomly taken measurements has component $\left(\frac{2}{p}(1-\bar{s})+\bar{s}\right)f_s$. At 10 randomly taken measurements order of frequency components with lowest to highest standard deviation value is $\left(\frac{2}{p}(1-\bar{s})+\bar{s}\right)f_s$, $(1+8\bar{s})f_s$, $\bar{s}f_s$, $(1-4\bar{s})f_s$, $(1+4\bar{s})f_s$, $\left(\frac{2}{p}(1-\bar{s})-\bar{s}\right)f_s$, $3\bar{s}f_s$ and $(1+2\bar{s})f_s$. Their corresponding values are 0.62 %, 2.09 %, 2.43 %, 2.69 %, 3.78 %, 4.08 %, 5.02 % and 5.74 %.

6.7. COMPARISON – Statistical Analysis

Since data for Končar group follows non-parametric distribution, for comparison of results only the non-parametric analysis from Siemens group will be taken into account. Results of Siemens and Končar Friedman test for BRB detection is shown in Figure 68. Exact numerical values can be found in Table 13 and Table 22.
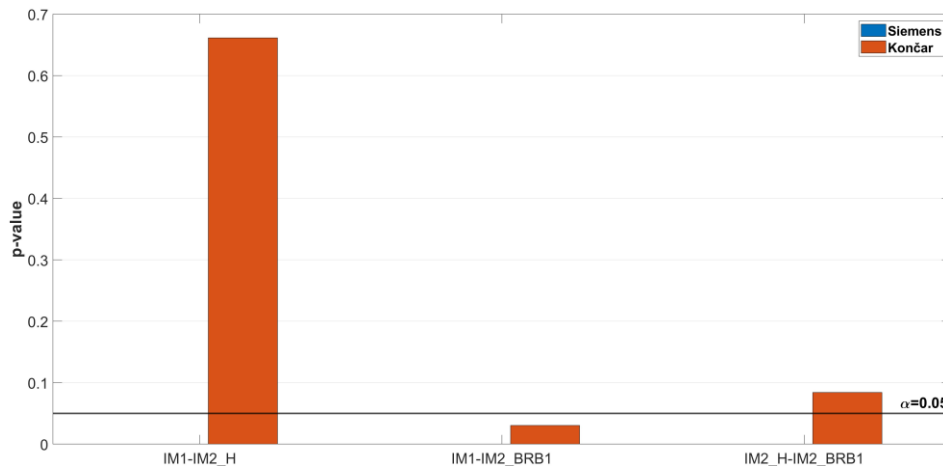
Figure 68. Broken rotor bar detection: p-values for Siemens and Končar motors.

From Figure 68 it can be observed that there is a statistically significant difference between two Siemens healthy motors. When comparing healthy Siemens motors to faulty Siemens motor, analysis shows a statistically significant difference. For Končar group Figure 63 show that for two healthy motors there is not enough evidence to reject the null hypothesis at 5 % significant level, which states that data of two healthy motors come from the same distribution. When comparing Končar motors IM1 and IM2_BRB1, analysis show that there is statistically significant difference. Comparison of IM2_H and IM2_BRB1 show that there is not enough evidence to reject the null hypothesis at 5 % significant level.

Based on the graph from Figure 63 one can conclude that triaxial sensor with random positioning approach and raw data statistical analysis, cannot detect broken rotor bar fault in the case of Siemens and Končar motor.

If the significant level is set to 10 % then it could be stated that for Končar motors triaxial sensor with random positioning approach and raw data statistical analysis, can detect broken rotor bar. This is not the case for Siemens motors because p-value for the healthy-healthy combination would still be lower than 0.1.

6.8. COMPARISON – Feature Analysis

When comparing Figures 36 and 37 it can be observed that features 14, 15 and 17 are common to Siemens and Končar motors. Percentage difference between Siemens and Končar for feature 14, relative to Siemens is -96.71 %. Percentage difference between Siemens and Končar for feature 15, relative to Siemens is -71.76 %. Percentage difference between Siemens and Končar for feature 17, relative to Siemens is -56.54 %.

Comparison between Siemens and Končar group based on maximum value for each feature is displayed on Figure 69.
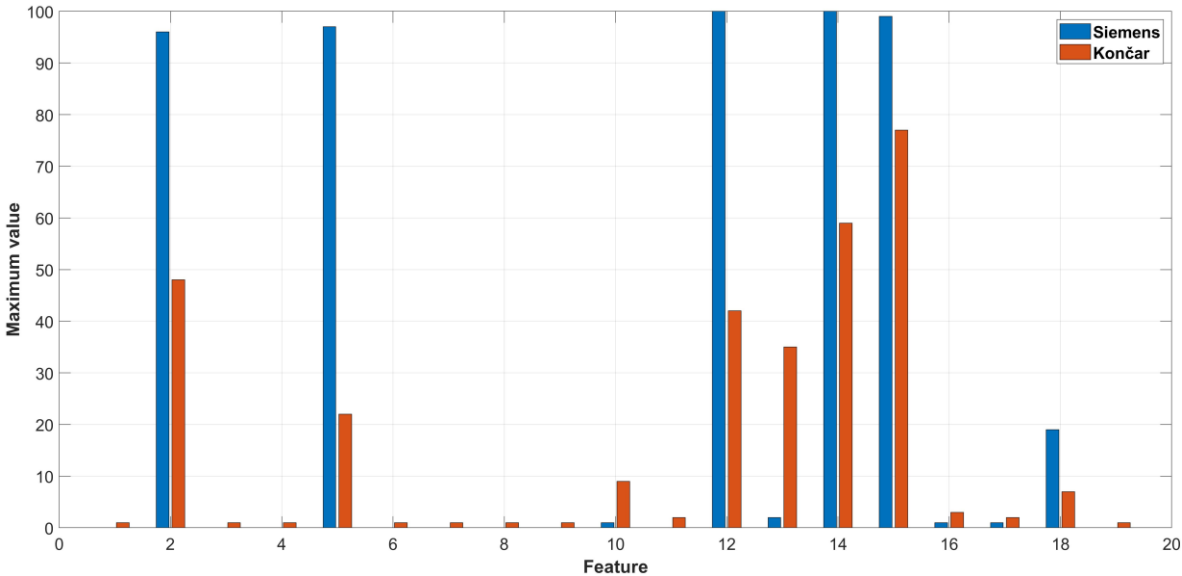
Figure 69. Comparison of Siemens and Končar group based on maximum value.

Figure 69 shows that BRB detection with feature approach for Siemens group is possible based on number of measurements that is lower than 1000. Six features of Siemens group (2, 5, 12, 14 and 15) have maximum value greater that 95 %. All maximum values of Končar group are lower than 80 %.

6.9. COMPARISON – FFT Analysis

Analysis of Siemens and Končar motors with FFT based on 1000 measurement (of each motor) and BRB indicators defined by Eq. 1, 2, 3 and 4 showed that broken rotor bar can be detected with random positioning of triaxial sensor.

Comparison of Siemens and Končar group by frequency components for 10 randomly taken measurements is shown in Figure 70.
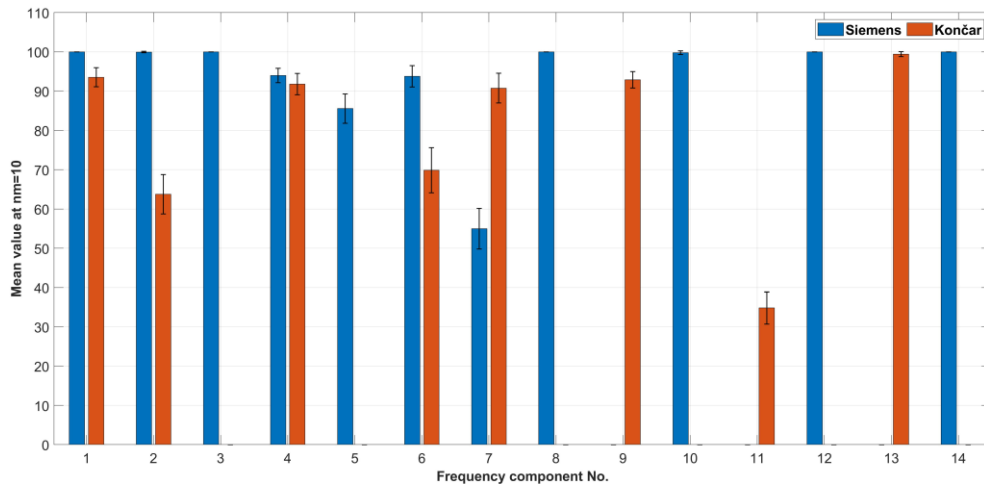
Figure 70. Comparison of Siemens and Končar group by frequency components for 10 randomly taken measurements

Frequency component No. on Figure 70 refers to numbering in Table 18 and Table 26. Black bar on Figure 65 represents the standard deviation. If the 90 % level is set as criterium for reliable BRB detection then in the case of Siemens group 9 out of 11 frequency components can serve as a BRB indicator for 10 randomly taken measurements. In the case of Končar group 3 out of 8 frequency components can serve as a BRB indicator for 10 randomly taken measurements. If the 95 % level is set that it is 7 out of 11 for Siemens group and 1 out of 8 for Končar group. Frequency component that satisfies 90 % level and is common for both groups is frequency component No.1, $\bar{s}f_s$.

7. CONCLUSION

This thesis investigates the possibility of detecting a broken rotor bar in a stationary state with stray magnetic flux by randomly positioning the triaxial air-core coil above the surface of the motor. The triaxial air-core coil consists of a 3D-printed body and hand-wound coils.

Before investigating the fault detection of broken bar, the validation of the measurement method is performed, which includes a triaxial coil and data recording. The reason for this was that the random positioning approach is novel approach and therefore needed to be analysed for consistency. In addition, there were no previously validated measurement devices or commercial equipment that could be used to compare the measurement results. Validation requires consistent measurement results for the unchanged condition of the motor. For example, if the motor is healthy, the measurement results obtained with the triaxial coil must show at all times that there are no quantitative differences in the measurement.

All experiments were conducted with two groups of motors (Siemens and Končar motors), each group consisting of two identical motors. One motor of the group was kept in a healthy state throughout the process, while the second motor was tested in a healthy state, after which the broken rotor bar was generated. For each motor and each motor condition, 1000 measurements were taken. One measurement involved randomly positioning the sensor on the surface of the motor and recording the data with a duration of 20 seconds and a sampling frequency of 5 kHz.

Three approaches to BRB detection were investigated: statistical analysis of raw data, feature analysis and Fast Fourier Transformation Analysis.

The first step in this thesis, the validation of the measurement method, was carried out with a statistical analysis of the raw data, i.e. the values of the induced electromotive force of the coils. The data was collected over a period of ten days, with 100 measurements per day. The statistical analysis of the data distribution was inconclusive. The normality tests performed in MATLAB did not show complete agreement with the quantile-quantile plots, which led to the use of two approaches: parametric and non-parametric. RM-ANOVA was used for the parametric approach. The results of the RM-ANOVA to validate the measurement method showed that the measurements for each motor and each motor condition are time-independent. The multiple comparison analysis was performed together with the Benjamini-Hochberg p-value correction for the daily measurement combinations. After applying the Benjamini-Hochberg correction, all p-values were above the 5% significance level, i.e., there was no

statistically significant difference between the daily measurements for a given motor, which that measurement method is valid.

In the first approach to BRB detection, a two-way RM-ANOVA and a Friedman test were used to statistically analyse the differences between the Siemens group. The data analysis of the Končar group revealed that the raw data was not parametric and therefore only the Friedman test was applied. The results of the parametric test and the non-parametric test for the Siemens motor provide the same conclusion: there is a statistically significant difference between all motors, which means that approach with statistical analysis of raw data is not a valid method for BRB detection since it can not provide statistical differentiation between healthy and faulty state. The statistical analysis of the Siemens group based on the raw data did not provide a positive result in terms of BRB detection, more specifically it showed that there is a statistically significant difference between healthy motors and faulty motor, which is a positive result, but also that there is a statistically significant difference between two healthy motors. However, the multiple comparison of the motors showed that the estimated differences in the mean values of the healthy-healthy combination are 7 to 8 times greater than the differences in the mean values of the healthy-BRB combination.

The statistical analysis of the Končar group based on the Friedman test did not provide a positive result regarding the detection of BRB. More specifically, the test showed that there is no statistically significant difference between two healthy motors, which is a positive result, but it also showed that there is no statistically significant difference between healthy motors and BRB motor. However, the analysis is based on a significance level of 5 %. If the significance level had been set at 10%, the results would have been positive in terms of BRB detection.

The second approach to BRB detection, feature analysis, is based on 19 time-domain features. The feature analysis is performed for all 1000 measurements for each motor of each group. The influence of the number of measurements is analysed afterwards. To avoid bias in the order of the measurements, the measurement matrices of each motor were shuffled by columns. The analysis was performed for 30 iterations and shuffling was performed 100 times in each iteration. For each of the 100 iterations, the features for the shuffled 1000 measurements of each motor/motor state were calculated. The calculated feature series served as input for the Friedman test. Based on the significance level of 5 %, the combinations that would yield positive results were counted. The series. Each count represents the number of positive results of the Friedman test out of 100 tests. For each feature, the mean and standard deviation are

calculated on the basis of the 30 counts. If the level for reliable BRB detection is set at 80%, the Siemens group would have 3 features as reliable indicators: peak-to-rms, impulse factor and clearance factor. The Končar group would have 1 feature/indicator: mean. If the level for reliable BRB detection is set to 90%, then the Siemens group would have 2 reliable indicators: peak-to-rms and impulse factor. The Končar group would have none. If the level for reliable BRB detection is set to 98%, then the Siemens group would have 1 reliable indicator: peak-to-rms.

The influence of the number of measurements was analysed in the same way as for all 1000 measurements, with the exception that there were no 30 iterations for each feature. The analysis is performed for the following series of number of measurements: nm=20, 40, 60, ..., 980, 1000. For each number of measurements, nm, the measurement matrix was shuffled and a random number of measurements were taken. This was followed by the feature calculation and the Friedman test. For each feature and each nm, 100 iterations were performed. The result of the process was counted, i.e. it was determined how many positive results of the Friedman test occurred in 100 tests. The overall results show that the number of appearances depends on the number of measurements, that different features have different dependency patterns and that there are some features that do not appear at all. If the level for reliable BRB detection is set at 90%, then the Siemens group would have 3 features/indicators, peak-to-rms, impulse factor and clearance factor, which would reliably detect BRB in the interval nm=520, ..., 1000. For the Siemens group in the nm=20, ..., 200 interval, the peak-to-rms, impulse factor and clearance factor have their number of appearances in the range of 35 % and 77 %. Relevant features for the Siemens group in the interval nm=20, ..., 200 are mean value and median. At nm=40 and 60, the mean value feature has an occurrence of 96 % and at nm=40 the median feature has an occurrence of 97 %. From nm=60, the mean and median have an overall decreasing trend, which reaches zero at nm=640. The maximum value across all features and the number of measurements for the Končar group is 77 %. At 90 % level, the Siemens group has 3 reliable features from nm=520 and 2 features for a low number of measurements, mean and median at nm=40. The feature approach can therefore be used to detect a broken rotor bar in Siemens motors. For Končar motors, the feature approach is not a reliable method for BRB detection.

The third approach to detect BRB is the FFT. The analysis is performed for all 1000 measurements for each motor of each group. The influence of the number of measurements is analysed afterwards. The measurement matrix of each motor is formed by adding the emf values of each coil. The FFT is then applied. The amplitudes are averaged over the frequencies for

each motor/motor state. The averaged frequency spectra are analysed for the frequency interval 0-100 Hz. For a given interval, two healthy and one faulty motor are graphically compared with averaged frequency spectra. First, the frequency values of the indicators for BRB fault are calculated based on the average speed of the motors. Then the frequency spectrum for the BRB indicators is analysed harmonic by harmonic. For the Siemens group, 11 frequency indicators are identified and for the Končar group 8. Based on 1000 measurements for each motor/motor state with the FFT approach, a BRB fault can be reliably detected.

The influence of the number of measurements was also analysed on the basis of the measurement matrix formed by emf adding of each coil. Corresponding intervals were determined using the determined frequency indicators based on 1000 measurements. The Siemens group has 11 reference intervals and the Končar group has 8. For each motor/motor state the selected number of measurements was randomly performed 100 times and this was repeated in 30 iterations. At each iteration, the number of times the faulty motor had a higher amplitude compared to healthy motors was counted. After a series of 30 counts had been performed, the mean and standard deviation were calculated. The number of measurements for which this approach was tested was: 1, 2, 3, 4, 5 and 10. For Siemens and the Končar group, the different frequency components were found to have a different dependency pattern. Some components decrease in mean value, for others the mean value increases slowly and for some the value converges to the maximum at 5 measurements. If the level for reliable BRB detection is set to 90% and 1 random measurement is taken, then the Siemens group would have 5 out of 11 frequency indicators, while the Končar group would have none. At a level of 90% and 5 random measurements, Siemens would have 7 out of 11 and Končar 2 out of 8 frequency indicators. Finally, with 10 random measurements, Siemens would have 9 out of 11 and Končar 3 out of 8 frequency indicators. The FFT approach with 10 random measurements can reliably detect BRB fault for Siemens and Končar. The only frequency component that fulfils 90% of the level in 10 random measurements and occurs in both groups is $\bar{s}f_s$.

Limitations of this study are the number and type of motors, i.e. the experiments were performed on four SCIMs, the severity of the fault, i.e. only the case of a one broken bar was investigated, the laboratory conditions, i.e. the absence of an industrial environment (electromagnetic interference from other electrical equipment), the duration and sampling frequency of the measurement were kept constant throughout the experiment, i.e. their influence on reliable BRB detection was not investigated, and the fact that the analysis of a healthy motor is needed as a reference for the detection of a broken rotor fault.

For future research, there are several possibilities to be explored: the influence of a shorter measurement time, which would contribute to the practical application of BRB detection with the random method, experiments with motors from different manufacturers (in this research it has been shown that even motors with the same rated power but not identical technical parameters show different behaviour in terms of statistical and feature analysis) and the effectiveness of the random method for detecting two broken rotor bars.

8. LITERATURE

[1]   D. F. de Souza, F. A. M. Salotti, I. L. Sauer, H. Tatizawa, A. T. de Almeida, and A. G. Kanashiro, "A Performance Evaluation of Three-Phase Induction Electric Motors between 1945 and 2020," *Energies*, vol. 15, no. 6, pp. 1–31, 2022, doi: 10.3390/en15062002.

[2]   Y. Merizalde, L. Hernández-Callejo, and O. Duque-Perez, "State of the art and trends in the monitoring, detection and diagnosis of failures in electric induction motors," *Energies*, vol. 10, no. 7, 2017, doi: 10.3390/en10071056.

[3]   A. H. Bonnett, "Root cause failure analysis for AC induction motors in the petroleum and chemical industry," *Rec. Conf. Pap. - Annu. Pet. Chem. Ind. Conf.*, pp. 1–13, 2010, doi: 10.1109/PCIC.2010.5666831.

[4]   S. K. Gundewar and P. V. Kane, *Condition Monitoring and Fault Diagnosis of Induction Motor*, vol. 9, no. 4. Springer Singapore, 2021.

[5]   K. Shang, Y. Zhang, M. Galea, V. Brusic, and S. Korposh, "Fibre optic sensors for the monitoring of rotating electric machines: a review," *Opt. Quantum Electron.*, vol. 53, no. 2, pp. 1–28, 2021, doi: 10.1007/s11082-020-02712-y.

[6]   A. H. Bonnett and T. Albers, "Squirrel-cage rotor options for AC induction motors," *IEEE Trans. Ind. Appl.*, vol. 37, no. 4, pp. 1197–1209, 2001, doi: 10.1109/28.936414.

[7]   O. E. Hassan, M. Amer, A. K. Abdelsalam, and B. W. Williams, "Induction motor broken rotor bar fault detection techniques based on fault signature analysis – A review," *IET Electr. Power Appl.*, vol. 12, no. 7, pp. 895–907, 2018, doi: 10.1049/iet-epa.2018.0054.

[8]   M. E. E. D. Atta, D. K. Ibrahim, and M. I. Gilany, "Broken Bar Fault Detection and Diagnosis Techniques for Induction Motors and Drives: State of the Art," *IEEE Access*, vol. 10, no. August, pp. 88504–88526, 2022, doi: 10.1109/ACCESS.2022.3200058.

[9]   D. Maestre-Cambronel, J. P. Rojas, and J. Duarte-Forero, "EVALUATION OF FAULTS IN THE SQUIRREL CAGE THREE-PHASE INDUCTION MOTORS," *Rev. Ing. Univ. Medellín*, vol. 21, no. 40, pp. 126–142, Dec. 2021, doi: 10.22395/rium.v21n40a8.

[10]   M. Garcia, P. A. Panagiotou, J. A. Antonino-Daviu, and K. N. Gyftakis, "Efficiency Assessment of Induction Motors Operating Under Different Faulty Conditions," *IEEE Trans. Ind. Electron.*, vol. 66, no. 10, pp. 8072–8081, Oct. 2019, doi: 10.1109/TIE.2018.2885719.

[11]   Y. Wu, S. Sun, Q. An, and X. Lie, "Treatment Strategy Research on a Squirrel-Cage Induction Motor with Broken Rotor Bar Faults," *Sensors*, vol. 22, no. 12, 2022, doi: 10.3390/s22124345.

[12]   R. Fišer and S. Ferkolj, "Magnetic field analysis of induction motor with rotor faults," *COMPEL - Int. J. Comput. Math. Electr. Electron. Eng.*, vol. 17, no. 1–3, pp. 206–211, 1998, doi: 10.1108/03321649810203143.

[13]   M. S. Rafaq, M. Faizan Shaikh, Y. Park, and S. Bin Lee, "Reliable Airgap Search Coil Based Detection of Induction Motor Rotor Faults under False Negative Motor Current Signature Analysis Indications," *IEEE Trans. Ind. Informatics*, vol. 18, no. 5, pp. 3276–3285, 2022, doi: 10.1109/TII.2020.3042195.

[14]   P. Zhang, Y. Du, T. G. Habetler, and B. Lu, "A survey of condition monitoring and protection methods for medium-voltage induction motors," *IEEE Trans. Ind. Appl.*, vol. 47, no. 1, pp. 34–46, 2011, doi: 10.1109/TIA.2010.2090839.

[15]   R. R. Kumar, M. Andriollo, G. Cirrincione, M. Cirrincione, and A. Tortella, "A Comprehensive Review of Conventional and Intelligence-Based Approaches for the Fault Diagnosis and Condition Monitoring of Induction Motors," *Energies*, vol. 15, no. 23, 2022, doi: 10.3390/en15238938.

[16]   P. F. Albrecht, J. C. Appiarius, R. M. McCoy, E. L. Owen, and D. K. Sharma, "Assessment of the Reliability of Motors in Utility Applications - Updated," *IEEE Trans. Energy Convers.*, vol. EC-1, no. 1, pp. 39–46, Mar. 1986, doi: 10.1109/TEC.1986.4765668.

[17]   O. V. Thorsen and M. Dalva, "A Survey of Faults on Induction Motors in Offshore Oil Industry, Petrochemical Industry, Gas Terminals, and Oil Refineries," *IEEE Trans. Ind. Appl.*, vol. 31, no. 5, pp.

1186–1196, 1995, doi: 10.1109/28.464536.

[18] W. Group *et al.*, "Report of Large Motor Reliability Survey of Industrial and Commercial Installations, Part I," *IEEE Trans. Ind. Appl.*, vol. IA-21, no. 4, pp. 853–864, 1985, doi: 10.1109/TIA.1985.349532.

[19] P. Spreij, *IEEE Recommended Practice for Design of Reliable Industrial and Commercial Power Systems*, vol. R-34, no. 4. 1985.

[20] A. Elez, S. Car, S. Tvorić, and B. Vaseghi, "Rotor Cage and Winding Fault Detection Based on Machine Differential Magnetic Field Measurement (DMFM)," *IEEE Trans. Ind. Appl.*, vol. 53, no. 3, pp. 3156–3163, 2017, doi: 10.1109/TIA.2016.2636800.

[21] Y. Park, H. Choi, J. Shin, J. Park, S. Bin Lee, and H. Jo, "Airgap flux based detection and classification of induction motor rotor and load defects during the starting transient," *IEEE Trans. Ind. Electron.*, vol. 67, no. 12, pp. 10075–10084, 2020, doi: 10.1109/TIE.2019.2962470.

[22] H. Henao, C. Demian, and G. A. Capolino, "A frequency-domain detection of stator winding faults in induction machines using an external flux sensor," *IEEE Trans. Ind. Appl.*, vol. 39, no. 5, pp. 1272–1279, 2003, doi: 10.1109/TIA.2003.816531.

[23] M. S. Erlicki, Y. Porat, and A. Alexandrovitz, "Leakage Field Changes of an Induction Motor as Indication of Nonsymmetric Supply," *IEEE Trans. Ind. Gen. Appl.*, vol. IGA-7, no. 6, pp. 713–717, Nov. 1971, doi: 10.1109/TIGA.1971.4181373.

[24] H. Pacaiova and J. Glatz, "Maintenance management system," *MM Sci. J.*, vol. 2015, no. OCTOBER, pp. 665–669, 2015, doi: 10.17973/MMSJ.2015_10_201532.

[25] S. K. Mishra, D. Mahapatra, and D. Making, "MAINTENANCE STRATEGY AND DECISION MAKING – AHP METHOD," *Int. J. Adv. Eng. Res. Stud.*, vol. IV, no. II, pp. 256–258, 2015.

[26] Y. Raptodimos, I. Lazakis, G. Theotokatos, T. Varelas, and L. Drikos, "Ship sensors data collection & analysis for condition monitoring of ship structures & machinery systems," *RINA, R. Inst. Nav. Archit. - Smart Sh. Technol. 2016, Pap.*, no. January, pp. 77–86, 2016, doi: 10.3940/rina.sst.2016.13.

[27] BUREAU VERITAS MARINE & OFFSHORE, "GUIDELINES FOR CONDITION BASED MAINTENANCE NI684 - SEPTEMBER 2022." BUREAU VERITAS MARINE & OFFSHORE, 2022, [Online]. Available: marine-offshore.bureauveritas.com/rules-guidelines.

[28] S. S. Patil, A. K. Bewoor, R. Kumar, M. H. Ahmadi, M. Sharifpur, and S. PraveenKumar, "Development of Optimized Maintenance Program for a Steam Boiler System Using Reliability-Centered Maintenance Approach," *Sustain.*, vol. 14, no. 16, 2022, doi: 10.3390/su141610073.

[29] P. Zhang *et al.*, "Marine Systems and Equipment Prognostics and Health Management: A Systematic Review from Health Condition Monitoring to Maintenance Strategy," *Machines*, vol. 10, no. 2, 2022, doi: 10.3390/machines10020072.

[30] N. S. Arunraj and J. Maiti, "Risk-based maintenance-Techniques and applications," *J. Hazard. Mater.*, vol. 142, no. 3, pp. 653–661, 2007, doi: 10.1016/j.jhazmat.2006.06.069.

[31] D. T. Hall, *Practical marine electrical knowledge*, Third. Witherby Seamanship International Ltd, 2014.

[32] E. Mazaheri-Tehrani and J. Faiz, "Airgap and stray magnetic flux monitoring techniques for fault diagnosis of electrical machines: An overview," *IET Electr. Power Appl.*, vol. 16, no. 3, pp. 277–299, 2022, doi: 10.1049/elp2.12157.

[33] I. Zamudio-Ramirez, R. A. Osornio-Rios, J. A. Antonino-Daviu, H. Razik, and R. Romero-Troncoso, "Magnetic Flux Analysis for the Condition Monitoring of Electric Machines: A Review," *IEEE Trans. Ind. Informatics*, vol. 18, no. 5, pp. 2895–2908, 2022, doi: 10.1109/TII.2021.3070581.

[34] P. Gangsar and R. Tiwari, "Signal based condition monitoring techniques for fault detection and diagnosis of induction motors: A state-of-the-art review," *Mech. Syst. Signal Process.*, vol. 144, p. 106908, 2020, doi: 10.1016/j.ymssp.2020.106908.

[35] S. Koroglu, A. A. Adam, N. Umurkan, and K. Gulez, "Leakage magnetic flux density in the vicinity of induction motor during operation," *Electr. Eng.*, vol. 91, no. 1, pp. 15–21, 2009, doi: 10.1007/s00202-009-0111-4.

[36] F. Filippetti, G. Franceschini, C. Tassoni, and P. Vas, "AI techniques in induction machines diagnosis including the speed ripple effect," *IEEE Trans. Ind. Appl.*, vol. 34, no. 1, pp. 98–108, 1998, doi: 10.1109/28.658729.

[37] V. Ghorbanian and J. Faiz, "A survey on time and frequency characteristics of induction motors with broken rotor bars in line-start and inverter-fed modes," *Mech. Syst. Signal Process.*, vol. 54, pp. 427–456, 2015, doi: 10.1016/j.ymssp.2014.08.022.

[38] A. Ceban, R. Pusca, and R. Romary, "Study of rotor faults in induction motors using external magnetic field analysis," *IEEE Trans. Ind. Electron.*, vol. 59, no. 5, pp. 2082–2093, 2012, doi: 10.1109/TIE.2011.2163285.

[39] S. Bin Lee, J. Shin, Y. Park, H. Kim, and J. Kim, "Reliable Flux-Based Detection of Induction Motor Rotor Faults from the Fifth Rotor Rotational Frequency Sideband," *IEEE Trans. Ind. Electron.*, vol. 68, no. 9, pp. 7874–7883, 2021, doi: 10.1109/TIE.2020.3016241.

[40] G. Chicco and A. Mazza, "100 Years of Symmetrical Components," *Energies*, vol. 12, no. 3, pp. 1–20, 2019, doi: 10.3390/en12030450.

[41] J. A. Ramirez-Nunez *et al.*, "Evaluation of the Detectability of Electromechanical Faults in Induction Motors Via Transient Analysis of the Stray Flux," *IEEE Trans. Ind. Appl.*, vol. 54, no. 5, pp. 4324–4332, 2018, doi: 10.1109/TIA.2018.2843371.

[42] P. A. Panagiotou, I. Arvanitakis, N. Lophitis, J. A. Antonino-Daviu, and K. N. Gyftakis, "A New Approach for Broken Rotor Bar Detection in Induction Motors Using Frequency Extraction in Stray Flux Signals," *IEEE Trans. Ind. Appl.*, vol. 55, no. 4, pp. 3501–3511, 2019, doi: 10.1109/TIA.2019.2905803.

[43] K. N. Gyftakis, P. A. Panagiotou, E. Palomeno, and S. Bin Lee, "Introduction of the Zero-Sequence Stray Flux as a Reliable Diagnostic Method of Rotor Electrical Faults in Induction Motors," *IECON Proc. (Industrial Electron. Conf.*, vol. 2019-Octob, pp. 6016–6021, 2019, doi: 10.1109/IECON.2019.8927775.

[44] M. E. Iglesias-Martinez, P. F. De Cordoba, J. A. Antonino-Daviu, and J. Alberto Conejero, "Detection of Nonadjacent Rotor Faults in Induction Motors via Spectral Subtraction and Autocorrelation of Stray Flux Signals," *IEEE Trans. Ind. Appl.*, vol. 55, no. 5, pp. 4585–4594, 2019, doi: 10.1109/TIA.2019.2917861.

[45] M. E. Iglesias-Martínez, J. A. Antonino-Daviu, P. Fernández de Córdoba, and J. Alberto Conejero, "Rotor fault detection in induction motors based on time-frequency analysis using the bispectrum and the autocovariance of stray flux signals," *Energies*, vol. 12, no. 4, 2019, doi: 10.3390/en12040597.

[46] P. A. Panagiotou, I. Arvanitakis, N. Lophitis, J. A. Antonino-Daviu, and K. N. Gyftakis, "On the broken rotor bar diagnosis using time-frequency analysis: 'Is one spectral representation enough for the characterisation of monitored signals?,'" *IET Electr. Power Appl.*, vol. 13, no. 7, pp. 932–942, 2019, doi: 10.1049/iet-epa.2018.5512.

[47] Y. Park *et al.*, "Stray flux monitoring for reliable detection of rotor faults under the influence of rotor axial air ducts," *IEEE Trans. Ind. Electron.*, vol. 66, no. 10, pp. 7561–7570, 2019, doi: 10.1109/TIE.2018.2880670.

[48] I. Zamudio-Ramirez *et al.*, "Automatic Diagnosis of Electromechanical Faults in Induction Motors Based on the Transient Analysis of the Stray Flux via MUSIC Methods," *IEEE Trans. Ind. Appl.*, vol. 56, no. 4, pp. 3604–3613, 2020, doi: 10.1109/TIA.2020.2988002.

[49] I. Zamudio-Ramírez, R. A. Osornio-Ríos, J. A. Antonino-Daviu, and A. Quijano-Lopez, "Smart-Sensor for the Automatic Detection of Electromechanical Faults in Induction Motors Based on the Transient Stray Flux Analysis," *Sensors*, vol. 20, no. 5, p. 1477, Mar. 2020, doi: 10.3390/s20051477.

[50] Y. Park, H. Choi, S. Bin Lee, and K. N. Gyftakis, "Search Coil-Based Detection of Nonadjacent Rotor Bar Damage in Squirrel Cage Induction Motors," *IEEE Trans. Ind. Appl.*, vol. 56, no. 5, pp. 4748–4757, 2020, doi: 10.1109/TIA.2020.3000461.

[51] K. N. Gyftakis, P. A. Panagiotou, and S. Bin Lee, "Generation of Mechanical Frequency Related Harmonics in the Stray Flux Spectra of Induction Motors Suffering from Rotor Electrical Faults," *IEEE Trans. Ind. Appl.*, vol. 56, no. 5, pp. 4796–4803, 2020, doi: 10.1109/TIA.2020.3002975.

[52] K. N. Gyftakis, P. A. Panagiotou, and D. Spyrakis, "Detection of simultaneous mechanical faults in 6-kV pumping induction motors using combined MCSA and stray flux methods," *IET Electr. Power Appl.*, vol. 15, no. 5, pp. 643–652, 2021, doi: 10.1049/elp2.12054.

[53] V. Biot-Monterde, Á. Navarro-Navarro, J. A. Antonino-Daviu, and H. Razik, "Stray flux analysis for the detection and severity categorization of rotor failures in induction machines driven by soft-starters," *Energies*, vol. 14, no. 18, 2021, doi: 10.3390/en14185757.

[54] I. Zamudio-Ramirez, R. A. Osornio-Rios, and J. A. Antonino-Daviu, "Smart Sensor for Fault Detection in Induction Motors Based on the Combined Analysis of Stray-Flux and Current Signals: A Flexible, Robust Approach," *IEEE Ind. Appl. Mag.*, vol. 28, no. 2, pp. 56–66, 2022, doi: 10.1109/MIAS.2021.3114647.

[55] I. Zamudio-Ramirez, J. A. Antonino-Daviu, M. Trejo-Hernandez, and R. A. Osornio-Rios, "Cutting Tool Wear Monitoring in CNC Machines Based in Spindle-Motor Stray Flux Signals," *IEEE Trans. Ind. Informatics*, vol. 18, no. 5, pp. 3267–3275, 2022, doi: 10.1109/TII.2020.3022677.

[56] A. Navarro-Navarro, I. Zamudio-Ramirez, V. Biot-Monterde, R. A. Osornio-Rios, and J. A. Antonino-Daviu, "Current and Stray Flux Combined Analysis for the Automatic Detection of Rotor Faults in Soft-Started Induction Motors," *Energies*, vol. 15, no. 7, pp. 1–19, 2022, doi: 10.3390/en15072511.

[57] V. Biot-Monterde, A. Navarro-Navarro, I. Zamudio-Ramirez, J. A. Antonino-Daviu, and R. A. Osornio-Rios, "Automatic Classification of Rotor Faults in Soft-Started Induction Motors, Based on Persistence Spectrum and Convolutional Neural Network Applied to Stray-Flux Signals," *Sensors*, vol. 23, no. 1, 2023, doi: 10.3390/s23010316.

[58] J. J. Saucedo-Dorantes, D. A. Elvira-Ortiz, A. Y. Jaen-Cuellar, J. A. Antonino-Daviu, and R. A. Osornio-Rios, "Automatic Methodology for Multiple Fault Detection in Induction Motor Under Periodic Low-Frequency Fluctuating Load Based on Stray Flux Signals," *IEEE Trans. Energy Convers.*, vol. 38, no. 4, pp. 2744–2753, 2023, doi: 10.1109/TEC.2023.3294392.

[59] X. Wang, Y. Zheng, Z. Zhao, and J. Wang, "Bearing fault diagnosis based on statistical locally linear embedding," *Sensors (Switzerland)*, vol. 15, no. 7, pp. 16225–16247, 2015, doi: 10.3390/s150716225.

[60] B. R. Nayana and P. Geethanjali, "Analysis of Statistical Time-Domain Features Effectiveness in Identification of Bearing Faults from Vibration Signal," *IEEE Sens. J.*, vol. 17, no. 17, pp. 5618–5625, 2017, doi: 10.1109/JSEN.2017.2727638.

[61] R. F. Ribeiro Junior, F. A. de Almeida, and G. F. Gomes, "Fault classification in three-phase motors based on vibration signal analysis and artificial neural networks," *Neural Comput. Appl.*, vol. 32, no. 18, pp. 15171–15189, 2020, doi: 10.1007/s00521-020-04868-w.

[62] S. Misra *et al.*, "Fault Detection in Induction Motor Using Time Domain and Spectral Imaging-Based Transfer Learning Approach on Vibration Data," *Sensors*, vol. 22, no. 21, 2022, doi: 10.3390/s22218210.

[63] I. Zamudio-Ramirez, J. M. Mendoza-Ortiz, R. A. Osomio-Rios, and J. A. Antonino-Daviu, "Stray Flux Signal Analysis for Faults Detection in Induction Motors During Startup Transient By Means Of Statistical Indicators," *Proc. 2023 IEEE 14th Int. Symp. Diagnostics Electr. Mach. Power Electron. Drives, SDEMPED 2023*, pp. 179–185, 2023, doi: 10.1109/SDEMPED54949.2023.10271497.

[64] B. Asad, T. Vaimann, A. Belahcen, A. Kallaste, A. Rassõlkin, and M. N. Iqbal, "Broken rotor bar fault detection of the grid and inverter-fed induction motor by effective attenuation of the fundamental component," *IET Electr. Power Appl.*, vol. 13, no. 12, pp. 2005–2014, 2019, doi: 10.1049/iet-epa.2019.0350.

[65] P. Guzik and B. Więckowska, "Data distribution analysis – a preliminary approach to quantitative data in biomedical research," *J. Med. Sci.*, vol. 92, no. 2, pp. 81–96, 2023, doi: 10.20883/medical.e869.

[66] H. Hernandez, "Testing for Normality: What is the Best Method?," *ForsChem Res. Reports*, vol. 6, no. April, pp. 2021–2026, 2021, doi: 10.13140/RG.2.2.13926.14406.

[67] A. Loy, L. Follett, and H. Hofmann, "Variations of Q–Q Plots: The Power of Our Eyes!," *Am. Stat.*, vol. 70, no. 2, pp. 202–214, 2016, doi: 10.1080/00031305.2015.1077728.

[68] T. K. Kim, "Practical statistics in pain research," *Korean J. Pain*, vol. 30, no. 4, pp. 243–249, 2017, doi: 10.3344/kjp.2017.30.4.243.

[69] L. N. Muhammad, "Guidelines for repeated measures statistical analysis approaches with basic science research considerations," *J. Clin. Invest.*, vol. 133, no. 11, pp. 2–4, 2023, doi: 10.1172/JCI171058.

[70] M. J. Blanca, J. Arnau, F. J. García-Castro, R. Alarcón, and R. Bono, "Non-normal Data in Repeated Measures ANOVA: Impact on Type I Error and Power," *Psicothema*, vol. 35, no. 1, pp. 21–29, 2023, doi: 10.7334/psicothema2022.292.

[71] M. J. Blanca, J. Arnau, F. J. García-Castro, R. Alarcón, and R. Bono, "Repeated measures ANOVA and adjusted F-tests when sphericity is violated: which procedure is best?," *Front. Psychol.*, vol. 14, no. August, pp. 1–11, 2023, doi: 10.3389/fpsyg.2023.1192453.

[72] S. Y. Chen, Z. Feng, and X. Yi, "A general introduction to adjustment for multiple comparisons," *J. Thorac. Dis.*, vol. 9, no. 6, pp. 1725–1729, 2017, doi: 10.21037/jtd.2017.05.34.

[73] S. Lee and D. K. Lee, "What is the proper way to apply the multiple comparison test?," *Korean J. Anesthesiol.*, vol. 71, no. 5, pp. 353–360, 2018, doi: 10.4097/kja.d.18.00242.

[74] M. A. Lindquist and A. Mejia, "Zen and the Art of Multiple Comparisons," *Psychosom. Med.*, vol. 77, no. 2, pp. 114–125, Feb. 2015, doi: 10.1097/PSY.0000000000000148.

[75] G. G. R. Leday, J. Hemerik, J. Engel, and H. van der Voet, "Improved family-wise error rate control in multiple equivalence testing," *Food Chem. Toxicol.*, vol. 178, no. April, 2023, doi: 10.1016/j.fct.2023.113928.

[76] A. Garrido-Trigo *et al.*, "Macrophage and neutrophil heterogeneity at single-cell spatial resolution in human inflammatory bowel disease," *Nat. Commun.*, vol. 14, no. 1, pp. 1–18, 2023, doi: 10.1038/s41467-023-40156-6.

[77] W. Dubitzky, *Encyclopedia of Systems Biology*. 2013.

[78] N. Pike, "Using false discovery rates for multiple comparisons in ecology and evolution," *Methods Ecol. Evol.*, vol. 2, no. 3, pp. 278–282, 2011, doi: 10.1111/j.2041-210X.2010.00061.x.

[79] R. Brinster, A. Köttgen, B. O. Tayo, M. Schumacher, and P. Sekula, "Control procedures and estimators of the false discovery rate and their application in low-dimensional settings: An empirical investigation," *BMC Bioinformatics*, vol. 19, no. 1, pp. 1–10, 2018, doi: 10.1186/s12859-018-2081-x.

[80] F. Emmert-Streib and M. Dehmer, "Large-Scale Simultaneous Inference with Hypothesis Testing: Multiple Testing Procedures in Practice," *Mach. Learn. Knowl. Extr.*, vol. 1, no. 2, pp. 653–683, 2019, doi: 10.3390/make1020039.

[81] F. S. Nahm, "Nonparametric statistical tests for the continuous data: The basic concept and the practical use," *Korean J. Anesthesiol.*, vol. 69, no. 1, pp. 8–14, 2016, doi: 10.4097/kjae.2016.69.1.8.

[82] M. Krzywinski and N. Altman, "Nonparametric tests," *Nat. Methods*, vol. 11, no. 5, pp. 467–468, May 2014, doi: 10.1038/nmeth.2937.

[83] M. R. Mowla, J. D. Gonzalez-Morales, J. Rico-Martinez, D. A. Ulichnie, and D. E. Thompson, "A comparison of classification techniques to predict brain-computer interfaces accuracy using classifier-based latency estimation," *Brain Sci.*, vol. 10, no. 10, pp. 1–13, 2020, doi: 10.3390/brainsci10100734.

[84] D. G. Pereira, A. Afonso, and F. M. Medeiros, "Overview of Friedman's Test and Post-hoc Analysis," *Commun. Stat. - Simul. Comput.*, vol. 44, no. 10, pp. 2636–2653, Nov. 2015, doi: 10.1080/03610918.2014.931971.

9. LIST OF FIGURES

10. LIST OF TABLES

11. BIOGRAPHY

- Born on September 19, 1988 in Split
- 2007 – 2012 attended Undergraduate and Master study at Faculty of Electrical Engineering, Mechanical Engineering and Naval Arhitecure, University of Split, Croatia
- 2012 – employment at KONČAR – Electrical Equioment, Inc. in Dicmo (Quality Control Department)
- 2015 – enrollment to PhD study at University of Zagreb, Faculty of Electrical Engineering and Computing
- March, 2017 - employment at University of Split, Faculty of Maritime Studies (assistant at Department for Marine Electrical Engineering and Information Technologies)
- September, 2022 – withdrawal from PhD study at University of Zagreb, Faculty of Electrical Engineering and Computing
- October, 2022 - enrollment to PhD study at University of Split, Faculty of Maritime Studies

Published papers and conference proceedings:

1. Krčum, Maja ; **Zubčić, Marko** ; Žanić-Mikuličić, Jelena
   Brodski elektroenergetski sustav - mreže istosmjerne struje // KoREMA 37 th Conference on transportation Systems with International Participation Automatio in Transportation 2017 / Šakić, Željko - Zagreb : KoREMA, Unska 3, Zagreb, Hrvatska, 2017. 2017. str. 125-128

2. Krčum, Maja ; **Zubčić, Marko** ; Gudelj, Anita
   A Review and Comparison of Ship Power Simulation Methods // Naše more : znanstveni časopis za more i pomorstvo, Vo. 65. No.4 (2018), 284-288. doi: 10.17818/NM/2018/4SI.22

3. **Zubcic, Marko** ; Krcum, Maja
   Power frequency withstand voltage type testing and FEM analysis of the medium-voltage switchgear busbar compartment // 2018 17th International Symposium INFOTEH-JAHORINA (INFOTEH 2018). Sarajevo: Institute of Electrical and Electronics Engineers (IEEE), 2018. str. 23-27 doi: 10.1109/infoteh.2018.8345514

4. Krčum, Maja ; **Zubčić, Marko** ; Plazibat, Veljko
   DOPRINOS ENERGETSKOJ UČINKOVITOSTI U PLOVIDBI HRVATSKIM LUKAMA // 38th Conference on Transportation Systems with International Participation AUTOMATON IN TRANSPORTATION 2018. 2018. str. 41-44

5. **Zubčić, Marko** ; Krčum, Maja ; Šakić, Zvonimir
   "Green ships" – perspective and development // 18th International Conference on Transport Science – ICTS 2018, CONFERENCE PROCEEDINGS / Zanne, Marina ; Bajec, Patricija - Portorož : Fakulteta za pomorstvo in promet Portorož, 2018. 2018. str. 426-432

6. Krčum, Maja ; **Zubčić, Marko** ; Dlabač, Tatjana
   Electromechanical Analysis of the Medium Voltage Earthing Switch due to Short-Time and Peak Withstand Current Test // Energies (Basel), 12 (2019), 16; 3189, 17. doi: 10.3390/en12163189

7. Petković, Miro ; **Zubčić, Marko** ; Krčum, Maja ; Vujović, Igor

   Maritime Green Solution for Traffic Congestion // TransNav 2019 / Weintrit, Adam ; Neumann, Tomasz (ur.). Gdynia, 2019. str. 48-48

8. Petković, Miro ; **Zubčić, Marko** ; Vujović, Igor ; Šoda, Joško

   Autonomno "Shuttle" plovilo za područje trajektne luke Split // 39th Conference on Transportation Systems with International Participation AUTOMATON IN TRANSPORTATION 2019. Split, 2019. str. 32-35

9. **Zubčić, Marko** ; Krčum, Maja ; Peša, Tomislav ; Bacalja, Bruna

   Koncept električnog katamarana za liniju Split - Zračna luka "Split" // 39th Conference on Transportation Systems with International Participation AUTOMATON IN TRANSPORTATION 2019. 2019. str. 36-41

10. Petković, Miro ; **Zubčić, Marko** ; Krčum, Maja ; Vujović, Igor

    Maritime Green Solution for Traffic Congestion // TransNav, 14 (2020), 1; 97-103. doi: 10.12716/1001.14.01.11

11. Peša, Tomislav ; Krčum, Maja ; **Zubčić, Marko** ; Bacalja, Bruna

    Implementation of renewable sources of energy on Croatian coast guard logistic support vessel PT-71 // 19th International Conference on Transport Science ICTS 2020 : Maritime, transport and logistics science - conference proceedings / Zanne, Marina ; Bajec, Patricija ; Twrdy, Elen (ur.). Portorož: Fakulteta za pomorstvo in promet Univerza v Ljubljani, 2020. str. 258-262

12. Petković, Miro ; **Zubčić, Marko** ; Krčum, Maja ; Pavić, Ivan

    Wind Assisted Ship Propulsion Technologies – Can they Help in Emissions Reduction? // Naše more : znanstveni časopis za more i pomorstvo, 68 (2021), 2; 102-109. doi: 10.17818/NM/2021/2.6

13. Bacalja, Bruna ; Krčum, Maja ; Peša, Tomislav ; **Zubčić, Marko**

    The Measurment of Exhaust gas Emissions by Testo 350 Maritime - Exhaust gas Analyzer // Pedagogika (Sofia), 93 (2021), S6; 186-195. doi: 10.53656/ped21-6s.16mea

14. Kaštelan, Nediljko ; **Zubčić, Marko** ; Krčum, Maja ; Petković, Miro

    Contribution to the reduction of the ship's switchboard by applying sensor technology // Pedagogika (Sofia), 93 (2021), 6s; 235-249. doi: 10.53656/ped21-6s.21con

15. Krčum, Maja ; **Zubčić, Marko** ; Kaštelan, Nediljko ; Gudelj, Anita

    Reducing the Dimensions of the Ship's Main Switchboard—A Contribution to Energy Efficiency // Energies (Basel), 14 (2021), 22; 7567, 21. doi: 10.3390/en14227567

16. **Zubčić, Marko** ; Kaštelan, Nediljko ; Krčum, Maja ; Peša, Tomislav

    Motor drive experimental setup parameters determination // 2nd International Conference of Maritime Science & Technology : Naše more 2021 - conference proceedings / Mišković, Darijo (ur.). Dubrovnik: Pomorski odjel Sveučilišta u Dubrovniku, 2021. str. 408-417

17. Kaštelan, Nediljko ; **Zubčić, Marko** ; Krčum, Maja ; Bacalja, Bruna

    Temperature Rise Prediction in Three-Phase Busbar Systems - A Step in Preparation for Medium-voltage Switchgear Type Testing // Book of Abstracts - 1st Kotor International Maritime Conference / Špiro, Ivošević ; Milena, Dževerdanović Pejović ; Zorica, Đurović (ur.). Kotor: Faculty of Maritime Studies Kotor, University of Montenegro, 2021. str. 5-5

18. **Zubčić, Marko** ; Berberović, Sead

Medium-Voltage Circuit Breaker Current Path 3D model: A Case Study. 2021. doi: 10.1109/ICECET52533.2021.9698585

19. Krčum, Maja ; Kaštelan, Nediljko ; **Zubčić, Marko** ; Peša, Tomislav

ENERGY EFFICIENCY - CONTRIBUTION BY OPTIMIZING THE LAYOUT OF THE SHIP'S SWITCHBOARD // 20th International Conference on Transport Science THE BOOK OF ABSTRACTS. Portorož: Fakulteta za pomorstvo in promet Univerze v Ljubljani, 2022. str. 33-33

20. **Zubčić, Marko** ; Kaštelan, Nediljko ; Krčum, Maja ; Peša, Tomislav

LABORATORY POWER CONVERTER – ANALYSIS AND MODELLING FOR STUDENT TRAINING // 20th International Conference on Transport Science- THE BOOK OF ABSTRACTS. Portorož: Fakulteta za pomorstvo in promet Univerze v Ljubljani, 2022. str. 74-74

21. **Zubčić, Marko**; Kaštelan Nediljko; Petković, Miro; Krčum, Maja

Estimation of CO2 Reduction due to Flettner Technology based on Online Calculator for Panamax and Capesize Bulk Carriers // 10th IMSC International Maritime Science Conference Book of Proceedings. Split: Pomorski fakultet Sveučilišta u Splitu, 2023. str. 365-371

22. **Zubčić,Marko**;Pavić,Ivan;Matić,Petar;Polak,Adam

Broken Rotor Bar Detection Based on Steady-State Stray Flux Signals Using Triaxial Sensor with Random Positioning // Sensors, 24 (2024), 10; 3080, 23. doi: 10.3390/s24103080

APPENDIX A: SPEED MEASUREMENT

Every measurement set containes 50 measuremets. After the last measurementof of each set the speed of the motor was read off from the Lucas-Nuelle module CO3636-6V display and writen in Measuremet log.

The speed for Siemens and Končar group is shown in Table A1.

No.	Speed [rpm]					
	SIEMENS			KONČAR		
	IM1	IM2_H	IM2_BRB1	IM1	IM2_H	IM2_BRB1
1	1439	1435	1428	2809	2795	2785
2	1438	1435	1427	2808	2794	2786
3	1438	1434	1427	2806	2795	2785
4	1439	1434	1428	2808	2796	2785
5	1440	1434	1427	2807	2796	2786
6	1438	1435	1427	2807	2794	2786
7	1437	1437	1427	2807	2794	2785
8	1437	1437	1428	2808	2795	2786
9	1438	1437	1427	2807	2795	2787
10	1437	1437	1428	2807	2796	2787
11	1436	1437	1427	2808	2797	2788
12	1436	1436	1426	2809	2796	2787
13	1437	1435	1426	2809	2797	2788
14	1437	1435	1428	2807	2796	2786
15	1437	1436	1428	2806	2795	2788
16	1436	1436	1428	2806	2795	2787
17	1436	1436	1428	2808	2796	2788
18	1437	1434	1427	2808	2795	2787
19	1437	1435	1429	2809	2796	2786
20	1437	1435	1427	2809	2796	2787
Mean	1437.35	1435.5	1427.4	2807,65	2795,45	2786,5
Std	1.08	1.10	0.75	1,04	0,89	1,05

APPENDIX B: MATLAB SCRIPTS

```matlab
clc; clear all; close all
%% %%%%%%%%%%%%%%%%%%%%%%%%%%%%%%%%%%%%%%%%%%%%%%%%%%%%%%%%%%%%%%%%%%%%%%%%
%% %%%%%%%%%%%%%%%%% MEASUREMENT MATRIX GENERATION %%%%%%%%%%%%%%%%%%%%%%%%%
%% %%%%%%%%%%%%%%%%%%%%%%%%%%%%%%%%%%%%%%%%%%%%%%%%%%%%%%%%%%%%%%%%%%%%%%%%

%% Sampling frequency = 5 kHz
%% Duration = 20 s

%% %%%%%%%%%%%%%%%%%%%%%%%%%%% SIEMENS %%%%%%%%%%%%%%%%%%%%%%%%%%%%%%%%%%%%
%% Load = 3.33 Nm
%% %%%%%%%%%%%%%%%%%%%%%%%%%%%%% HEALTHY - IM1  %%%%%%%%%%%%%%%%%%%%%%%%%%%

% QH(1)   =load('C:\Users\PFST-User\Desktop\PhD DATA\SIEMENS\IM1\H_IM1_M1_TAC41.mat');
% QH(2)   =load('C:\Users\PFST-User\Desktop\PhD DATA\SIEMENS\IM1\H_IM1_M2_TAC41.mat');
% QH(3)   =load('C:\Users\PFST-User\Desktop\PhD DATA\SIEMENS\IM1\H_IM1_M3_TAC41.mat');
% QH(4)   =load('C:\Users\PFST-User\Desktop\PhD DATA\SIEMENS\IM1\H_IM1_M4_TAC41.mat');
% QH(5)   =load('C:\Users\PFST-User\Desktop\PhD DATA\SIEMENS\IM1\H_IM1_M5_TAC41.mat');
% QH(6)   =load('C:\Users\PFST-User\Desktop\PhD DATA\SIEMENS\IM1\H_IM1_M6_TAC41.mat');
% QH(7)   =load('C:\Users\PFST-User\Desktop\PhD DATA\SIEMENS\IM1\H_IM1_M7_TAC41.mat');
% QH(8)   =load('C:\Users\PFST-User\Desktop\PhD DATA\SIEMENS\IM1\H_IM1_M8_TAC41.mat');
% QH(9)   =load('C:\Users\PFST-User\Desktop\PhD DATA\SIEMENS\IM1\H_IM1_M9_TAC41.mat');
% QH(10)  =load('C:\Users\PFST-User\Desktop\PhD DATA\SIEMENS\IM1\H_IM1_M10_TAC41.mat');
% QH(11)  =load('C:\Users\PFST-User\Desktop\PhD DATA\SIEMENS\IM1\H_IM1_M11_TAC41.mat');
% QH(12)  =load('C:\Users\PFST-User\Desktop\PhD DATA\SIEMENS\IM1\H_IM1_M12_TAC41.mat');
% QH(13)  =load('C:\Users\PFST-User\Desktop\PhD DATA\SIEMENS\IM1\H_IM1_M13_TAC41.mat');
% QH(14)  =load('C:\Users\PFST-User\Desktop\PhD DATA\SIEMENS\IM1\H_IM1_M14_TAC41.mat');
% QH(15)  =load('C:\Users\PFST-User\Desktop\PhD DATA\SIEMENS\IM1\H_IM1_M15_TAC41.mat');
% QH(16)  =load('C:\Users\PFST-User\Desktop\PhD DATA\SIEMENS\IM1\H_IM1_M16_TAC41.mat');
% QH(17)  =load('C:\Users\PFST-User\Desktop\PhD DATA\SIEMENS\IM1\H_IM1_M17_TAC41.mat');
% QH(18)  =load('C:\Users\PFST-User\Desktop\PhD DATA\SIEMENS\IM1\H_IM1_M18_TAC41.mat');
% QH(19)  =load('C:\Users\PFST-User\Desktop\PhD DATA\SIEMENS\IM1\H_IM1_M19_TAC41.mat');
% QH(20)  =load('C:\Users\PFST-User\Desktop\PhD DATA\SIEMENS\IM1\H_IM1_M20_TAC41.mat');


%% %%%%%%%%%%%%%%%%%%%%%%%%%%%%% HEALTHY - IM2  %%%%%%%%%%%%%%%%%%%%%%%%%%%

% QH(1)   =load('C:\Users\PFST-User\Desktop\PhD DATA\SIEMENS\IM2_H\H_IM2_M1_TAC41.mat');
% QH(2)   =load('C:\Users\PFST-User\Desktop\PhD DATA\SIEMENS\IM2_H\H_IM2_M2_TAC41.mat');
% QH(3)   =load('C:\Users\PFST-User\Desktop\PhD DATA\SIEMENS\IM2_H\H_IM2_M3_TAC41.mat');
% QH(4)   =load('C:\Users\PFST-User\Desktop\PhD DATA\SIEMENS\IM2_H\H_IM2_M4_TAC41.mat');
% QH(5)   =load('C:\Users\PFST-User\Desktop\PhD DATA\SIEMENS\IM2_H\H_IM2_M5_TAC41.mat');
% QH(6)   =load('C:\Users\PFST-User\Desktop\PhD DATA\SIEMENS\IM2_H\H_IM2_M6_TAC41.mat');
% QH(7)   =load('C:\Users\PFST-User\Desktop\PhD DATA\SIEMENS\IM2_H\H_IM2_M7_TAC41.mat');
% QH(8)   =load('C:\Users\PFST-User\Desktop\PhD DATA\SIEMENS\IM2_H\H_IM2_M8_TAC41.mat');
% QH(9)   =load('C:\Users\PFST-User\Desktop\PhD DATA\SIEMENS\IM2_H\H_IM2_M9_TAC41.mat');
% QH(10)  =load('C:\Users\PFST-User\Desktop\PhD DATA\SIEMENS\IM2_H\H_IM2_M10_TAC41.mat');
% QH(11)  =load('C:\Users\PFST-User\Desktop\PhD DATA\SIEMENS\IM2_H\H_IM2_M11_TAC41.mat');
% QH(12)  =load('C:\Users\PFST-User\Desktop\PhD DATA\SIEMENS\IM2_H\H_IM2_M12_TAC41.mat');
% QH(13)  =load('C:\Users\PFST-User\Desktop\PhD DATA\SIEMENS\IM2_H\H_IM2_M13_TAC41.mat');
% QH(14)  =load('C:\Users\PFST-User\Desktop\PhD DATA\SIEMENS\IM2_H\H_IM2_M14_TAC41.mat');
% QH(15)  =load('C:\Users\PFST-User\Desktop\PhD DATA\SIEMENS\IM2_H\H_IM2_M15_TAC41.mat');
% QH(16)  =load('C:\Users\PFST-User\Desktop\PhD DATA\SIEMENS\IM2_H\H_IM2_M16_TAC41.mat');
% QH(17)  =load('C:\Users\PFST-User\Desktop\PhD DATA\SIEMENS\IM2_H\H_IM2_M17_TAC41.mat');
% QH(18)  =load('C:\Users\PFST-User\Desktop\PhD DATA\SIEMENS\IM2_H\H_IM2_M18_TAC41.mat');
% QH(19)  =load('C:\Users\PFST-User\Desktop\PhD DATA\SIEMENS\IM2_H\H_IM2_M19_TAC41.mat');
% QH(20)  =load('C:\Users\PFST-User\Desktop\PhD DATA\SIEMENS\IM2_H\H_IM2_M20_TAC41.mat');


%% %%%%%%%%%%%%%%%%%%%%%%%%%%%%% BRB 1 - IM2 %%%%%%%%%%%%%%%%%%%%%%%%%%%%%

QBRB1(1)   =load('C:\Users\PFST-User\Desktop\PhD DATA\SIEMENS\IM2_BRB1\BRB1_IM2_M1_TAC41.mat');
QBRB1(2)   =load('C:\Users\PFST-User\Desktop\PhD DATA\SIEMENS\IM2_BRB1\BRB1_IM2_M2_TAC41.mat');
QBRB1(3)   =load('C:\Users\PFST-User\Desktop\PhD DATA\SIEMENS\IM2_BRB1\BRB1_IM2_M3_TAC41.mat');
QBRB1(4)   =load('C:\Users\PFST-User\Desktop\PhD DATA\SIEMENS\IM2_BRB1\BRB1_IM2_M4_TAC41.mat');
QBRB1(5)   =load('C:\Users\PFST-User\Desktop\PhD DATA\SIEMENS\IM2_BRB1\BRB1_IM2_M5_TAC41.mat');
QBRB1(6)   =load('C:\Users\PFST-User\Desktop\PhD DATA\SIEMENS\IM2_BRB1\BRB1_IM2_M6_TAC41.mat');
QBRB1(7)   =load('C:\Users\PFST-User\Desktop\PhD DATA\SIEMENS\IM2_BRB1\BRB1_IM2_M7_TAC41.mat');
QBRB1(8)   =load('C:\Users\PFST-User\Desktop\PhD DATA\SIEMENS\IM2_BRB1\BRB1_IM2_M8_TAC41.mat');
QBRB1(9)   =load('C:\Users\PFST-User\Desktop\PhD DATA\SIEMENS\IM2_BRB1\BRB1_IM2_M9_TAC41.mat');
QBRB1(10)  =load('C:\Users\PFST-User\Desktop\PhD DATA\SIEMENS\IM2_BRB1\BRB1_IM2_M10_TAC41.mat');
QBRB1(11)  =load('C:\Users\PFST-User\Desktop\PhD DATA\SIEMENS\IM2_BRB1\BRB1_IM2_M11_TAC41.mat');
QBRB1(12)  =load('C:\Users\PFST-User\Desktop\PhD DATA\SIEMENS\IM2_BRB1\BRB1_IM2_M12_TAC41.mat');
QBRB1(13)  =load('C:\Users\PFST-User\Desktop\PhD DATA\SIEMENS\IM2_BRB1\BRB1_IM2_M13_TAC41.mat');
QBRB1(14)  =load('C:\Users\PFST-User\Desktop\PhD DATA\SIEMENS\IM2_BRB1\BRB1_IM2_M14_TAC41.mat');
QBRB1(15)  =load('C:\Users\PFST-User\Desktop\PhD DATA\SIEMENS\IM2_BRB1\BRB1_IM2_M15_TAC41.mat');
QBRB1(16)  =load('C:\Users\PFST-User\Desktop\PhD DATA\SIEMENS\IM2_BRB1\BRB1_IM2_M16_TAC41.mat');
QBRB1(17)  =load('C:\Users\PFST-User\Desktop\PhD DATA\SIEMENS\IM2_BRB1\BRB1_IM2_M17_TAC41.mat');
QBRB1(18)  =load('C:\Users\PFST-User\Desktop\PhD DATA\SIEMENS\IM2_BRB1\BRB1_IM2_M18_TAC41.mat');
QBRB1(19)  =load('C:\Users\PFST-User\Desktop\PhD DATA\SIEMENS\IM2_BRB1\BRB1_IM2_M19_TAC41.mat');
QBRB1(20)  =load('C:\Users\PFST-User\Desktop\PhD DATA\SIEMENS\IM2_BRB1\BRB1_IM2_M20_TAC41.mat');
```

```matlab
%% %%%%%%%%%%%%%%%%%%%%%%%%% KONCAR %%%%%%%%%%%%%%%%%%%%%%%%%%%%%%%%%%%%%
%% Load = 1.69 Nm
%% %%%%%%%%%%%%%%%%%%%%%%%%% HEALTHY - IM1  %%%%%%%%%%%%%%%%%%%%%%%%%%%%%

% QH(1)    =load('C:\Users\PFST-User\Desktop\PhD DATA\KONCAR\IM1\H_IM1_M1_TAC41.mat');
% QH(2)    =load('C:\Users\PFST-User\Desktop\PhD DATA\KONCAR\IM1\H_IM1_M2_TAC41.mat');
% QH(3)    =load('C:\Users\PFST-User\Desktop\PhD DATA\KONCAR\IM1\H_IM1_M3_TAC41.mat');
% QH(4)    =load('C:\Users\PFST-User\Desktop\PhD DATA\KONCAR\IM1\H_IM1_M4_TAC41.mat');
% QH(5)    =load('C:\Users\PFST-User\Desktop\PhD DATA\KONCAR\IM1\H_IM1_M5_TAC41.mat');
% QH(6)    =load('C:\Users\PFST-User\Desktop\PhD DATA\KONCAR\IM1\H_IM1_M6_TAC41.mat');
% QH(7)    =load('C:\Users\PFST-User\Desktop\PhD DATA\KONCAR\IM1\H_IM1_M7_TAC41.mat');
% QH(8)    =load('C:\Users\PFST-User\Desktop\PhD DATA\KONCAR\IM1\H_IM1_M8_TAC41.mat');
% QH(9)    =load('C:\Users\PFST-User\Desktop\PhD DATA\KONCAR\IM1\H_IM1_M9_TAC41.mat');
% QH(10)   =load('C:\Users\PFST-User\Desktop\PhD DATA\KONCAR\IM1\H_IM1_M10_TAC41.mat');
% QH(11)   =load('C:\Users\PFST-User\Desktop\PhD DATA\KONCAR\IM1\H_IM1_M11_TAC41.mat');
% QH(12)   =load('C:\Users\PFST-User\Desktop\PhD DATA\KONCAR\IM1\H_IM1_M12_TAC41.mat');
% QH(13)   =load('C:\Users\PFST-User\Desktop\PhD DATA\KONCAR\IM1\H_IM1_M13_TAC41.mat');
% QH(14)   =load('C:\Users\PFST-User\Desktop\PhD DATA\KONCAR\IM1\H_IM1_M14_TAC41.mat');
% QH(15)   =load('C:\Users\PFST-User\Desktop\PhD DATA\KONCAR\IM1\H_IM1_M15_TAC41.mat');
% QH(16)   =load('C:\Users\PFST-User\Desktop\PhD DATA\KONCAR\IM1\H_IM1_M16_TAC41.mat');
% QH(17)   =load('C:\Users\PFST-User\Desktop\PhD DATA\KONCAR\IM1\H_IM1_M17_TAC41.mat');
% QH(18)   =load('C:\Users\PFST-User\Desktop\PhD DATA\KONCAR\IM1\H_IM1_M18_TAC41.mat');
% QH(19)   =load('C:\Users\PFST-User\Desktop\PhD DATA\KONCAR\IM1\H_IM1_M19_TAC41.mat');
% QH(20)   =load('C:\Users\PFST-User\Desktop\PhD DATA\KONCAR\IM1\H_IM1_M20_TAC41.mat');

%% %%%%%%%%%%%%%%%%%%%%%%%%% HEALTHY - IM2  %%%%%%%%%%%%%%%%%%%%%%%%%%%%%

% QH(1)    =load('C:\Users\PFST-User\Desktop\PhD DATA\KONCAR\IM2_H\H_IM2_M1_TAC41.mat');
% QH(2)    =load('C:\Users\PFST-User\Desktop\PhD DATA\KONCAR\IM2_H\H_IM2_M2_TAC41.mat');
% QH(3)    =load('C:\Users\PFST-User\Desktop\PhD DATA\KONCAR\IM2_H\H_IM2_M3_TAC41.mat');
% QH(4)    =load('C:\Users\PFST-User\Desktop\PhD DATA\KONCAR\IM2_H\H_IM2_M4_TAC41.mat');
% QH(5)    =load('C:\Users\PFST-User\Desktop\PhD DATA\KONCAR\IM2_H\H_IM2_M5_TAC41.mat');
% QH(6)    =load('C:\Users\PFST-User\Desktop\PhD DATA\KONCAR\IM2_H\H_IM2_M6_TAC41.mat');
% QH(7)    =load('C:\Users\PFST-User\Desktop\PhD DATA\KONCAR\IM2_H\H_IM2_M7_TAC41.mat');
% QH(8)    =load('C:\Users\PFST-User\Desktop\PhD DATA\KONCAR\IM2_H\H_IM2_M8_TAC41.mat');
% QH(9)    =load('C:\Users\PFST-User\Desktop\PhD DATA\KONCAR\IM2_H\H_IM2_M9_TAC41.mat');
% QH(10)   =load('C:\Users\PFST-User\Desktop\PhD DATA\KONCAR\IM2_H\H_IM2_M10_TAC41.mat');
% QH(11)   =load('C:\Users\PFST-User\Desktop\PhD DATA\KONCAR\IM2_H\H_IM2_M11_TAC41.mat');
% QH(12)   =load('C:\Users\PFST-User\Desktop\PhD DATA\KONCAR\IM2_H\H_IM2_M12_TAC41.mat');
% QH(13)   =load('C:\Users\PFST-User\Desktop\PhD DATA\KONCAR\IM2_H\H_IM2_M13_TAC41.mat');
% QH(14)   =load('C:\Users\PFST-User\Desktop\PhD DATA\KONCAR\IM2_H\H_IM2_M14_TAC41.mat');
% QH(15)   =load('C:\Users\PFST-User\Desktop\PhD DATA\KONCAR\IM2_H\H_IM2_M15_TAC41.mat');
% QH(16)   =load('C:\Users\PFST-User\Desktop\PhD DATA\KONCAR\IM2_H\H_IM2_M16_TAC41.mat');
% QH(17)   =load('C:\Users\PFST-User\Desktop\PhD DATA\KONCAR\IM2_H\H_IM2_M17_TAC41.mat');
% QH(18)   =load('C:\Users\PFST-User\Desktop\PhD DATA\KONCAR\IM2_H\H_IM2_M18_TAC41.mat');
% QH(19)   =load('C:\Users\PFST-User\Desktop\PhD DATA\KONCAR\IM2_H\H_IM2_M19_TAC41.mat');
% QH(20)   =load('C:\Users\PFST-User\Desktop\PhD DATA\KONCAR\IM2_H\H_IM2_M20_TAC41.mat');

%% %%%%%%%%%%%%%%%%%%%%%%%%%%% BRB 1 - IM2 %%%%%%%%%%%%%%%%%%%%%%%%%%%%%%

% QBRB1(1)   =load('C:\Users\PFST-User\Desktop\PhD DATA\KONCAR\IM2_BRB1\BRB1_IM2_M1_TAC41.mat');
% QBRB1(2)   =load('C:\Users\PFST-User\Desktop\PhD DATA\KONCAR\IM2_BRB1\BRB1_IM2_M2_TAC41.mat');
% QBRB1(3)   =load('C:\Users\PFST-User\Desktop\PhD DATA\KONCAR\IM2_BRB1\BRB1_IM2_M3_TAC41.mat');
% QBRB1(4)   =load('C:\Users\PFST-User\Desktop\PhD DATA\KONCAR\IM2_BRB1\BRB1_IM2_M4_TAC41.mat');
% QBRB1(5)   =load('C:\Users\PFST-User\Desktop\PhD DATA\KONCAR\IM2_BRB1\BRB1_IM2_M5_TAC41.mat');
% QBRB1(6)   =load('C:\Users\PFST-User\Desktop\PhD DATA\KONCAR\IM2_BRB1\BRB1_IM2_M6_TAC41.mat');
% QBRB1(7)   =load('C:\Users\PFST-User\Desktop\PhD DATA\KONCAR\IM2_BRB1\BRB1_IM2_M7_TAC41.mat');
% QBRB1(8)   =load('C:\Users\PFST-User\Desktop\PhD DATA\KONCAR\IM2_BRB1\BRB1_IM2_M8_TAC41.mat');
% QBRB1(9)   =load('C:\Users\PFST-User\Desktop\PhD DATA\KONCAR\IM2_BRB1\BRB1_IM2_M9_TAC41.mat');
% QBRB1(10)  =load('C:\Users\PFST-User\Desktop\PhD DATA\KONCAR\IM2_BRB1\BRB1_IM2_M10_TAC41.mat');
% QBRB1(11)  =load('C:\Users\PFST-User\Desktop\PhD DATA\KONCAR\IM2_BRB1\BRB1_IM2_M11_TAC41.mat');
% QBRB1(12)  =load('C:\Users\PFST-User\Desktop\PhD DATA\KONCAR\IM2_BRB1\BRB1_IM2_M12_TAC41.mat');
% QBRB1(13)  =load('C:\Users\PFST-User\Desktop\PhD DATA\KONCAR\IM2_BRB1\BRB1_IM2_M13_TAC41.mat');
% QBRB1(14)  =load('C:\Users\PFST-User\Desktop\PhD DATA\KONCAR\IM2_BRB1\BRB1_IM2_M14_TAC41.mat');
% QBRB1(15)  =load('C:\Users\PFST-User\Desktop\PhD DATA\KONCAR\IM2_BRB1\BRB1_IM2_M15_TAC41.mat');
% QBRB1(16)  =load('C:\Users\PFST-User\Desktop\PhD DATA\KONCAR\IM2_BRB1\BRB1_IM2_M16_TAC41.mat');
% QBRB1(17)  =load('C:\Users\PFST-User\Desktop\PhD DATA\KONCAR\IM2_BRB1\BRB1_IM2_M17_TAC41.mat');
% QBRB1(18)  =load('C:\Users\PFST-User\Desktop\PhD DATA\KONCAR\IM2_BRB1\BRB1_IM2_M18_TAC41.mat');
% QBRB1(19)  =load('C:\Users\PFST-User\Desktop\PhD DATA\KONCAR\IM2_BRB1\BRB1_IM2_M19_TAC41.mat');
% QBRB1(20)  =load('C:\Users\PFST-User\Desktop\PhD DATA\KONCAR\IM2_BRB1\BRB1_IM2_M20_TAC41.mat');

%% %%%%%%%%%%%%%%%%%%%%%%%%%%%%%%%%%%%%%%%%%%%%%%%%%%%%%%%%%%%%%%%%%%%%%%%
%% %%%%%%%%%%%%%%%%%%%%%%%%%%%%%%%%%%%%%%%%%%%%%%%%%%%%%%%%%%%%%%%%%%%%%%%

N=50;                  % Number of random triaxial coil positions
NF_H=20;               % Number of files for healthy state
NF_BRB1=20;            % Number of files for BRB1 state

%% %%%%%%%%%%%%%%%%%%%%%%% DATA LOADING - HEALTHY %%%%%%%%%%%%%%%%%%%%%%%%
%% %%%%%%%%%%%%%%%%%% Separate signals e1(t), e2(t), e3(t) %%%%%%%%%%%%%%%%%%

% for i=1:NF_H
%     fnH=fieldnames(QH(i));
% for j=1:N
%
%     tH{j,i}=seconds(QH(i).(fnH{j}).Time);    % Time vector - Healthy
%     YH_s1{j,i}=QH(i).(fnH{j}).Dev1_ai0;
%     YH_s2{j,i}=QH(i).(fnH{j}).Dev1_ai1;
```

```matlab
%       YH_s3{j,i}=QH(i).(fnH{j}).Dev1_ai2;
% end
% end

%% %%%%%%%%%%%%%%%%%%%%% DATA LOADING - BRB1 %%%%%%%%%%%%%%%%%%%%%%%%%%%%%
%% %%%%%%%%%%%%%%%%%% Separate signals e1(t), e2(t), e3(t) %%%%%%%%%%%%%%%%%%

for i=1:NF_BRB1
    fnBRB1=fieldnames(QBRB1(i));
for j=1:N

    tBRB1{j,i}=seconds(QBRB1(i).(fnBRB1{j}).Time);   % Time vector - BRB1
    YBRB1_s1{j,i}=QBRB1(i).(fnBRB1{j}).Dev1_ai0;
    YBRB1_s2{j,i}=QBRB1(i).(fnBRB1{j}).Dev1_ai1;
    YBRB1_s3{j,i}=QBRB1(i).(fnBRB1{j}).Dev1_ai2;
end
end

%% HEALTHY %%%%%%%%%%%%%%%%%%%%%%%%%%%%%%%%%%%%%%%%%%%%%%%%%%%%%%%%%%%%%%%%%

% t_H=tH{1,1}(:);
%
% count1=0;
% counter1=0;
% for i=1:NF_H
% for j=1:N
% for k=1:length(tH{1,1})
%
% % S1_H_IM1_M1000(k,j+count1)=YH_s1{j,i}(k);
% % S2_H_IM1_M1000(k,j+count1)=YH_s2{j,i}(k);
% % S3_H_IM1_M1000(k,j+count1)=YH_s3{j,i}(k);
%
% % S1_H_IM2_M1000(k,j+count1)=YH_s1{j,i}(k);
% % S2_H_IM2_M1000(k,j+count1)=YH_s2{j,i}(k);
% % S3_H_IM2_M1000(k,j+count1)=YH_s3{j,i}(k);
%
% end
% counter1=counter1+1;
% end
% count1=counter1;
% end

% save('C:\Users\PFST-User\Desktop\PhD DATA/S_H_IM1_M1000.mat',...
% 'S1_H_IM1_M1000',...
% 'S2_H_IM1_M1000',...
% 'S3_H_IM1_M1000');

% save('C:\Users\PFST-User\Desktop\PhD DATA/S_H_IM2_M1000.mat',...
% 'S1_H_IM2_M1000',...
% 'S2_H_IM2_M1000',...
% 'S3_H_IM2_M1000');

% save('C:\Users\PFST-User\Desktop\PhD DATA/K_H_IM1_M1000.mat',...
% 'S1_H_IM1_M1000',...
% 'S2_H_IM1_M1000',...
% 'S3_H_IM1_M1000');

% save('C:\Users\PFST-User\Desktop\PhD DATA/K_H_IM2_M1000.mat',...
% 'S1_H_IM2_M1000',...
% 'S2_H_IM2_M1000',...
% 'S3_H_IM2_M1000');


%% BRB1 %%%%%%%%%%%%%%%%%%%%%%%%%%%%%%%%%%%%%%%%%%%%%%%%%%%%%%%%%%%%%%%%%%%%%

t_BRB1=tBRB1{1,1}(:);

count2=0;
counter2=0;
for i=1:NF_BRB1
for j=1:N
for k=1:length(tBRB1{1,1})

S1_BRB1_IM2_M1000(k,j+count2)=YBRB1_s1{j,i}(k);
S2_BRB1_IM2_M1000(k,j+count2)=YBRB1_s2{j,i}(k);
S3_BRB1_IM2_M1000(k,j+count2)=YBRB1_s3{j,i}(k);


end
counter2=counter2+1;
end
count2=counter2;
end


save('C:\Users\PFST-User\Desktop\PhD DATA/S_BRB1_IM2_M1000.mat',...
'S1_BRB1_IM2_M1000',...
'S2_BRB1_IM2_M1000',...
```

```
'S3_BRB1_IM2_M1000');

% save('C:\Users\PFST-User\Desktop\PhD DATA/K_BRB1_IM2_M1000.mat',...
% 'S1_BRB1_IM2_M1000',...
% 'S2_BRB1_IM2_M1000',...
% 'S3_BRB1_IM2_M1000');


%-----------------------------------------------------------------



clear all;close all;clc

%% %%%%%%%%%%%%%%%%%%%%%%%%%%%%%%%%%%%%%%%%%%%%%%%%%%%%%%%%%%%%%%%%%%%
%% %%%%%%%%%%%%%%%%%%%% HISTOGRAM & QQ plot %%%%%%%%%%%%%%%%%%%%%%%%%%
%% %%%%%%%%%%%%%%%%%%%%%%%%%%%%%%%%%%%%%%%%%%%%%%%%%%%%%%%%%%%%%%%%%%%

%% SIEMENS %%%%%%%%%%%%%%%%%%%%%%%%%%%%%%%%%%%%%%%%%%%%%%%%%%%%%%%%%%%%

% load('C:\Users\PFST-User\Desktop\PhD DATA\S_H_IM1_M1000.mat')
% load('C:\Users\PFST-User\Desktop\PhD DATA\S_H_IM2_M1000.mat')
% load('C:\Users\PFST-User\Desktop\PhD DATA\S_BRB1_IM2_M1000.mat')

%% KONCAR %%%%%%%%%%%%%%%%%%%%%%%%%%%%%%%%%%%%%%%%%%%%%%%%%%%%%%%%%%%%

load('C:\Users\PFST-User\Desktop\PhD DATA\K_H_IM1_M1000.mat')
load('C:\Users\PFST-User\Desktop\PhD DATA\K_H_IM2_M1000.mat')
load('C:\Users\PFST-User\Desktop\PhD DATA\K_BRB1_IM2_M1000.mat')

%% %%%%%%%%%%%%%%%%%%%%%%%%%%%%%%%%%%%%%%%%%%%%%%%%%%%%%%%%%%%%%%%%%%%
IM1_C1=reshape(S1_H_IM1_M1000,[],1);
IM1_C2=reshape(S2_H_IM1_M1000,[],1);
IM1_C3=reshape(S3_H_IM1_M1000,[],1);

IM2_H_C1=reshape(S1_H_IM2_M1000,[],1);
IM2_H_C2=reshape(S2_H_IM2_M1000,[],1);
IM2_H_C3=reshape(S3_H_IM2_M1000,[],1);

IM2_BRB1_C1=reshape(S1_BRB1_IM2_M1000,[],1);
IM2_BRB1_C2=reshape(S2_BRB1_IM2_M1000,[],1);
IM2_BRB1_C3=reshape(S3_BRB1_IM2_M1000,[],1);

IM1_C123=[IM1_C1 IM1_C2 IM1_C3];
IM2_H_C123=[IM2_H_C1 IM2_H_C2 IM2_H_C3];
IM2_BRB1_C123=[IM2_BRB1_C1 IM2_BRB1_C2 IM2_BRB1_C3];

%%
l=length(IM1_C1);
x=l/10;

IM1_C123_1=IM1_C123(1:x,:);
IM1_C123_2=IM1_C123(1*x+1:2*x,:);
IM1_C123_3=IM1_C123(2*x+1:3*x,:);
IM1_C123_4=IM1_C123(3*x+1:4*x,:);
IM1_C123_5=IM1_C123(4*x+1:5*x,:);
IM1_C123_6=IM1_C123(5*x+1:6*x,:);
IM1_C123_7=IM1_C123(6*x+1:7*x,:);
IM1_C123_8=IM1_C123(7*x+1:8*x,:);
IM1_C123_9=IM1_C123(8*x+1:9*x,:);
IM1_C123_10=IM1_C123(9*x+1:10*x,:);

IM2_H_C123_1=IM2_H_C123(1:x,:);
IM2_H_C123_2=IM2_H_C123(1*x+1:2*x,:);
IM2_H_C123_3=IM2_H_C123(2*x+1:3*x,:);
IM2_H_C123_4=IM2_H_C123(3*x+1:4*x,:);
IM2_H_C123_5=IM2_H_C123(4*x+1:5*x,:);
IM2_H_C123_6=IM2_H_C123(5*x+1:6*x,:);
IM2_H_C123_7=IM2_H_C123(6*x+1:7*x,:);
IM2_H_C123_8=IM2_H_C123(7*x+1:8*x,:);
IM2_H_C123_9=IM2_H_C123(8*x+1:9*x,:);
IM2_H_C123_10=IM2_H_C123(9*x+1:10*x,:);

IM2_BRB1_C123_1=IM2_BRB1_C123(1:x,:);
IM2_BRB1_C123_2=IM2_BRB1_C123(1*x+1:2*x,:);
IM2_BRB1_C123_3=IM2_BRB1_C123(2*x+1:3*x,:);
IM2_BRB1_C123_4=IM2_BRB1_C123(3*x+1:4*x,:);
IM2_BRB1_C123_5=IM2_BRB1_C123(4*x+1:5*x,:);
IM2_BRB1_C123_6=IM2_BRB1_C123(5*x+1:6*x,:);
IM2_BRB1_C123_7=IM2_BRB1_C123(6*x+1:7*x,:);
IM2_BRB1_C123_8=IM2_BRB1_C123(7*x+1:8*x,:);
IM2_BRB1_C123_9=IM2_BRB1_C123(8*x+1:9*x,:);
IM2_BRB1_C123_10=IM2_BRB1_C123(9*x+1:10*x,:);
%%
IM1_R_C123_1=reshape(IM1_C123_1,[],1);
IM1_R_C123_2=reshape(IM1_C123_2,[],1);
IM1_R_C123_3=reshape(IM1_C123_3,[],1);
```

```matlab
IM1_R_C123_4=reshape(IM1_C123_4,[],1);
IM1_R_C123_5=reshape(IM1_C123_5,[],1);
IM1_R_C123_6=reshape(IM1_C123_6,[],1);
IM1_R_C123_7=reshape(IM1_C123_7,[],1);
IM1_R_C123_8=reshape(IM1_C123_8,[],1);
IM1_R_C123_9=reshape(IM1_C123_9,[],1);
IM1_R_C123_10=reshape(IM1_C123_10,[],1);

IM2_H_R_C123_1=reshape(IM2_H_C123_1,[],1);
IM2_H_R_C123_2=reshape(IM2_H_C123_2,[],1);
IM2_H_R_C123_3=reshape(IM2_H_C123_3,[],1);
IM2_H_R_C123_4=reshape(IM2_H_C123_4,[],1);
IM2_H_R_C123_5=reshape(IM2_H_C123_5,[],1);
IM2_H_R_C123_6=reshape(IM2_H_C123_6,[],1);
IM2_H_R_C123_7=reshape(IM2_H_C123_7,[],1);
IM2_H_R_C123_8=reshape(IM2_H_C123_8,[],1);
IM2_H_R_C123_9=reshape(IM2_H_C123_9,[],1);
IM2_H_R_C123_10=reshape(IM2_H_C123_10,[],1);

IM2_BRB1_R_C123_1=reshape(IM2_BRB1_C123_1,[],1);
IM2_BRB1_R_C123_2=reshape(IM2_BRB1_C123_2,[],1);
IM2_BRB1_R_C123_3=reshape(IM2_BRB1_C123_3,[],1);
IM2_BRB1_R_C123_4=reshape(IM2_BRB1_C123_4,[],1);
IM2_BRB1_R_C123_5=reshape(IM2_BRB1_C123_5,[],1);
IM2_BRB1_R_C123_6=reshape(IM2_BRB1_C123_6,[],1);
IM2_BRB1_R_C123_7=reshape(IM2_BRB1_C123_7,[],1);
IM2_BRB1_R_C123_8=reshape(IM2_BRB1_C123_8,[],1);
IM2_BRB1_R_C123_9=reshape(IM2_BRB1_C123_9,[],1);
IM2_BRB1_R_C123_10=reshape(IM2_BRB1_C123_10,[],1);

%%
IM1_R_C123=[IM1_R_C123_1 IM1_R_C123_2 IM1_R_C123_3 IM1_R_C123_4 IM1_R_C123_5 IM1_R_C123_6 IM1_R_C123_7
IM1_R_C123_8 IM1_R_C123_9 IM1_R_C123_10];
IM2_H_R_C123=[IM2_H_R_C123_1 IM2_H_R_C123_2 IM2_H_R_C123_3 IM2_H_R_C123_4 IM2_H_R_C123_5 IM2_H_R_C123_6
IM2_H_R_C123_7 IM2_H_R_C123_8 IM2_H_R_C123_9 IM2_H_R_C123_10];
IM2_BRB1_R_C123=[IM2_BRB1_R_C123_1 IM2_BRB1_R_C123_2 IM2_BRB1_R_C123_3 IM2_BRB1_R_C123_4 IM2_BRB1_R_C123_5
IM2_BRB1_R_C123_6 IM2_BRB1_R_C123_7 IM2_BRB1_R_C123_8 IM2_BRB1_R_C123_9 IM2_BRB1_R_C123_10];

%% HISTOGRAM - IM1 %%%%%%%%%%%%%%%%%%%%%%%%%%%%%%%%%%%%%%%%%%%%%%%%%%%

NB=100; % NB - number of bins
figure,histogram(IM1_R_C123(:,1),NB);
hold on;
histogram(IM1_R_C123(:,2),NB);
histogram(IM1_R_C123(:,3),NB);
histogram(IM1_R_C123(:,4),NB);
histogram(IM1_R_C123(:,5),NB);
histogram(IM1_R_C123(:,6),NB);
histogram(IM1_R_C123(:,7),NB);
histogram(IM1_R_C123(:,8),NB);
histogram(IM1_R_C123(:,9),NB);
histogram(IM1_R_C123(:,10),NB);
grid on
xlim([-0.1 0.1])      % for Siemens
ylim([0 15e4])        % for Siemens

% xlim([-0.6 0.60000001]) % for KONCAR
% ylim([0 20e4])          % for KONCAR
set(gca,'FontSize',16)
    xlabel('Data value - emf [V]','FontSize',16,'FontWeight','bold')
    ylabel('Frequency','FontSize',16,'FontWeight','bold')
legend({    'Day 1', 'Day 2','Day 3','Day 4','Day 5',...
            'Day 6', 'Day 7','Day 8','Day 9','Day 10'},...

'Location','northeast','Orientation','horizontal','NumColumns',1,'FontSize',14,'FontWeight','bold')


%% HISTOGRAM - IM2_H %%%%%%%%%%%%%%%%%%%%%%%%%%%%%%%%%%%%%%%%%%%%%%%%%%%%

figure,histogram(IM2_H_R_C123(:,1),NB);
hold on;
histogram(IM2_H_R_C123(:,2),NB);
histogram(IM2_H_R_C123(:,3),NB);
histogram(IM2_H_R_C123(:,4),NB);
histogram(IM2_H_R_C123(:,5),NB);
histogram(IM2_H_R_C123(:,6),NB);
histogram(IM2_H_R_C123(:,7),NB);
histogram(IM2_H_R_C123(:,8),NB);
histogram(IM2_H_R_C123(:,9),NB);
histogram(IM2_H_R_C123(:,10),NB);
grid on
xlim([-0.1 0.1])       % for Siemens
ylim([0 15e4])         % for Siemens

% xlim([-0.6 0.60000001])     % for KONCAR
% ylim([0 20e4])              % for KONCAR
set(gca,'FontSize',16)
    xlabel('Data value - emf [V]','FontSize',16,'FontWeight','bold')
```

```matlab
    ylabel('Frequency','FontSize',16,'FontWeight','bold')
legend({    'Day 1', 'Day 2','Day 3','Day 4','Day 5',...
                'Day 6', 'Day 7','Day 8','Day 9','Day 10'},...

'Location','northeast','Orientation','horizontal','NumColumns',1,'FontSize',14,'FontWeight','bold')

%% HISTOGRAM - IM2_BRB1 %%%%%%%%%%%%%%%%%%%%%%%%%%%%%%%%%%%%%%%%%%%%

figure,histogram(IM2_BRB1_R_C123(:,1),NB);
hold on;
histogram(IM2_BRB1_R_C123(:,2),NB);
histogram(IM2_BRB1_R_C123(:,3),NB);
histogram(IM2_BRB1_R_C123(:,4),NB);
histogram(IM2_BRB1_R_C123(:,5),NB);
histogram(IM2_BRB1_R_C123(:,6),NB);
histogram(IM2_BRB1_R_C123(:,7),NB);
histogram(IM2_BRB1_R_C123(:,8),NB);
histogram(IM2_BRB1_R_C123(:,9),NB);
histogram(IM2_BRB1_R_C123(:,10),NB);
grid on
xlim([-0.1 0.1])        % for Siemens
ylim([0 15e4])          % for Siemens

% xlim([-0.6 0.60000001])     % for KONCAR
% ylim([0 20e4])              % for KONCAR
set(gca,'FontSize',16)
    xlabel('Data value - emf [V]','FontSize',16,'FontWeight','bold')
    ylabel('Frequency','FontSize',16,'FontWeight','bold')
legend({    'Day 1', 'Day 2','Day 3','Day 4','Day 5',...
                'Day 6', 'Day 7','Day 8','Day 9','Day 10'},...

'Location','northeast','Orientation','horizontal','NumColumns',1,'FontSize',14,'FontWeight','bold')

%%
figure,

hqqp = qqplot(IM1_R_C123);
% hqqp(1).MarkerSize = 20;
% hqqp(2).LineWidth = 5;
% hqqp(3).Color = 'g';

legend({    'day 1', 'day 2','day 3','day 4','day 5',...
                'day 6', 'day 7','day 8','day 9','day 10'},...
                'Location','southeast','Orientation','horizontal','NumColumns',2,'FontSize',16)
%%
figure, qqplot(IM2_H_R_C123)
legend({    'day 1', 'day 2','day 3','day 4','day 5',...
                'day 6', 'day 7','day 8','day 9','day 10'},...
                'Location','southeast','Orientation','horizontal','NumColumns',2,'FontSize',16)


%%
figure, qqplot(IM2_BRB1_R_C123)
legend({    'day 1', 'day 2','day 3','day 4','day 5',...
                'day 6', 'day 7','day 8','day 9','day 10'},...
                'Location','southeast','Orientation','horizontal','NumColumns',2,'FontSize',16)

%% %%%%%%%%%%%%%%%%%%%%%%%%%%%%%%%%%%%%%%%%%%%%%%%%%%%%%%%%%%%%%%%%%%%%

% save('C:\Users\PFST-User\Desktop\PhD DATA/SIEMENS_C123_M1000.mat',...
% 'IM1_R_C123',...
% 'IM2_H_R_C123',...
% 'IM2_BRB1_R_C123');

% save('C:\Users\PFST-User\Desktop\PhD DATA/KONCAR_C123_M1000.mat',...
% 'IM1_R_C123',...
% 'IM2_H_R_C123',...
% 'IM2_BRB1_R_C123');

%% %%%%%%%%%%%%%%%%%%%%%%%%%%%%%%%%%%%%%%%%%%%%%%%%%%%%%%%%%%%%%%%%%%%%


----------------------------------------------------------------
```

```matlab
clc; clear all; close all

%% %%%%%%%%%%%%%%%%%%%%%%%%%%%%%%%%%%%%%%%%%%%%%%%%%%%%%%%%%%%%%%%%%%%%%%%%%%
%% %%%%%%%%%%%%%%%% RM-ANOVA and Benjamini-Hochberg  %%%%%%%%%%%%%%%%%%%%%%%%
%% %%%%%%%%%%%%%%%%%%%%%%%%%%%%%%%%%%%%%%%%%%%%%%%%%%%%%%%%%%%%%%%%%%%%%%%%%%

% load('C:\Users\PFST-User\Desktop\PhD DATA\SIEMENS_C123_M1000.mat')

load('C:\Users\PFST-User\Desktop\PhD DATA\KONCAR_C123_M1000.mat')


%% ONE-WAY REPEATED MEASURES ANOVA %%%%%%%%%%%%%%%%%%%%%%%%%%%%%%%%%%%%%%%%%%


t_IM1 = table(      IM1_R_C123(:,1),IM1_R_C123(:,2),IM1_R_C123(:,3),IM1_R_C123(:,4),IM1_R_C123(:,5),...
                    IM1_R_C123(:,6),IM1_R_C123(:,7),IM1_R_C123(:,8),IM1_R_C123(:,9),IM1_R_C123(:,10),...
                    'VariableNames',{'d1','d2','d3','d4','d5','d6','d7','d8','d9','d10'});

t_IM2_H = table(
IM2_H_R_C123(:,1),IM2_H_R_C123(:,2),IM2_H_R_C123(:,3),IM2_H_R_C123(:,4),IM2_H_R_C123(:,5),...

IM2_H_R_C123(:,6),IM2_H_R_C123(:,7),IM2_H_R_C123(:,8),IM2_H_R_C123(:,9),IM2_H_R_C123(:,10),...
                    'VariableNames',{'d1','d2','d3','d4','d5','d6','d7','d8','d9','d10'});

t_IM2_BRB1 = table(
IM2_BRB1_R_C123(:,1),IM2_BRB1_R_C123(:,2),IM2_BRB1_R_C123(:,3),IM2_BRB1_R_C123(:,4),IM2_BRB1_R_C123(:,5),..
.

IM2_BRB1_R_C123(:,6),IM2_BRB1_R_C123(:,7),IM2_BRB1_R_C123(:,8),IM2_BRB1_R_C123(:,9),IM2_BRB1_R_C123(:,10),.
..
                    'VariableNames',{'d1','d2','d3','d4','d5','d6','d7','d8','d9','d10'});

%% %%%%%%%%%%%%%%%%%%%%%%%%%%%%%%%%%%%%%%%%%%%%%%%%%%%%%%%%%%%%%%%%%%%%%%%%%%


T = table([1 2 3 4 5 6 7 8 9 10]','VariableNames',{'day'});

% withinDesign = table([1 2 3 4 5 6 7 8 9 10]', 'VariableNames', {'Time'});
% withinDesign.Time = categorical(withinDesign.Time);

rm_IM1 = fitrm(t_IM1,'d1-d10 ~ 1','WithinDesign', T);
rm_IM2_H = fitrm(t_IM2_H,'d1-d10 ~ 1','WithinDesign', T);
rm_IM2_BRB1 = fitrm(t_IM2_BRB1,'d1-d10 ~ 1','WithinDesign', T);

RMAT_IM1 = ranova(rm_IM1)
RMAT_IM2_H = ranova(rm_IM2_H)
RMAT_IM2_BRB1 = ranova(rm_IM2_BRB1)

% tbl=multcompare(rm,'day')

% tbl_H4=multcompare(rm_H4,'day','ComparisonType','bonferroni')
% tbl_H5=multcompare(rm_H5,'day','ComparisonType','bonferroni')
% tbl_B=multcompare(rm_B,'day','ComparisonType','bonferroni')

%% ComparisonType = 'lsd' - PRETPOSTAVKA ZA Benjamini-Hochberg correction
%% MATLAB Definition: Least significant difference. This option uses plain t-tests...
%% ...It provides no protection against the multiple comparison problem.
str1='lsd';
tbl_IM1=multcompare(rm_IM1,'day','ComparisonType',str1)
tbl_IM2_H=multcompare(rm_IM2_H,'day','ComparisonType',str1)
tbl_IM2_BRB1=multcompare(rm_IM2_BRB1,'day','ComparisonType',str1)

TBL_IM1=
[tbl_IM1(1:9,:);tbl_IM1(11:18,:);tbl_IM1(21:27,:);tbl_IM1(31:36,:);tbl_IM1(41:45,:);tbl_IM1(51:54,:);tbl_IM
1(61:63,:);tbl_IM1(71:72,:);tbl_IM1(81,:)];
TBL_IM2_H=
[tbl_IM2_H(1:9,:);tbl_IM2_H(11:18,:);tbl_IM2_H(21:27,:);tbl_IM2_H(31:36,:);tbl_IM2_H(41:45,:);tbl_IM2_H(51:
54,:);tbl_IM2_H(61:63,:);tbl_IM2_H(71:72,:);tbl_IM2_H(81,:)];
TBL_IM2_BRB1=
[tbl_IM2_BRB1(1:9,:);tbl_IM2_BRB1(11:18,:);tbl_IM2_BRB1(21:27,:);tbl_IM2_BRB1(31:36,:);tbl_IM2_BRB1(41:45,:
);tbl_IM2_BRB1(51:54,:);tbl_IM2_BRB1(61:63,:);tbl_IM2_BRB1(71:72,:);tbl_IM2_BRB1(81,:)];

% figure,stem(TBL_H4.pValue)
% figure,stem(TBL_H5.pValue)
% figure,stem(TBL_B.pValue)

mm_IM1=margmean(rm_IM1,'day');
mm_IM2_H=margmean(rm_IM2_H,'day');
mm_IM2_BRB1=margmean(rm_IM2_BRB1,'day');

mTEST_IM1=mauchly(rm_IM1);
mTEST_IM2_H=mauchly(rm_IM2_H);
mTEST_IM2_BRB1=mauchly(rm_IM2_BRB1);

%% STEM PLOT IM1 %%%%%%%%%%%%%%%%%%%%%%%%%%%%%%%%%%%%%%%%%%%%%%%%%%%%%%%%%%%%
figure,stem(TBL_IM1.pValue,'filled','LineWidth',2)
hold on
yline(0.05,'r-','\alpha=0.05','LineWidth',2,'FontSize',18,'FontWeight','bold')
```

```matlab
set(gca,'FontSize',18)
xticks([1:1:45])
xticklabels({   '1-2','1-3','1-4','1-5','1-6','1-7','1-8','1-9','1-10',...
                '2-3','2-4','2-5','2-6','2-7','2-8','2-9','2-10',...
                '3-4','3-5','3-6','3-7','3-8','3-9','3-10',...
                '4-5','4-6','4-7','4-8','4-9','4-10',...
                '5-6','5-7','5-8','5-9','5-10',...
                '6-7','6-8','6-9','6-10',...
                '7-8','7-9','7-10',...
                '8-9','8-10',...
                '9-10'})
xtickangle(90)
xlabel('day combination','FontSize',18,'FontWeight','bold')
ylabel('p-value','FontSize',18,'FontWeight','bold')
% title('Multiple comparison - IM1')

%% STEM PLOT IM2_H %%%%%%%%%%%%%%%%%%%%%%%%%%%%%%%%%%%%%%%%%%%%%%%%%%%%%%
figure,stem(TBL_IM2_H.pValue,'filled','LineWidth',2)
hold on
yline(0.05,'r-','\alpha=0.05','LineWidth',2,'FontSize',18,'FontWeight','bold')
set(gca,'FontSize',18)
xticks([1:1:45])
xticklabels({   '1-2','1-3','1-4','1-5','1-6','1-7','1-8','1-9','1-10',...
                '2-3','2-4','2-5','2-6','2-7','2-8','2-9','2-10',...
                '3-4','3-5','3-6','3-7','3-8','3-9','3-10',...
                '4-5','4-6','4-7','4-8','4-9','4-10',...
                '5-6','5-7','5-8','5-9','5-10',...
                '6-7','6-8','6-9','6-10',...
                '7-8','7-9','7-10',...
                '8-9','8-10',...
                '9-10'})
xtickangle(90)
xlabel('day combination','FontSize',18,'FontWeight','bold')
ylabel('p-value','FontSize',18,'FontWeight','bold')
% title('Multiple comparison - IM1')

%% STEM PLOT IM2_BRB1 %%%%%%%%%%%%%%%%%%%%%%%%%%%%%%%%%%%%%%%%%%%%%%%%%%%%
figure,stem(TBL_IM2_BRB1.pValue,'filled','LineWidth',2)
hold on
yline(0.05,'r-','\alpha=0.05','LineWidth',2,'FontSize',18,'FontWeight','bold')
set(gca,'FontSize',18)
xticks([1:1:45])
xticklabels({   '1-2','1-3','1-4','1-5','1-6','1-7','1-8','1-9','1-10',...
                '2-3','2-4','2-5','2-6','2-7','2-8','2-9','2-10',...
                '3-4','3-5','3-6','3-7','3-8','3-9','3-10',...
                '4-5','4-6','4-7','4-8','4-9','4-10',...
                '5-6','5-7','5-8','5-9','5-10',...
                '6-7','6-8','6-9','6-10',...
                '7-8','7-9','7-10',...
                '8-9','8-10',...
                '9-10'})
xtickangle(90)
xlabel('day combination','FontSize',18,'FontWeight','bold')
ylabel('p-value','FontSize',18,'FontWeight','bold')
% title('Multiple comparison - IM1')

%% Benjamini-Hochberg correction - IM1 %%%%%%%%%%%%%%%%%%%%%%%%%%%%%%%%%%%

Comb=nchoosek([1:1:10],2);

P_IM1=[Comb TBL_IM1.pValue];
Sort_IM1=sortrows(P_IM1,3);
BiH_IM1=[Sort_IM1 (((1:1:45)./45)*0.05)'];

figure,plot(BiH_IM1(:,3),'LineWidth',3)
hold on
plot(BiH_IM1(:,4),'LineWidth',3)
set(gca,'FontSize',18)
xticks([1:1:45])

 str1=string(Sort_IM1(:,1));
 str2=string(Sort_IM1(:,2));
 str_IM1=append(str1,'-',str2);

xticklabels(str_IM1)
xtickangle(90)
xlabel('day combination','FontSize',18,'FontWeight','bold')
ylabel('p-Value','FontSize',18,'FontWeight','bold')
title('Benjamini-Hochberg correction - IM1')
legend({'Sorted p-Values','y=(i/45)Q, i=1,2,...,45'},...

'Location','east','Orientation','horizontal','NumColumns',1,'FontSize',20,'FontWeight','bold')

%% Benjamini-Hochberg correction - IM2_H %%%%%%%%%%%%%%%%%%%%%%%%%%%%%%%%%

P_IM2_H=[Comb TBL_IM2_H.pValue];
Sort_IM2_H=sortrows(P_IM2_H,3);
BiH_IM2_H=[Sort_IM2_H (((1:1:45)./45)*0.05)'];
```

```matlab
figure,plot(BiH_IM2_H(:,3),'LineWidth',3)
hold on
plot(BiH_IM2_H(:,4),'LineWidth',3)
set(gca,'FontSize',18)
xticks([1:1:45])

 str1=string(Sort_IM2_H(:,1));
 str2=string(Sort_IM2_H(:,2));
 str_IM2_H=append(str1,'-',str2);

xticklabels(str_IM2_H)
xtickangle(90)
xlabel('day combination','FontSize',18,'FontWeight','bold')
ylabel('p-Value','FontSize',18,'FontWeight','bold')
title('Benjamini-Hochberg correction - IM2\_H')
legend({'Sorted p-Values','y=(i/45)Q, i=1,2,...,45'},...

'Location','east','Orientation','horizontal','NumColumns',1,'FontSize',20,'FontWeight','bold')

%% Benjamini-Hochberg correction - IM2_BRB1 %%%%%%%%%%%%%%%%%%%%%%%%%%%%%%%

P_IM2_BRB1=[Comb TBL_IM2_BRB1.pValue];
Sort_IM2_BRB1=sortrows(P_IM2_BRB1,3);
BiH_IM2_BRB1=[Sort_IM2_BRB1 (((1:1:45)./45)*0.05)'];

figure,plot(BiH_IM2_BRB1(:,3),'LineWidth',3)
hold on
plot(BiH_IM2_BRB1(:,4),'LineWidth',3)
set(gca,'FontSize',18)
xticks([1:1:45])

 str1=string(Sort_IM2_BRB1(:,1));
 str2=string(Sort_IM2_BRB1(:,2));
 str_IM2_BRB1=append(str1,'-',str2);

xticklabels(str_IM2_BRB1)
xtickangle(90)
xlabel('day combination','FontSize',18,'FontWeight','bold')
ylabel('p-Value','FontSize',18,'FontWeight','bold')
title('Benjamini-Hochberg correction - IM2\_BRB1')
legend({'Sorted p-Values','y=(i/45)Q, i=1,2,...,45'},...

'Location','east','Orientation','horizontal','NumColumns',1,'FontSize',20,'FontWeight','bold')

%% Benjamini-Hochberg correction - IM1, IM2_H and IM2_BRB1 %%%%%%%%%%%%%%%%

figure,plot(BiH_IM1(:,3),'LineWidth',3)
hold on
plot(BiH_IM2_H(:,3),'LineWidth',3)
plot(BiH_IM2_BRB1(:,3),'LineWidth',3)
plot(BiH_IM1(:,4),'LineWidth',3)

set(gca,'FontSize',18)
xticks([1:1:45])

xticklabels(str_IM1)
xtickangle(90)
xlabel('day combination','FontSize',18,'FontWeight','bold')
ylabel('p-value','FontSize',18,'FontWeight','bold')

lgd=legend({'Sorted p-values - IM1','Sorted p-values - IM2\_H','Sorted p-values - IM2\_BRB1','y=(i/45)Q,
i=1,2,...,45; Q=0.05'},...

'Location','east','Orientation','horizontal','NumColumns',1,'FontSize',20,'FontWeight','bold')

set(lgd,'position',[ 0.4 0.2 0.7311  0.3331 ])



--------------------------------------------------------------------



clc; clear all; close all

%% %%%%%%%%%%%%%%%%%%%%%%%%%%%%%%%%%%%%%%%%%%%%%%%%%%%%%%%%%%%%%%%%%%%%%%%%%
%% %%%%%%%%%%%%%%%%%%%% RM-ANOVA BRB detection  %%%%%%%%%%%%%%%%%%%%%%%%%%%%
%% %%%%%%%%%%%%%%%%%%%%%%%%%%%%%%%%%%%%%%%%%%%%%%%%%%%%%%%%%%%%%%%%%%%%%%%%%

% load('C:\Users\PFST-User\Desktop\PhD DATA\SIEMENS_C123_M1000.mat')

load('C:\Users\PFST-User\Desktop\PhD DATA\KONCAR_C123_M1000.mat')

%% %%%%%%%%%%%%%%%%%%%%%%%%%%%%%%%%%%%%%%%%%%%%%%%%%%%%%%%%%%%%%%%%%%%%%%%%%
```

```matlab
Mot1=repmat('Mot1',90005400,1);
Mot2=repmat('Mot2',90005400,1);
Mot3=repmat('Mot3',90005400,1);

MOT=[Mot1;Mot2;Mot3];

X=[ IM1_R_C123(:,1) IM1_R_C123(:,2) IM1_R_C123(:,3) IM1_R_C123(:,4) IM1_R_C123(:,5)...
    IM1_R_C123(:,6) IM1_R_C123(:,7) IM1_R_C123(:,8) IM1_R_C123(:,9) IM1_R_C123(:,10);...
    IM2_H_R_C123(:,1) IM2_H_R_C123(:,2) IM2_H_R_C123(:,3) IM2_H_R_C123(:,4) IM2_H_R_C123(:,5)...
    IM2_H_R_C123(:,6) IM2_H_R_C123(:,7) IM2_H_R_C123(:,8) IM2_H_R_C123(:,9) IM2_H_R_C123(:,10);...
    IM2_BRB1_R_C123(:,1) IM2_BRB1_R_C123(:,2) IM2_BRB1_R_C123(:,3) IM2_BRB1_R_C123(:,4)
IM2_BRB1_R_C123(:,5),...
    IM2_BRB1_R_C123(:,6) IM2_BRB1_R_C123(:,7) IM2_BRB1_R_C123(:,8) IM2_BRB1_R_C123(:,9)
IM2_BRB1_R_C123(:,10)];

%%
t = table(  MOT,X(:,1),X(:,2),X(:,3),X(:,4),X(:,5),X(:,6),X(:,7),X(:,8),X(:,9),X(:,10),...
            'VariableNames',{'Motor','d1','d2','d3','d4','d5','d6','d7','d8','d9','d10'});


T = table([1 2 3 4 5 6 7 8 9 10]','VariableNames',{'day'});
withinDesign = table([1 2 3 4 5 6 7 8 9 10]', 'VariableNames', {'day'});
withinDesign.day = categorical(withinDesign.day);

%%
rm = fitrm(t,'d1-d10 ~ Motor', 'WithinDesign', withinDesign);

RMAT = ranova(rm,'WithinModel', 'day')

ROW1=RMAT(4,1:5) % Intercept(day)
ROW2=RMAT(2,1:5) % Motor
ROW3=RMAT(5,1:5) % Mot:day
ROW4=RMAT(6,1:5) % Mot:day

mm_day=margmean(rm,'day');

mTEST=mauchly(rm);

tbl_Mot=multcompare(rm,'Motor','ComparisonType','lsd')
tbl_day=multcompare(rm,'day','ComparisonType','lsd')


%%

mm_Mot=margmean(rm,'Motor')

EB1=errorbar([1],[tbl_Mot.Difference(1)],[(tbl_Mot.Upper(1)-tbl_Mot.Lower(1))./2
],'o','MarkerSize',2.5,'Color', 'b','MarkerFaceColor','b');
hold on
EB2=errorbar([2],[tbl_Mot.Difference(2)],[(tbl_Mot.Upper(2)-tbl_Mot.Lower(2))./2
],'o','MarkerSize',2.5,'Color', 'r','MarkerFaceColor','r');
EB3=errorbar([3],[tbl_Mot.Difference(4)],[(tbl_Mot.Upper(4)-tbl_Mot.Lower(4))./2
],'o','MarkerSize',2.5,'Color', 'r','MarkerFaceColor','r');
grid on
set(gca,'FontSize',16)
xlim([0.7 3.3])
xticks([0 1 2 3 4])
xticklabels({'','IM1-IM2\_H','IM1-IM2\_BRB1','IM2\_H-IM2\_BRB1',''})
ylabel('Estimated difference of means [V]','FontSize',16,'FontWeight','bold')
xlabel('Motor combination','FontSize',16,'FontWeight','bold')


%-----------------------------------------------------------------------


clc; clear all; close all

%% %%%%%%%%%%%%%%%%%%%%%%%%%%%%%%%%%%%%%%%%%%%%%%%%%%%%%%%%%%%%%%%%%%%%%%%%%
%% %%%%%%%%%%%%%%%%% FRIEDMAN and Benjamini-Hochberg  %%%%%%%%%%%%%%%%%%%%%%
%% %%%%%%%%%%%%%%%%%%%%%%%%%%%%%%%%%%%%%%%%%%%%%%%%%%%%%%%%%%%%%%%%%%%%%%%%%

load('C:\Users\PFST-User\Desktop\PhD DATA\SIEMENS_C123_M1000.mat')

% load('C:\Users\PFST-User\Desktop\PhD DATA\KONCAR_C123_M1000.mat')

%%
[p_IM1,tbl_IM1,stats_IM1] = friedman(IM1_R_C123);
[p_IM2_H,tbl_IM2_H,stats_IM2_H] = friedman(IM2_H_R_C123);
[p_IM2_BRB1,tbl_IM2_BRB1,stats_IM2_BRB1] = friedman(IM2_BRB1_R_C123);

% multcompare za Friedman test: http://www.ece.northwestern.edu/local-
apps/matlabhelp/toolbox/stats/multcompare.html
c_IM1 = multcompare(stats_IM1,0.05,'on','lsd');
c_IM2_H = multcompare(stats_IM2_H,0.05,'on','lsd');
c_IM2_BRB1 = multcompare(stats_IM2_BRB1,0.05,'on','lsd');
```

```matlab
%% STEM - IM1 %%%%%%%%%%%%%%%%%%%%%%%%%%%%%%%%%%%%%%%%%%%%%%%%%%%%%%%%%%%
figure,stem(c_IM1(:,6),'filled','LineWidth',2)
hold on
yline(0.05,'r-','\alpha=0.05','LineWidth',2,'FontSize',18,'FontWeight','bold')
set(gca,'FontSize',18)
xticks([1:1:45])
xticklabels({   '1-2','1-3','1-4','1-5','1-6','1-7','1-8','1-9','1-10',...
                '2-3','2-4','2-5','2-6','2-7','2-8','2-9','2-10',...
                '3-4','3-5','3-6','3-7','3-8','3-9','3-10',...
                '4-5','4-6','4-7','4-8','4-9','4-10',...
                '5-6','5-7','5-8','5-9','5-10',...
                '6-7','6-8','6-9','6-10',...
                '7-8','7-9','7-10',...
                '8-9','8-10',...
                '9-10'})
xtickangle(90)
xlabel('day combination','FontSize',18,'FontWeight','bold')
ylabel('p-value','FontSize',18,'FontWeight','bold')

%% STEM - IM2_H %%%%%%%%%%%%%%%%%%%%%%%%%%%%%%%%%%%%%%%%%%%%%%%%%%%%%%%%%%
figure,stem(c_IM2_H(:,6),'filled','LineWidth',2)
hold on
yline(0.05,'r-','\alpha=0.05','LineWidth',2,'FontSize',18,'FontWeight','bold')
set(gca,'FontSize',18)
xticks([1:1:45])
xticklabels({   '1-2','1-3','1-4','1-5','1-6','1-7','1-8','1-9','1-10',...
                '2-3','2-4','2-5','2-6','2-7','2-8','2-9','2-10',...
                '3-4','3-5','3-6','3-7','3-8','3-9','3-10',...
                '4-5','4-6','4-7','4-8','4-9','4-10',...
                '5-6','5-7','5-8','5-9','5-10',...
                '6-7','6-8','6-9','6-10',...
                '7-8','7-9','7-10',...
                '8-9','8-10',...
                '9-10'})
xtickangle(90)
xlabel('day combination','FontSize',18,'FontWeight','bold')
ylabel('p-value','FontSize',18,'FontWeight','bold')

%% STEM - IM2_BRB1 %%%%%%%%%%%%%%%%%%%%%%%%%%%%%%%%%%%%%%%%%%%%%%%%%%%%%%%
figure,stem(c_IM2_BRB1(:,6),'filled','LineWidth',2)
hold on
yline(0.05,'r-','\alpha=0.05','LineWidth',2,'FontSize',18,'FontWeight','bold')
set(gca,'FontSize',18)
xticks([1:1:45])
xticklabels({   '1-2','1-3','1-4','1-5','1-6','1-7','1-8','1-9','1-10',...
                '2-3','2-4','2-5','2-6','2-7','2-8','2-9','2-10',...
                '3-4','3-5','3-6','3-7','3-8','3-9','3-10',...
                '4-5','4-6','4-7','4-8','4-9','4-10',...
                '5-6','5-7','5-8','5-9','5-10',...
                '6-7','6-8','6-9','6-10',...
                '7-8','7-9','7-10',...
                '8-9','8-10',...
                '9-10'})
xtickangle(90)
xlabel('day combination','FontSize',18,'FontWeight','bold')
ylabel('p-value','FontSize',18,'FontWeight','bold')

%% Benjamini-Hochberg correction - IM1 %%%%%%%%%%%%%%%%%%%%%%%%%%%%%%%%%%%

Comb=nchoosek([1:1:10],2);

P_IM1=[Comb c_IM1(:,6)];
Sort_IM1=sortrows(P_IM1,3);
BiH_IM1=[Sort_IM1 (((1:1:45)./45)*0.05)'];

figure,plot(BiH_IM1(:,3),'LineWidth',3)
hold on
plot(BiH_IM1(:,4),'LineWidth',3)
set(gca,'FontSize',18)
xticks([1:1:45])

 str1=string(Sort_IM1(:,1));
 str2=string(Sort_IM1(:,2));
 str_IM1=append(str1,'-',str2);

xticklabels(str_IM1)
xtickangle(90)
xlabel('day combination','FontSize',18,'FontWeight','bold')
ylabel('p-Value','FontSize',18,'FontWeight','bold')
title('Benjamini-Hochberg correction - IM1')
legend({'Sorted p-Values','y=(i/45)Q, i=1,2,...,45'},...

'Location','east','Orientation','horizontal','NumColumns',1,'FontSize',20,'FontWeight','bold')

%% Benjamini-Hochberg correction - IM2_H %%%%%%%%%%%%%%%%%%%%%%%%%%%%%%%%%

Comb=nchoosek([1:1:10],2);
```

```matlab
P_IM2_H=[Comb c_IM2_H(:,6)];
Sort_IM2_H=sortrows(P_IM2_H,3);
BiH_IM2_H=[Sort_IM2_H (((1:1:45)./45)*0.05)'];

figure,plot(BiH_IM2_H(:,3),'LineWidth',3)
hold on
plot(BiH_IM2_H(:,4),'LineWidth',3)
set(gca,'FontSize',18)
xticks([1:1:45])

 str1=string(Sort_IM2_H(:,1));
 str2=string(Sort_IM2_H(:,2));
 str_IM2_H=append(str1,'-',str2);

xticklabels(str_IM2_H)
xtickangle(90)
xlabel('day combination','FontSize',18,'FontWeight','bold')
ylabel('p-Value','FontSize',18,'FontWeight','bold')
title('Benjamini-Hochberg correction - IM2\_H')
legend({'Sorted p-Values','y=(i/45)Q, i=1,2,...,45'},...

'Location','east','Orientation','horizontal','NumColumns',1,'FontSize',20,'FontWeight','bold')

%% Benjamini-Hochberg correction - IM2_BRB1 %%%%%%%%%%%%%%%%%%%%%%%%%%%%%%%%

Comb=nchoosek([1:1:10],2);

P_IM2_BRB1=[Comb c_IM2_BRB1(:,6)];
Sort_IM2_BRB1=sortrows(P_IM2_BRB1,3);
BiH_IM2_BRB1=[Sort_IM2_BRB1 (((1:1:45)./45)*0.05)'];

figure,plot(BiH_IM2_BRB1(:,3),'LineWidth',3)
hold on
plot(BiH_IM2_BRB1(:,4),'LineWidth',3)
set(gca,'FontSize',18)
xticks([1:1:45])

 str1=string(Sort_IM2_BRB1(:,1));
 str2=string(Sort_IM2_BRB1(:,2));
 str_IM2_BRB1=append(str1,'-',str2);

xticklabels(str_IM2_BRB1)
xtickangle(90)
xlabel('day combination','FontSize',18,'FontWeight','bold')
ylabel('p-Value','FontSize',18,'FontWeight','bold')
title('Benjamini-Hochberg correction - IM2\_BRB1')
legend({'Sorted p-Values','y=(i/45)Q, i=1,2,...,45'},...

'Location','east','Orientation','horizontal','NumColumns',1,'FontSize',20,'FontWeight','bold')
%% Benjamini-Hochberg correction - IM1, IM2_H and IM2_BRB1 %%%%%%%%%%%%%%%%%

figure,plot(BiH_IM1(:,3),'LineWidth',3)
hold on
plot(BiH_IM2_H(:,3),'LineWidth',3)
plot(BiH_IM2_BRB1(:,3),'LineWidth',3)
plot(BiH_IM1(:,4),'LineWidth',3)

set(gca,'FontSize',18)
xticks([1:1:45])

xticklabels(str_IM1)
xtickangle(90)
xlabel('day combination','FontSize',18,'FontWeight','bold')
ylabel('p-Value','FontSize',18,'FontWeight','bold')
ylabel('p-Value','FontSize',18,'FontWeight','bold')

lgd=legend({'Sorted p-values - IM1','Sorted p-values - IM2\_H','Sorted p-values - IM2\_BRB1','y=(i/45)Q,
i=1,2,...,45; Q=0.05'},...

'Location','east','Orientation','horizontal','NumColumns',1,'FontSize',20,'FontWeight','bold')

set(lgd,'position',[ 0.4 0.2 0.7311  0.3331 ])


%---------------------------------------------------------------------



clc; clear all; close all

%% %%%%%%%%%%%%%%%%%%%%%%%%%%%%%%%%%%%%%%%%%%%%%%%%%%%%%%%%%%%%%%%%%%%%%%%%%%
%% %%%%%%%%%%%%%%%%%%%% FRIEDMAN BRB detection  %%%%%%%%%%%%%%%%%%%%%%%%%%%%%%
%% %%%%%%%%%%%%%%%%%%%%%%%%%%%%%%%%%%%%%%%%%%%%%%%%%%%%%%%%%%%%%%%%%%%%%%%%%%

% load('C:\Users\PFST-User\Desktop\PhD DATA\SIEMENS_C123_M1000.mat')

load('C:\Users\PFST-User\Desktop\PhD DATA\KONCAR_C123_M1000.mat')
```

```matlab
%% %%%%%%%%%%%%%%%%%%%%%%%%%%%%%%%%%%%%%%%%%%%%%%%%%%%%%%%%%%%%%%%%%%%%%%%%%%

IM1=[ IM1_R_C123(:,1)' IM1_R_C123(:,2)' IM1_R_C123(:,3)' IM1_R_C123(:,4)' IM1_R_C123(:,5)'...
     IM1_R_C123(:,6)' IM1_R_C123(:,7)' IM1_R_C123(:,8)' IM1_R_C123(:,9)' IM1_R_C123(:,10)']';

IM2_H=[ IM2_H_R_C123(:,1)' IM2_H_R_C123(:,2)' IM2_H_R_C123(:,3)' IM2_H_R_C123(:,4)' IM2_H_R_C123(:,5)'...
     IM2_H_R_C123(:,6)' IM2_H_R_C123(:,7)' IM2_H_R_C123(:,8)' IM2_H_R_C123(:,9)' IM2_H_R_C123(:,10)']';

IM2_BRB1=[ IM2_BRB1_R_C123(:,1)' IM2_BRB1_R_C123(:,2)' IM2_BRB1_R_C123(:,3)' IM2_BRB1_R_C123(:,4)'
IM2_BRB1_R_C123(:,5)'...
     IM2_BRB1_R_C123(:,6)' IM2_BRB1_R_C123(:,7)' IM2_BRB1_R_C123(:,8)' IM2_BRB1_R_C123(:,9)'
IM2_BRB1_R_C123(:,10)']';

MOT=[IM1 IM2_H IM2_BRB1];

[p_M,tbl_M,stats_M] = friedman(MOT)

% c_M = multcompare(stats_M,0.05,'on','lsd')
%%
[c,m,h,gnames] = multcompare(stats_M,0.05,'on','lsd')
%%
tbl = array2table(c,"VariableNames",["Group A","Group B","Lower Limit","A-B","Upper Limit","P-value"])


%% %%%%%%%%%%%%%%%%%%%%%%%%%%%%%%%%%%%%%%%%%%%%%%%%%%%%%%%%%%%%%%%%%%%%%%%%%%

EB1=errorbar([1],[c(1,4)],[(c(1,5)-c(1,3))./2 ],'o','MarkerSize',2.5,'Color', 'b','MarkerFaceColor','b');
hold on
EB2=errorbar([2],[c(2,4)],[(c(2,5)-c(2,3))./2 ],'o','MarkerSize',2.5,'Color', 'r','MarkerFaceColor','r');
EB3=errorbar([3],[c(3,4)],[(c(3,5)-c(3,3))./2 ],'o','MarkerSize',2.5,'Color', 'r','MarkerFaceColor','r');

set(gca,'FontSize',16)
xlim([0.5 3.5])

xticks([0 1 2 3 4])
xticklabels({'','IM1-IM2\_H','IM1-IM2\_BRB1','IM2\_H-IM2\_BRB1',''})
ylabel('Estimated difference of means ranks','FontSize',16,'FontWeight','bold')
xlabel('Motor combination','FontSize',16,'FontWeight','bold')


%% %%%%%%%%%%%%%%%%%%%%%%%%%%%%%%%%%%%%%%%%%%%%%%%%%%%%%%%%%%%%%%%%%%%%%%%%%%


--------------------------------------------------------------------------------



tic
clc; clear all; close all

%% %%%%%%%%%%%%%%%%%%%%%%%%%%%%%%%%%%%%%%%%%%%%%%%%%%%%%%%%%%%%%%%%%%%%%%%%%%
%% %%%%%%%%%%%%%%%%%%%%%%%%%% FEATURE Analysis   %%%%%%%%%%%%%%%%%%%%%%%%%%%%
%% %%%%%%%%%%%%%%%%%%%%%%%%%%%%%%%%%%%%%%%%%%%%%%%%%%%%%%%%%%%%%%%%%%%%%%%%%%

%% SIEMENS %%%%%%%%%%%%%%%%%%%%%%%%%%%%%%%%%%%%%%%%%%%%%%%%%%%%%%%%%%%%%%%%%%

load('C:\Users\PFST-User\Desktop\PhD DATA\S_H_IM1_M1000.mat')
load('C:\Users\PFST-User\Desktop\PhD DATA\S_H_IM2_M1000.mat')
load('C:\Users\PFST-User\Desktop\PhD DATA\S_BRB1_IM2_M1000.mat')

%% KONCAR %%%%%%%%%%%%%%%%%%%%%%%%%%%%%%%%%%%%%%%%%%%%%%%%%%%%%%%%%%%%%%%%%%%

% load('C:\Users\PFST-User\Desktop\PhD DATA\K_H_IM1_M1000.mat')
% load('C:\Users\PFST-User\Desktop\PhD DATA\K_H_IM2_M1000.mat')
% load('C:\Users\PFST-User\Desktop\PhD DATA\K_BRB1_IM2_M1000.mat')

%% EQ1 %%%%%%%%%%%%%%%%%%%%%%%%%%%%%%%%%%%%%%%%%%%%%%%%%%%%%%%%%%%%%%%%%%%%%%

M1=S1_H_IM1_M1000+S2_H_IM1_M1000+S3_H_IM1_M1000;
M2=S1_H_IM2_M1000+S2_H_IM2_M1000+S3_H_IM2_M1000;
M3=S1_BRB1_IM2_M1000+S2_BRB1_IM2_M1000+S3_BRB1_IM2_M1000;

%% %%%%%%%%%%%%%%%%%%%%%%%%%%%%%%%%%%%%%%%%%%%%%%%%%%%%%%%%%%%%%%%%%%%%%%%%%%

% nm=[20:20:1000]; % nm - number of mesurements

nm=[10]; % nm - number of mesurements
L_nm=length(nm);

Feature=zeros(19,L_nm);
Repeat_Count=zeros(19,L_nm);

% If one number of measurement is set, e.g., nm=[60], then use for loop
% ppp=1:30. If vector nm=[20:20:1000] is used, set ppp=1:1 or erase line
% for ppp=1:30 and the corresponding end
```

```matlab
for ppp=1:30

for yy=1:L_nm

NoR=100; % Number of repetition

for zz=1:NoR


M1=M1(:, randperm(size(M1, 2)));
M2=M2(:, randperm(size(M2, 2)));
M3=M3(:, randperm(size(M3, 2)));


%% %%%%%%%%%%%%%%%%%%%%%%%%%%%%%%%%%%%%%%%%%%%%%%%%%%%%%%%%%%%%%%%%%%%%%%%

nd=10; % nd - number of days

nmpd=nm(yy)./nd; % nmpd - number of measurements per day

%% %%%%%%%%%%%%%%%%%%%%%%%%%%%%%%%%%%%%%%%%%%%%%%%%%%%%%%%%%%%%%%%%%%%%%%%

for i=1:nd
for j=1:nmpd

%% FEATURES %%%%%%%%%%%%%%%%%%%%%%%%%%%%%%%%%%%%%%%%%%%%%%%%%%%%%%%%%%%%%%%
%% F1 - Energy %%%%%%%%%%%%%%%%%%%%%%%%%%%%%%%%%%%%%%%%%%%%%%%%%%%%%%%%%%%%
    M1_energy(j,i)=sum((abs(M1(:,j+nmpd*(i-1)))).^2,1);
    M2_energy(j,i)=sum((abs(M2(:,j+nmpd*(i-1)))).^2,1);
    M3_energy(j,i)=sum((abs(M3(:,j+nmpd*(i-1)))).^2,1);
%% F2 - Mean %%%%%%%%%%%%%%%%%%%%%%%%%%%%%%%%%%%%%%%%%%%%%%%%%%%%%%%%%%%%%%
    M1_mean(j,i)=mean(M1(:,j+nmpd*(i-1)),1);
    M2_mean(j,i)=mean(M2(:,j+nmpd*(i-1)),1);
    M3_mean(j,i)=mean(M3(:,j+nmpd*(i-1)),1);
%% F3 - Std %%%%%%%%%%%%%%%%%%%%%%%%%%%%%%%%%%%%%%%%%%%%%%%%%%%%%%%%%%%%%%%
    M1_std(j,i)=std(M1(:,j+nmpd*(i-1)),0,1);
    M2_std(j,i)=std(M2(:,j+nmpd*(i-1)),0,1);
    M3_std(j,i)=std(M3(:,j+nmpd*(i-1)),0,1);
%% F4 - Var %%%%%%%%%%%%%%%%%%%%%%%%%%%%%%%%%%%%%%%%%%%%%%%%%%%%%%%%%%%%%%%
    M1_var(j,i)=var(M1(:,j+nmpd*(i-1)),0,1);
    M2_var(j,i)=var(M2(:,j+nmpd*(i-1)),0,1);
    M3_var(j,i)=var(M3(:,j+nmpd*(i-1)),0,1);
%% F5 - Median %%%%%%%%%%%%%%%%%%%%%%%%%%%%%%%%%%%%%%%%%%%%%%%%%%%%%%%%%%%%
    M1_median(j,i)=median(M1(:,j+nmpd*(i-1)),1);
    M2_median(j,i)=median(M2(:,j+nmpd*(i-1)),1);
    M3_median(j,i)=median(M3(:,j+nmpd*(i-1)),1);
%% F6 - Kurtosis %%%%%%%%%%%%%%%%%%%%%%%%%%%%%%%%%%%%%%%%%%%%%%%%%%%%%%%%%%
    M1_kurtosis(j,i)=kurtosis(M1(:,j+nmpd*(i-1)),1);
    M2_kurtosis(j,i)=kurtosis(M2(:,j+nmpd*(i-1)),1);
    M3_kurtosis(j,i)=kurtosis(M3(:,j+nmpd*(i-1)),1);
%% F7 - Skewness %%%%%%%%%%%%%%%%%%%%%%%%%%%%%%%%%%%%%%%%%%%%%%%%%%%%%%%%%%
    M1_skewness(j,i)=skewness(M1(:,j+nmpd*(i-1)),1);
    M2_skewness(j,i)=skewness(M2(:,j+nmpd*(i-1)),1);
    M3_skewness(j,i)=skewness(M3(:,j+nmpd*(i-1)),1);
%% F8 - RMS %%%%%%%%%%%%%%%%%%%%%%%%%%%%%%%%%%%%%%%%%%%%%%%%%%%%%%%%%%%%%%%
    M1_rms(j,i)=rms(M1(:,j+nmpd*(i-1)),1);
    M2_rms(j,i)=rms(M2(:,j+nmpd*(i-1)),1);
    M3_rms(j,i)=rms(M3(:,j+nmpd*(i-1)),1);
%% F9 - RSSQ %%%%%%%%%%%%%%%%%%%%%%%%%%%%%%%%%%%%%%%%%%%%%%%%%%%%%%%%%%%%%%
    M1_rssq(j,i)=rssq(M1(:,j+nmpd*(i-1)),1);
    M2_rssq(j,i)=rssq(M2(:,j+nmpd*(i-1)),1);
    M3_rssq(j,i)=rssq(M3(:,j+nmpd*(i-1)),1);
%% F10 - IQR %%%%%%%%%%%%%%%%%%%%%%%%%%%%%%%%%%%%%%%%%%%%%%%%%%%%%%%%%%%%%%
    M1_iqr(j,i)=iqr(M1(:,j+nmpd*(i-1)),1);
    M2_iqr(j,i)=iqr(M2(:,j+nmpd*(i-1)),1);
    M3_iqr(j,i)=iqr(M3(:,j+nmpd*(i-1)),1);
%% F11 - peak2peak %%%%%%%%%%%%%%%%%%%%%%%%%%%%%%%%%%%%%%%%%%%%%%%%%%%%%%%%
    M1_peak2peak(j,i)=peak2peak(M1(:,j+nmpd*(i-1)),1);
    M2_peak2peak(j,i)=peak2peak(M2(:,j+nmpd*(i-1)),1);
    M3_peak2peak(j,i)=peak2peak(M3(:,j+nmpd*(i-1)),1);
%% F12 - peak2rms %%%%%%%%%%%%%%%%%%%%%%%%%%%%%%%%%%%%%%%%%%%%%%%%%%%%%%%%%
    M1_peak2rms(j,i)=peak2rms(M1(:,j+nmpd*(i-1)),1);
    M2_peak2rms(j,i)=peak2rms(M2(:,j+nmpd*(i-1)),1);
    M3_peak2rms(j,i)=peak2rms(M3(:,j+nmpd*(i-1)),1);
%% F13 - Shape factor %%%%%%%%%%%%%%%%%%%%%%%%%%%%%%%%%%%%%%%%%%%%%%%%%%%%%
    M1_shapefactor(j,i)=rms(M1(:,j+nmpd*(i-1)),1)./(1/length(M1(:,j+nmpd*(i-1))).*sum(abs(M1(:,j+nmpd*(i-1))),1));
    M2_shapefactor(j,i)=rms(M2(:,j+nmpd*(i-1)),1)./(1/length(M2(:,j+nmpd*(i-1))).*sum(abs(M2(:,j+nmpd*(i-1))),1));
    M3_shapefactor(j,i)=rms(M3(:,j+nmpd*(i-1)),1)./(1/length(M3(:,j+nmpd*(i-1))).*sum(abs(M3(:,j+nmpd*(i-1))),1));
%% F14 - Impulse factor %%%%%%%%%%%%%%%%%%%%%%%%%%%%%%%%%%%%%%%%%%%%%%%%%%%
    M1_impulsefactor(j,i)=max(abs(M1(:,j+nmpd*(i-1))),[],1)./(1/length(M1(:,j+nmpd*(i-1))).*sum(abs(M1(:,j+nmpd*(i-1))),1));
    M2_impulsefactor(j,i)=max(abs(M2(:,j+nmpd*(i-1))),[],1)./(1/length(M2(:,j+nmpd*(i-1))).*sum(abs(M2(:,j+nmpd*(i-1))),1));
    M3_impulsefactor(j,i)=max(abs(M3(:,j+nmpd*(i-1))),[],1)./(1/length(M3(:,j+nmpd*(i-1))).*sum(abs(M3(:,j+nmpd*(i-1))),1));
```

```matlab
%% F15 - Clearance factor %%%%%%%%%%%%%%%%%%%%%%%%%%%%%%%%%%%%%%%%%%
    M1_clearancefactor(j,i)=max(abs(M1(:,j+nmpd*(i-1))),[],1)./(1/length(M1(:,j+nmpd*(i-
1))).*sum(sqrt(abs(M1(:,j+nmpd*(i-1)))),1)).^2;
    M2_clearancefactor(j,i)=max(abs(M2(:,j+nmpd*(i-1))),[],1)./(1/length(M2(:,j+nmpd*(i-
1))).*sum(sqrt(abs(M2(:,j+nmpd*(i-1)))),1)).^2;
    M3_clearancefactor(j,i)=max(abs(M3(:,j+nmpd*(i-1))),[],1)./(1/length(M3(:,j+nmpd*(i-
1))).*sum(sqrt(abs(M3(:,j+nmpd*(i-1)))),1)).^2;
%% F16 - Harmonic mean %%%%%%%%%%%%%%%%%%%%%%%%%%%%%%%%%%%%%%%%%%%%%
    M1_harmmean(j,i)=harmmean(M1(:,j+nmpd*(i-1)),1);
    M2_harmmean(j,i)=harmmean(M2(:,j+nmpd*(i-1)),1);
    M3_harmmean(j,i)=harmmean(M3(:,j+nmpd*(i-1)),1);
%% F17 - Central moment 5 %%%%%%%%%%%%%%%%%%%%%%%%%%%%%%%%%%%%%%%%%%
    M1_moment5(j,i)=moment(M1(:,j+nmpd*(i-1)),5);
    M2_moment5(j,i)=moment(M2(:,j+nmpd*(i-1)),5);
    M3_moment5(j,i)=moment(M3(:,j+nmpd*(i-1)),5);
%% F18 - Central moment 6 %%%%%%%%%%%%%%%%%%%%%%%%%%%%%%%%%%%%%%%%%%
    M1_moment6(j,i)=moment(M1(:,j+nmpd*(i-1)),6);
    M2_moment6(j,i)=moment(M2(:,j+nmpd*(i-1)),6);
    M3_moment6(j,i)=moment(M3(:,j+nmpd*(i-1)),6);

end
end


%% F19 - Waveform length N=1 %%%%%%%%%%%%%%%%%%%%%%%%%%%%%%%%%%%%%%%%
N=1;
M1_waveformlength=zeros(1,nm(yy));
M2_waveformlength=zeros(1,nm(yy));
M3_waveformlength=zeros(1,nm(yy));
LM=length(M1);


for ii=1:nm
for jj=1:(LM-N)

    M1_waveformlength(:,ii)=M1_waveformlength(:,ii)+abs( M1(jj+N,ii)-M1(jj,ii) );
    M2_waveformlength(:,ii)=M2_waveformlength(:,ii)+abs( M2(jj+N,ii)-M2(jj,ii) );
    M3_waveformlength(:,ii)=M3_waveformlength(:,ii)+abs( M3(jj+N,ii)-M3(jj,ii) );

end
end
%% %%%%%%%%%%%%%%%%%%%%%%%%%%%%%%%%%%%%%%%%%%%%%%%%%%%%%%%%%%%%%%%%%%

for i=1:nd
for j=1:nmpd

    M1_WL(j,i)=M1_waveformlength(:,j+nmpd*(i-1));
    M2_WL(j,i)=M2_waveformlength(:,j+nmpd*(i-1));
    M3_WL(j,i)=M3_waveformlength(:,j+nmpd*(i-1));

end
end


%% %%%%%%%%%%%%%%%%%%%%%%%%%%%%%%%%%%%%%%%%%%%%%%%%%%%%%%%%%%%%%%%%%%

MOT_energy=[reshape(M1_energy,[],1) reshape(M2_energy,[],1) reshape(M3_energy,[],1)];
MOT_mean=[reshape(M1_mean,[],1) reshape(M2_mean,[],1) reshape(M3_mean,[],1)];
MOT_std=[reshape(M1_std,[],1) reshape(M2_std,[],1) reshape(M3_std,[],1)];
MOT_var=[reshape(M1_var,[],1) reshape(M2_var,[],1) reshape(M3_var,[],1)];
MOT_median=[reshape(M1_median,[],1) reshape(M2_median,[],1) reshape(M3_median,[],1)];
MOT_kurtosis=[reshape(M1_kurtosis,[],1) reshape(M2_kurtosis,[],1) reshape(M3_kurtosis,[],1)];
MOT_skewness=[reshape(M1_skewness,[],1) reshape(M2_skewness,[],1) reshape(M3_skewness,[],1)];
MOT_rms=[reshape(M1_rms,[],1) reshape(M2_rms,[],1) reshape(M3_rms,[],1)];
MOT_rssq=[reshape(M1_rssq,[],1) reshape(M2_rssq,[],1) reshape(M3_rssq,[],1)];
MOT_iqr=[reshape(M1_iqr,[],1) reshape(M2_iqr,[],1) reshape(M3_iqr,[],1)];
MOT_peak2peak=[reshape(M1_peak2peak,[],1) reshape(M2_peak2peak,[],1) reshape(M3_peak2peak,[],1)];
MOT_peak2rms=[reshape(M1_peak2rms,[],1) reshape(M2_peak2rms,[],1) reshape(M3_peak2rms,[],1)];
MOT_shapefactor=[reshape(M1_shapefactor,[],1) reshape(M2_shapefactor,[],1) reshape(M3_shapefactor,[],1)];
MOT_impulsefactor=[reshape(M1_impulsefactor,[],1) reshape(M2_impulsefactor,[],1)
reshape(M3_impulsefactor,[],1)];
MOT_clearancefactor=[reshape(M1_clearancefactor,[],1) reshape(M2_clearancefactor,[],1)
reshape(M3_clearancefactor,[],1)];
MOT_harmmean=[reshape(M1_harmmean,[],1) reshape(M2_harmmean,[],1) reshape(M3_harmmean,[],1)];
MOT_moment5=[reshape(M1_moment5,[],1) reshape(M2_moment5,[],1) reshape(M3_moment5,[],1)];
MOT_moment6=[reshape(M1_moment6,[],1) reshape(M2_moment6,[],1) reshape(M3_moment6,[],1)];
MOT_WL=[reshape(M1_WL,[],1) reshape(M2_WL,[],1) reshape(M3_WL,[],1)];


[pF_energyM,tbl_energyM,stats_energyM] = friedman(MOT_energy,1,'off');
[pF_meanM,tbl_meanM,stats_meanM] = friedman(MOT_mean,1,'off');
[pF_stdM,tbl_stdM,stats_stdM] = friedman(MOT_std,1,'off');
[pF_varM,tbl_varM,stats_varM] = friedman(MOT_var,1,'off');
[pF_medianM,tbl_medianM,stats_medianM] = friedman(MOT_median,1,'off');
[pF_kurtosisM,tbl_kurtosisM,stats_kurtosisM] = friedman(MOT_kurtosis,1,'off');
[pF_skewnessM,tbl_skewnessM,stats_skewnessM] = friedman(MOT_skewness,1,'off');
[pF_rmsM,tbl_rmsM,stats_rmsM] = friedman(MOT_rms,1,'off');
[pF_rssqM,tbl_rssqM,stats_rssqM] = friedman(MOT_rssq,1,'off');
[pF_iqrM,tbl_iqrM,stats_iqrM] = friedman(MOT_iqr,1,'off');
[pF_peak2peakM,tbl_peak2peakM,stats_peak2peakM] = friedman(MOT_peak2peak,1,'off');
```

```matlab
[pF_peak2rmsM,tbl_peak2rmsM,stats_peak2rmsM] = friedman(MOT_peak2rms,1,'off');
[pF_shapefactorM,tbl_shapefactorM,stats_shapefactorM] = friedman(MOT_shapefactor,1,'off');
[pF_impulsefactorM,tbl_impulsefactorM,stats_impulsefactorM] = friedman(MOT_impulsefactor,1,'off');
[pF_clearancefactorM,tbl_clearancefactorM,stats_clearancefactorM] = friedman(MOT_clearancefactor,1,'off');
[pF_harmmeanM,tbl_harmmeanM,stats_harmmeanM] = friedman(MOT_harmmean,1,'off');
[pF_moment5M,tbl_moment5M,stats_moment5M] = friedman(MOT_moment5,1,'off');
[pF_moment6M,tbl_moment6M,stats_moment6M] = friedman(MOT_moment6,1,'off');
[pF_WLM,tbl_WLM,stats_WLM] = friedman(MOT_WL,1,'off');

%
str2='lsd';
[c_energyMOT,m_energyMOT,h_energyMOT,gnames_energyMOT] = multcompare(stats_energyM,0.05,'on',str2);
[c_meanMOT,m_meanMOT,h_meanMOT,gnames_meanMOT] = multcompare(stats_meanM,0.05,'on',str2);
[c_stdMOT,m_stdMOT,h_stdMOT,gnames_stdMOT] = multcompare(stats_stdM,0.05,'on',str2);
[c_varMOT,m_varMOT,h_varMOT,gnames_varMOT] = multcompare(stats_varM,0.05,'on',str2);
[c_medianMOT,m_medianMOT,h_medianMOT,gnames_medianMOT] = multcompare(stats_medianM,0.05,'on',str2);
[c_kurtosisMOT,m_kurtosisMOT,h_kurtosisMOT,gnames_kurtosisMOT] = multcompare(stats_rmsM,0.05,'on',str2);
[c_skewnessMOT,m_skewnessMOT,h_skewnessMOT,gnames_skewnessMOT] = multcompare(stats_rmsM,0.05,'on',str2);
[c_rmsMOT,m_rmsMOT,h_rmsMOT,gnames_rmsMOT] = multcompare(stats_rmsM,0.05,'on',str2);
[c_rssqMOT,m_rssqMOT,h_rssqMOT,gnames_rssqMOT] = multcompare(stats_rssqM,0.05,'on',str2);
[c_iqrMOT,m_iqrMOT,h_iqrMOT,gnames_iqrMOT] = multcompare(stats_iqrM,0.05,'on',str2);
[c_peak2peakMOT,m_peak2peakMOT,h_peak2peakMOT,gnames_peak2peakMOT] =
multcompare(stats_peak2peakM,0.05,'on',str2);
[c_peak2rmsMOT,m_peak2rmsMOT,h_peak2rmsMOT,gnames_peak2rmsMOT] =
multcompare(stats_peak2rmsM,0.05,'on',str2);
[c_shapefactorMOT,m_shapefactorMOT,h_shapefactorMOT,gnames_shapefactorMOT] =
multcompare(stats_shapefactorM,0.05,'on',str2);
[c_impulsefactorMOT,m_impulsefactorMOT,h_impulsefactorMOT,gnames_impulsefactorMOT] =
multcompare(stats_impulsefactorM,0.05,'on',str2);
[c_clearancefactorMOT,m_clearancefactorMOT,h_clearancefactorMOT,gnames_clearancefactorMOT] =
multcompare(stats_clearancefactorM,0.05,'on',str2);
[c_harmmeanMOT,m_harmmeanMOT,h_harmmeanMOT,gnames_harmmeanMOT] =
multcompare(stats_harmmeanM,0.05,'on',str2);
[c_moment5MOT,m_moment5MOT,h_moment5MOT,gnames_moment5MOT] = multcompare(stats_moment5M,0.05,'on',str2);
[c_moment6MOT,m_moment6MOT,h_moment6MOT,gnames_moment6MOT] = multcompare(stats_moment6M,0.05,'on',str2);
[c_WLMOT,m_WLMOT,h_WLMOT,gnames_WLMOT] = multcompare(stats_WLM,0.05,'on',str2);

                c_energyMOT_nm(:,zz)=c_energyMOT(:,6)';
                c_meanMOT_nm(:,zz)=c_meanMOT(:,6)';
                c_stdMOT_nm(:,zz)=c_stdMOT(:,6)';
                c_varMOT_nm(:,zz)=c_varMOT(:,6)';
                c_medianMOT_nm(:,zz)=c_medianMOT(:,6)';
                c_kurtosisMOT_nm(:,zz)=c_kurtosisMOT(:,6)';
                c_skewnessMOT_nm(:,zz)=c_skewnessMOT(:,6)';
                c_rmsMOT_nm(:,zz)=c_rmsMOT(:,6)';
                c_rssqMOT_nm(:,zz)=c_rssqMOT(:,6)';
                c_iqrMOT_nm(:,zz)=c_iqrMOT(:,6)';
                c_peak2peakMOT_nm(:,zz)=c_peak2peakMOT(:,6)';
                c_peak2rmsMOT_nm(:,zz)=c_peak2rmsMOT(:,6)';
                c_shapefactorMOT_nm(:,zz)=c_shapefactorMOT(:,6)';
                c_impulsefactorMOT_nm(:,zz)=c_impulsefactorMOT(:,6)';
                c_clearancefactorMOT_nm(:,zz)=c_clearancefactorMOT(:,6)';
                c_harmmeanMOT_nm(:,zz)=c_harmmeanMOT(:,6)';
                c_moment5MOT_nm(:,zz)=c_moment5MOT(:,6)';
                c_moment6MOT_nm(:,zz)=c_moment6MOT(:,6)';
                c_WLMOT_nm(:,zz)=c_WLMOT(:,6)';


end

 %%
c_MOT=[ c_energyMOT_nm c_meanMOT_nm c_stdMOT_nm c_varMOT_nm c_medianMOT_nm...
        c_kurtosisMOT_nm c_skewnessMOT_nm c_rmsMOT_nm c_rssqMOT_nm c_iqrMOT_nm...
        c_peak2peakMOT_nm c_peak2rmsMOT_nm c_shapefactorMOT_nm c_impulsefactorMOT_nm...
        c_clearancefactorMOT_nm....
        c_harmmeanMOT_nm c_moment5MOT_nm c_moment6MOT_nm c_WLMOT_nm ];

%%
clear Fno_cMOT InIn_cMOT inInt_NoR_cMOT Lo_cMOT Up_cMOT Int_NoR_cMOT indx_cMOT

 for tt=1:length(c_MOT)

     if(c_MOT(1,tt)>0.05 && c_MOT(2,tt)<0.05 && c_MOT(3,tt)<0.05)

         indx_cMOT(tt)=1;
     else
         indx_cMOT(tt)=0;

     end
end
%%
InIn_cMOT=find(indx_cMOT);   % InIn - Index Indices
Fno_cMOT=(ceil([InIn_cMOT]./NoR)); % Fno - Feature Number

Feature(1:length(unique(Fno_cMOT)),yy)=unique(Fno_cMOT)';
%%

for ww=1:length(Fno_cMOT)
```

```matlab
        Lo_cMOT=NoR.*Fno_cMOT(ww)-(NoR-1); % First number in interval, e.g., 5 (ww=1)
        Up_cMOT=NoR.*Fno_cMOT(ww);   % Last number in interval, e.g., 8 (ww=1)
        Int_NoR_cMOT=[Lo_cMOT:1:Up_cMOT]; % Int_NMind - interval of 4 numbers, e.g., [5 6 7 8]

        for www=1:NoR

            if(Int_NoR_cMOT(www)==InIn_cMOT(ww))
                inInt_NoR_cMOT(ww)=www; % returns the indice of number in interval, e.g., Interval=[5 6 7 8],
Indice=[1 2 3 4];


            else

            end
        end
end

%%

  [~,~,ix] = unique(Fno_cMOT);
CC = accumarray(ix,1);

Repeat_Count(1:length(CC),yy)=CC;
end
%%

Feature( ~any(Feature,2), : ) = [];
Repeat_Count( ~any(Repeat_Count,2), : ) = [];
FFF=nm.*ones(19,L_nm);

%%
for hh=1:L_nm
    for rr=1:length(nonzeros(Feature(:,hh)))

        stem3(Feature(rr,hh),FFF(rr,hh),Repeat_Count(rr,hh))
        hold on

    end
end
%%
SFeat=size(Feature);
SFeat_rows=SFeat(1,1);
SFeat_columns=SFeat(1,2);

%%
xyz=zeros(19,L_nm);

    for gg2=1:SFeat_columns

        for gg3=1:SFeat_rows

          for gg=1:19

            if(Feature(gg3,gg2)==gg)

                xyz(gg,gg2)=Repeat_Count(gg3,gg2);

            else

            end

          end

    end
end
%%
close all
XYZ(:,ppp)=xyz; % Use only when code is running for one number of measurement,e.g., nm=[80]...
                % ... if vector is used nm=[20:20:1000], Comment line: XYZ(:,ppp)=xyz;

% figure,plot(nm,xyz(:,1:L_nm))

%%

end
toc


------------------------------------------------------------------
```

```matlab
clc; clear all; close all;

%% %%%%%%%%%%%%%%%%%%%%%%%%%%%%%%%%%%%%%%%%%%%%%%%%%%%%%%%%%%%%%%%%%%%%%%%
%% %%%%%%%%%%%%%%%%%%% FFT - Matrix Generation  %%%%%%%%%%%%%%%%%%%%%%%%%%
%% %%%%%%%%%%%%%%%%%%%%%%%%%%%%%%%%%%%%%%%%%%%%%%%%%%%%%%%%%%%%%%%%%%%%%%%


%% SIEMENS %%%%%%%%%%%%%%%%%%%%%%%%%%%%%%%%%%%%%%%%%%%%%%%%%%%%%%%%%%%%%%%%

load('C:\Users\PFST-User\Desktop\PhD DATA\S_H_IM1_M1000.mat')
load('C:\Users\PFST-User\Desktop\PhD DATA\S_H_IM2_M1000.mat')
load('C:\Users\PFST-User\Desktop\PhD DATA\S_BRB1_IM2_M1000.mat')

%% KONCAR %%%%%%%%%%%%%%%%%%%%%%%%%%%%%%%%%%%%%%%%%%%%%%%%%%%%%%%%%%%%%%%%%

% load('C:\Users\PFST-User\Desktop\PhD DATA\K_H_IM1_M1000.mat')
% load('C:\Users\PFST-User\Desktop\PhD DATA\K_H_IM2_M1000.mat')
% load('C:\Users\PFST-User\Desktop\PhD DATA\K_BRB1_IM2_M1000.mat')

%% %%%%%%%%%%%%%%%%%%%%%%%%%%%%%%%%%%%%%%%%%%%%%%%%%%%%%%%%%%%%%%%%%%%%%%%

load('C:\Users\PFST-User\Desktop\PhD DATA\time_vector.mat')
t=t_H;
%% %%%%%%%%%%%%%%%%%%%%%%%%%%%%%%%%%%%%%%%%%%%%%%%%%%%%%%%%%%%%%%%%%%%%%%%
%% %%%%%%%%%%%%%%%%%%%%%%%%% FFT - HEALTHY - IM1 %%%%%%%%%%%%%%%%%%%%%%%%%
%% %%%%%%%%%%%%%%%%%%%%%%%%%%%%%%%%%%%%%%%%%%%%%%%%%%%%%%%%%%%%%%%%%%%%%%%
% LtH=length(t);
% FsH=1./(t(5001)-t(5000));
% TH=1./FsH;
% f_H = FsH*(0:(LtH/2))/LtH;
% LfH=length(f_H);
% FFT_H=zeros(LtH,1);
%
% for i=1:1000
%
%     FFT_S1(:,i)=fft(S1_H_IM1_M1000(:,i));
%     P2_FFT_S1(:,i) = abs(FFT_S1(:,i)./LtH);
%     P1_FFT_S1(:,i) = P2_FFT_S1(1:LtH./2+1,i);
%     P1_FFT_S1(2:end-1,i) = 2*P1_FFT_S1(2:end-1,i);
%
%     FFT_IM1_S1(:,i)=P1_FFT_S1(:,i);
%
%     FFT_S2(:,i)=fft(S2_H_IM1_M1000(:,i));
%     P2_FFT_S2(:,i) = abs(FFT_S2(:,i)./LtH);
%     P1_FFT_S2(:,i) = P2_FFT_S2(1:LtH./2+1,i);
%     P1_FFT_S2(2:end-1,i) = 2*P1_FFT_S2(2:end-1,i);
%
%     FFT_IM1_S2(:,i)=P1_FFT_S2(:,i);
%
%     FFT_S3(:,i)=fft(S3_H_IM1_M1000(:,i));
%     P2_FFT_S3(:,i) = abs(FFT_S3(:,i)./LtH);
%     P1_FFT_S3(:,i) = P2_FFT_S3(1:LtH./2+1,i);
%     P1_FFT_S3(2:end-1,i) = 2*P1_FFT_S3(2:end-1,i);
%
%     FFT_IM1_S3(:,i)=P1_FFT_S3(:,i);
%
% end

% save('C:\Users\PFST-User\Desktop\PhD DATA/S_FFT_H_IM1_M1000.mat',...
% 'FFT_IM1_S1',...
% 'FFT_IM1_S2',...
% 'FFT_IM1_S3');


%% %%%%%%%%%%%%%%%%%%%%%%%%%%%%%%%%%%%%%%%%%%%%%%%%%%%%%%%%%%%%%%%%%%%%%%%
%% %%%%%%%%%%%%%%%%%%%%%%%%% FFT - HEALTHY - IM2_H %%%%%%%%%%%%%%%%%%%%%%%
%% %%%%%%%%%%%%%%%%%%%%%%%%%%%%%%%%%%%%%%%%%%%%%%%%%%%%%%%%%%%%%%%%%%%%%%%


% LtH=length(t);
% FsH=1./(t(5001)-t(5000));
% TH=1./FsH;
% f_H = FsH*(0:(LtH/2))/LtH;
% LfH=length(f_H);
% FFT_H=zeros(LtH,1);
%
% for i=1:1000
%
%     FFT_S1(:,i)=fft(S1_H_IM2_M1000(:,i));
%     P2_FFT_S1(:,i) = abs(FFT_S1(:,i)./LtH);
%     P1_FFT_S1(:,i) = P2_FFT_S1(1:LtH./2+1,i);
%     P1_FFT_S1(2:end-1,i) = 2*P1_FFT_S1(2:end-1,i);
%
%     FFT_IM2_H_S1(:,i)=P1_FFT_S1(:,i);
%
%     FFT_S2(:,i)=fft(S2_H_IM2_M1000(:,i));
```

```matlab
%     P2_FFT_S2(:,i) = abs(FFT_S2(:,i)./LtH);
%     P1_FFT_S2(:,i) = P2_FFT_S2(1:LtH./2+1,i);
%     P1_FFT_S2(2:end-1,i) = 2*P1_FFT_S2(2:end-1,i);
%
%     FFT_IM2_H_S2(:,i)=P1_FFT_S2(:,i);
%
%     FFT_S3(:,i)=fft(S3_H_IM2_M1000(:,i));
%     P2_FFT_S3(:,i) = abs(FFT_S3(:,i)./LtH);
%     P1_FFT_S3(:,i) = P2_FFT_S3(1:LtH./2+1,i);
%     P1_FFT_S3(2:end-1,i) = 2*P1_FFT_S3(2:end-1,i);
%
%     FFT_IM2_H_S3(:,i)=P1_FFT_S3(:,i);
%
% end
%
%
% save('C:\Users\PFST-User\Desktop\PhD DATA/S_FFT_H_IM2_M1000.mat',...
% 'FFT_IM2_H_S1',...
% 'FFT_IM2_H_S2',...
% 'FFT_IM2_H_S3');

%% %%%%%%%%%%%%%%%%%%%%%%%%%%%%%%%%%%%%%%%%%%%%%%%%%%%%%%%%%%%%%%%%%%%%%%%%%%
%% %%%%%%%%%%%%%%%%%%%%%%%% FFT - BRB1 - IM2_BRB1 %%%%%%%%%%%%%%%%%%%%%%%%%%%%
%% %%%%%%%%%%%%%%%%%%%%%%%%%%%%%%%%%%%%%%%%%%%%%%%%%%%%%%%%%%%%%%%%%%%%%%%%%%%%


LtB=length(t);
FsB=1./(t(5001)-t(5000));
TB=1./FsB;
f_B = FsB*(0:(LtB/2))/LtB;
LfB=length(f_B);
FFT_B=zeros(LtB,1);

for i=1:1000

    FFT_S1(:,i)=fft(S1_BRB1_IM2_M1000(:,i));
    P2_FFT_S1(:,i) = abs(FFT_S1(:,i)./LtB);
    P1_FFT_S1(:,i) = P2_FFT_S1(1:LtB./2+1,i);
    P1_FFT_S1(2:end-1,i) = 2*P1_FFT_S1(2:end-1,i);

    FFT_IM2_BRB1_S1(:,i)=P1_FFT_S1(:,i);

    FFT_S2(:,i)=fft(S2_BRB1_IM2_M1000(:,i));
    P2_FFT_S2(:,i) = abs(FFT_S2(:,i)./LtB);
    P1_FFT_S2(:,i) = P2_FFT_S2(1:LtB./2+1,i);
    P1_FFT_S2(2:end-1,i) = 2*P1_FFT_S2(2:end-1,i);

    FFT_IM2_BRB1_S2(:,i)=P1_FFT_S2(:,i);

    FFT_S3(:,i)=fft(S3_BRB1_IM2_M1000(:,i));
    P2_FFT_S3(:,i) = abs(FFT_S3(:,i)./LtB);
    P1_FFT_S3(:,i) = P2_FFT_S3(1:LtB./2+1,i);
    P1_FFT_S3(2:end-1,i) = 2*P1_FFT_S3(2:end-1,i);

    FFT_IM2_BRB1_S3(:,i)=P1_FFT_S3(:,i);

end


% save('C:\Users\PFST-User\Desktop\PhD DATA/S_FFT_BRB1_IM2_M1000.mat',...
% 'FFT_IM2_BRB1_S1',...
% 'FFT_IM2_BRB1_S2',...
% 'FFT_IM2_BRB1_S3');



%-------------------------------------------------------------------------


tic
clc;clear all;close all

%% %%%%%%%%%%%%%%%%%%%%%%%%%%%%%%%%%%%%%%%%%%%%%%%%%%%%%%%%%%%%%%%%%%%%%%%%%%
%% %%%%%%%%%%%%%%%%%%%%%%%%% FFT SIEMENS Analysis  %%%%%%%%%%%%%%%%%%%%%%%%%%
%% %%%%%%%%%%%%%%%%%%%%%%%%%%%%%%%%%%%%%%%%%%%%%%%%%%%%%%%%%%%%%%%%%%%%%%%%%%%

%% %%%%%%%%%%%%%%%%%%%%%%%%%%%%%%%%%%%%%%%%%%%%%%%%%%%%%%%%%%%%%%%%%%%%%%%%%%%

load('C:\Users\PFST-User\Desktop\PhD DATA/S_FFT_H_IM1_M1000.mat');
load('C:\Users\PFST-User\Desktop\PhD DATA/S_FFT_H_IM2_M1000.mat');
load('C:\Users\PFST-User\Desktop\PhD DATA/S_FFT_BRB1_IM2_M1000.mat');

FFT_IM1=FFT_IM1_S1+FFT_IM1_S2+FFT_IM1_S3;
FFT_IM2_H=FFT_IM2_H_S1+FFT_IM2_H_S2+FFT_IM2_H_S3;
FFT_IM2_BRB1=FFT_IM2_BRB1_S1+FFT_IM2_BRB1_S2+FFT_IM2_BRB1_S3;
```

```matlab
%% %%%%%%%%%%%%%%%%%%%%%%%%%%%%%%%%%%%%%%%%%%%%%%%%%%%%%%%%%%%%%%%%%%%%%%%%
load('C:\Users\PFST-User\Desktop\KONCAR/frequency_vector.mat'); % ff - frequency vector 1x50004

%% %%%%%%%%%%%%%%%%%%%%%%%%%%%%%%%%%%%%%%%%%%%%%%%%%%%%%%%%%%%%%%%%%%%%%%%%
%% 1 %%%%%%%%%%%%%%%%%%%%%%%%%%%%%%%%%%%%%%%%%%%%%%%%%%%%%%%%%%%%%%%%%%%%%%%
% f1=1.8;
% f2=2.8;
%% 2 %%%%%%%%%%%%%%%%%%%%%%%%%%%%%%%%%%%%%%%%%%%%%%%%%%%%%%%%%%%%%%%%%%%%%%%
% f1=7;
% f2=8;
%% 3 %%%%%%%%%%%%%%%%%%%%%%%%%%%%%%%%%%%%%%%%%%%%%%%%%%%%%%%%%%%%%%%%%%%%%%%
% f1=20;
% f2=23;
%% 4 %%%%%%%%%%%%%%%%%%%%%%%%%%%%%%%%%%%%%%%%%%%%%%%%%%%%%%%%%%%%%%%%%%%%%%%
% f1=40;
% f2=41;
%% 5 %%%%%%%%%%%%%%%%%%%%%%%%%%%%%%%%%%%%%%%%%%%%%%%%%%%%%%%%%%%%%%%%%%%%%%%
% f1=44.6;
% f2=46;
%% 6 %%%%%%%%%%%%%%%%%%%%%%%%%%%%%%%%%%%%%%%%%%%%%%%%%%%%%%%%%%%%%%%%%%%%%%%
% f1=54;
% f2=56;
%% 7 %%%%%%%%%%%%%%%%%%%%%%%%%%%%%%%%%%%%%%%%%%%%%%%%%%%%%%%%%%%%%%%%%%%%%%%
% f1=58;
% f2=60;
%% 8 %%%%%%%%%%%%%%%%%%%%%%%%%%%%%%%%%%%%%%%%%%%%%%%%%%%%%%%%%%%%%%%%%%%%%%%
% f1=68;
% f2=71;
%% 9 %%%%%%%%%%%%%%%%%%%%%%%%%%%%%%%%%%%%%%%%%%%%%%%%%%%%%%%%%%%%%%%%%%%%%%%
% f1=82;
% f2=85;
%% 10 %%%%%%%%%%%%%%%%%%%%%%%%%%%%%%%%%%%%%%%%%%%%%%%%%%%%%%%%%%%%%%%%%%%%%%
% f1=91;
% f2=95;
%% 11 %%%%%%%%%%%%%%%%%%%%%%%%%%%%%%%%%%%%%%%%%%%%%%%%%%%%%%%%%%%%%%%%%%%%%%
f1=96;
f2=98;
%% %%%%%%%%%%%%%%%%%%%%%%%%%%%%%%%%%%%%%%%%%%%%%%%%%%%%%%%%%%%%%%%%%%%%%%%%

indx1= find(abs(ff-f1) < 0.001);
indx2= find(abs(ff-f2) < 0.001);

%% %%%%%%%%%%%%%%%%%%%%%%%%%%%%%%%%%%%%%%%%%%%%%%%%%%%%%%%%%%%%%%%%%%%%%%%%
NoM=2; % NoM - Number of measurements
NoI=30; % NoI - Number of iterations
for jj=1:NoI

clear IM1 IM2_H IM2_BRB1 IM1_mean IM2_H_mean IM2_BRB1_mean IM1_std IM2_H_std IM2_BRB1_std
clear IM1_indx IM2_H_indx IM2_BRB1_indx IM1_max IM2_H_max IM2_BRB1_max

for i=1:100

FFT_IM1=FFT_IM1(:, randperm(size(FFT_IM1, 2)));
FFT_IM2_H=FFT_IM2_H(:, randperm(size(FFT_IM2_H, 2)));
FFT_IM2_BRB1=FFT_IM2_BRB1(:, randperm(size(FFT_IM2_BRB1, 2)));



IM1=FFT_IM1(:,1:NoM);
IM2_H=FFT_IM2_H(:,1:NoM);
IM2_BRB1=FFT_IM2_BRB1(:,1:NoM);


IM1_mean=mean(IM1,2);
IM2_H_mean=mean(IM2_H,2);
IM2_BRB1_mean=mean(IM2_BRB1,2);

IM1_std=std(IM1,0,2);
IM2_H_std=std(IM2_H,0,2);
IM2_BRB1_std=std(IM2_BRB1,0,2);


IM1_indx=IM1_mean(indx1:indx2,:);
IM2_H_indx=IM2_H_mean(indx1:indx2,:);
IM2_BRB1_indx=IM2_BRB1_mean(indx1:indx2,:);

IM1_max(i)=max(IM1_indx);
IM2_H_max(i)=max(IM2_H_indx);
IM2_BRB1_max(i)=max(IM2_BRB1_indx);

end
%%
figure, plot(IM1_max,'b');hold on;plot(IM2_H_max,'k');plot(IM2_BRB1_max,'r')
%%
count=0;
for j=1:1:100
```

```matlab
        if (IM2_BRB1_max(j)>IM1_max(j) & IM2_BRB1_max(j)>IM2_H_max(j))

        count=count+1;
    else
    end


end

 CC(jj)=count;

end

toc


----------------------------------------------------------------------


tic
clc;clear all;close all

%% %%%%%%%%%%%%%%%%%%%%%%%%%%%%%%%%%%%%%%%%%%%%%%%%%%%%%%%%%%%%%%%%%%%%%%%%

load('C:\Users\PFST-User\Desktop\PhD DATA/K_FFT_H_IM1_M1000.mat');
load('C:\Users\PFST-User\Desktop\PhD DATA/K_FFT_H_IM2_M1000.mat');
load('C:\Users\PFST-User\Desktop\PhD DATA/K_FFT_BRB1_IM2_M1000.mat');

FFT_IM1=FFT_IM1_S1+FFT_IM1_S2+FFT_IM1_S3;
FFT_IM2_H=FFT_IM2_H_S1+FFT_IM2_H_S2+FFT_IM2_H_S3;
FFT_IM2_BRB1=FFT_IM2_BRB1_S1+FFT_IM2_BRB1_S2+FFT_IM2_BRB1_S3;


%% %%%%%%%%%%%%%%%%%%%%%%%%%%%%%%%%%%%%%%%%%%%%%%%%%%%%%%%%%%%%%%%%%%%%%%%%

load('C:\Users\PFST-User\Desktop\KONCAR/frequency_vector.mat'); % ff - frequency vector 1x50004

%% %%%%%%%%%%%%%%%%%%%%%%%%%%%%%%%%%%%%%%%%%%%%%%%%%%%%%%%%%%%%%%%%%%%%%%%%
%% 1 %%%%%%%%%%%%%%%%%%%%%%%%%%%%%%%%%%%%%%%%%%%%%%%%%%%%%%%%%%%%%%%%%%%%%%%
% f1=3;
% f2=4;
%% 2 %%%%%%%%%%%%%%%%%%%%%%%%%%%%%%%%%%%%%%%%%%%%%%%%%%%%%%%%%%%%%%%%%%%%%%%
% f1=9;
% f2=11;
%% 3 %%%%%%%%%%%%%%%%%%%%%%%%%%%%%%%%%%%%%%%%%%%%%%%%%%%%%%%%%%%%%%%%%%%%%%%
% f1=35;
% f2=38;
%% 4 %%%%%%%%%%%%%%%%%%%%%%%%%%%%%%%%%%%%%%%%%%%%%%%%%%%%%%%%%%%%%%%%%%%%%%%
f1=56;
f2=58;
%% 5 %%%%%%%%%%%%%%%%%%%%%%%%%%%%%%%%%%%%%%%%%%%%%%%%%%%%%%%%%%%%%%%%%%%%%%%
% f1=62;
% f2=65;
%% 6 %%%%%%%%%%%%%%%%%%%%%%%%%%%%%%%%%%%%%%%%%%%%%%%%%%%%%%%%%%%%%%%%%%%%%%%
% f1=78;
% f2=80;
%% 7 %%%%%%%%%%%%%%%%%%%%%%%%%%%%%%%%%%%%%%%%%%%%%%%%%%%%%%%%%%%%%%%%%%%%%%%
% f1=88;
% f2=90.6;
%% 8 %%%%%%%%%%%%%%%%%%%%%%%%%%%%%%%%%%%%%%%%%%%%%%%%%%%%%%%%%%%%%%%%%%%%%%%
% f1=96;
% f2=97;
%% %%%%%%%%%%%%%%%%%%%%%%%%%%%%%%%%%%%%%%%%%%%%%%%%%%%%%%%%%%%%%%%%%%%%%%%%

indx1= find(abs(ff-f1) < 0.001);
indx2= find(abs(ff-f2) < 0.001);

%% %%%%%%%%%%%%%%%%%%%%%%%%%%%%%%%%%%%%%%%%%%%%%%%%%%%%%%%%%%%%%%%%%%%%%%%%
NoM=2; % NoM - Number of measurements
NoI=30; % NoI - Number of iterations
for jj=1:NoI

clear IM1 IM2_H IM2_BRB1 IM1_mean IM2_H_mean IM2_BRB1_mean IM1_std IM2_H_std IM2_BRB1_std
clear IM1_indx IM2_H_indx IM2_BRB1_indx IM1_max IM2_H_max IM2_BRB1_max

for i=1:100

FFT_IM1=FFT_IM1(:, randperm(size(FFT_IM1, 2)));
FFT_IM2_H=FFT_IM2_H(:, randperm(size(FFT_IM2_H, 2)));
FFT_IM2_BRB1=FFT_IM2_BRB1(:, randperm(size(FFT_IM2_BRB1, 2)));



IM1=FFT_IM1(:,1:NoM);
IM2_H=FFT_IM2_H(:,1:NoM);
IM2_BRB1=FFT_IM2_BRB1(:,1:NoM);
```

```matlab
IM1_mean=mean(IM1,2);
IM2_H_mean=mean(IM2_H,2);
IM2_BRB1_mean=mean(IM2_BRB1,2);

IM1_std=std(IM1,0,2);
IM2_H_std=std(IM2_H,0,2);
IM2_BRB1_std=std(IM2_BRB1,0,2);


IM1_indx=IM1_mean(indx1:indx2,:);
IM2_H_indx=IM2_H_mean(indx1:indx2,:);
IM2_BRB1_indx=IM2_BRB1_mean(indx1:indx2,:);

IM1_max(i)=max(IM1_indx);
IM2_H_max(i)=max(IM2_H_indx);
IM2_BRB1_max(i)=max(IM2_BRB1_indx);

end
%%
figure, plot(IM1_max,'b');hold on;plot(IM2_H_max,'k');plot(IM2_BRB1_max,'r')
%%
count=0;
for j=1:1:100

        if (IM2_BRB1_max(j)>IM1_max(j) & IM2_BRB1_max(j)>IM2_H_max(j))

        count=count+1;
    else
    end


end

 CC(jj)=count;

end

toc
```